Pathogenic Mechanisms Underlying Immune Dysregulation Associated To Hypomorphic RAG2 Mutation: Role Of Microbiota At Mucosal Interfaces

Thesis

Rosita Rigoni

Personal identifier: C810628X

Master Degree in Biotechnology

PATHOGENIC MECHANISMS UNDERLYING IMMUNE DYSREGULATION ASSOCIATED TO HYPOMORPHIC RAG2 MUTATION: ROLE OF MICROBIOTA AT MUCOSAL INTERFACES

A thesis submitted for the degree of

DOCTOR OF PHILOSOPHY

The Open University

School of Life, Health and Chemical Sciences

Affiliated Research Center: IRCCS Istituto Clinico Humanitas

Date of submission: February 2018

LIST OF CONTENTS

1. ABSTRACT

Hypomorphic mutations in the *RAG* genes cause a profound immunodeficiency associated with multisystem autoimmune–like manifestations, mediated by oligoclonal self-reactive T and B cells, named Omenn Syndrome (OS). The clinical and immunological spectrum of OS presentation is extremely broad. Commonly, patients present symptoms very similar to graft-versus-host disease (GVHD) as inflammatory reactions particularly involve the environmental interfaces such as the skin and gut, leading to distinctive early onset erythroderma and protracted diarrhea. However, the complete comprehension of the molecular and cellular mechanisms underlying such autoimmune-like manifestations in OS is still puzzling. Furthermore, the role played by environmental triggers in the disease pathogenesis remains largely unknown. In this thesis, we demonstrated that in hypomorphic $Rag2^{R229Q\backslash R229Q}$ mice, the OS murine counterpart, mucosal B cell deficiency alters the composition of the gut microbiota and causes bacterial translocation across the intestinal epithelium. Furthermore, loss of T cell tolerance to the commensal microbiota leads to gut inflammation sustained by Th1 and Th17 cells. Interestingly, we provided evidence that these gut-derived inflammatory cells disseminate in the periphery, infiltrating target organs. Decreasing gut bacterial load in $Rag2^{R229Q\backslash R229Q}$ mice with long-term dosing of antibiotics reverses most of these abnormalities and normalizes serum hyper-IgE, a hallmark of the disease. Similar mechanisms are involved in the development of skin degeneration in mutant mice. Indeed, we found that compromised skin barrier integrity results in altered microbial load and composition, and dysregulated production of T cell recruiting chemokines by stimulated epithelial cells. Importantly, we found that the chronic intestinal inflammation synergistically supports the activation of skin epithelial cells and the recruitment of gut-derived pathogenic T cells at the cutaneous barrier. Overall, this work provided first time evidence that commensals and/or commensal-derived signals might play a substantial role in shaping immune response and autoimmunity at barrier sites and beyond in RAG-associated immune deficiency.

2. DECLARATION

The work described in this dissertation was performed in the IRCSS Istituto Clinico Humanitas (ICH), between February 2014 and December 2017. I declare that this dissertation has not been submitted in part or in whole to any other academic institution. The work reported here was carried out entirely by the author, unless otherwise indicated. Part of the results discussed here generated a paper that was accepted for publication in the Journal of Experimental Medicine (Rigoni R et al., 2016 Mar 7;213(3):355-75. doi: 10.1084/jem.20151116).

3. PREFACE

Publications obtained during the course of this thesis:

Rigoni R, Fontana E, Guglielmetti S, Fosso B, D'Erchia AM, Maina V, Taverniti V, Castiello MC, Mantero S, Pacchiana G, Musio S, Pedotti R, Selmi C, Mora JR, Pesole G, Vezzoni P, Poliani PL, Grassi F, Villa A, Cassani B. Intestinal microbiota sustains inflammation and autoimmunity induced by hypomorphic RAG defects, **J Exp Med**. 2016 Mar 7;213(3):355-75

Farini A, Sitzia C, Cassani B, Cassinelli L, **Rigoni R**, Colleoni F, Fusco N, Gatti S, Bella P, Villa C, Napolitano F, Maiavacca R, Bosari S, Villa A, Torrente Y. Therapeutic Potential of Immunoproteasome Inhibition in Duchenne Muscular Dystrophy, **Mol Ther.** 2016 Sep 27

Rigoni R, Grassi F, Villa A, Cassani B, RAGs and BUGS: An alliance for autoimmunity, **Gut Microbes**. 2016 Aug 30:1-9

Capo V, Castiello MC, Fontana E, Penna S, Bosticardo M, Draghici E, Poliani LP, Sergi Sergi L, **Rigoni R**, Cassani B, Zanussi M, Carrera P, Uva P, Dobbs K, Notarangelo LD, van Til NP, Wagemaker G, Villa A, Efficacy of lentiviral mediated gene therapy in an Omenn syndrome Rag2 mouse model is not hindered by inflammation and immune dysregulation, **JACI**. 2017 Dec 11

4. LIST OF FIGURES AND TABLES

5. ABBREVIATIONS

A.U.	Arbitrary unit
ABX	Antibiotic
ADA	Adenosine deaminase
ADAM-17	Disintegrin and metalloproteinase domain-containing protein 17
AID	Activation-induced cytidine deaminase
AIRE	Autoimmune regulator
AMPs	Antimicrobial peptides
APC	Antigen presenting cells
APECED	Autoimmune polyendocrinopathy-candidiasis-ectodermal dystrophy
APRIL	Proliferation inducing ligand
ASF	Altered Schaedler flora
ATP	Adenosine triphosphate
BAFF	B cell-activating factor
BAFFR	B cell-activating factor receptor
Bcl-6	B-cell lymphoma 6 protein
Blimp-1	B lymphocyte-induced maturation protein 1
BTK	Bruton's tyrosine kinase
CCL	CC-chemokine-ligand
CD	Crohn Disease
CD40L	CD40 ligand
CF	Cystic fibrosis
CGD	Chronic granulomatous disease
CHD7	Chromodomain helicase DNA binding protein 7

CID	Combined immunodeficiency
CK5	Keratin 5
CLA	Cutaneous lymphocyte associated antigen
CMD	Corticomedullary demarcation
CNS	Central nervous system
CSR	Class switch recombination
CT	Cholera toxin
CVID	Common variable immunodeficiency
CXCL	CX-chemokine-ligand
DC	Dendritic cells
DETCs	Dendritic epidermal T cells
DGS	DiGeorge syndrome
DLNs	Draining lymph nodes
DN3	Double negative 3
DNA-PK	DNA-dependent protein kinase
DNA-PKcs	DNA-PK catalytic subunit
DOCK8	Dedicator of cytokinesis ptotein 8
DP	Double positive
DSS	Dextran sulfate sodium
EAE	Experimental autoimmune encephalomyelitis
EBV	Epstein Barr virus
FACS	Fluorescence-activated cell sorting
FLG	Filaggrin
FOXN1	Forkhead box N1
FSC	Forward scatter
GALT	Gut-associated lymphoid tissues

GC	Germinal centers
GF	Germ free
GFP	Green fluorescent protein
GI	Gastrointestinal tract
GT	Gene therapy
GVHD	Graft-versus host disease
GWAS	Genome-wide association studies
H&E	Hematoxilin and Eosin
HIGMs	Hyper-IgM syndromes
HLA	Human leucocyte antigen
HSCT	Hematopoietic stem cell transplantation
HSV	Herpes simplex virus
IBD	Inflammatory bowel disease
ICOS	Inducible T cell costimulator
IECs	Intestinal epithelial cells
IELs	Intraepithelial lymphocytes
IFN	Interferon
IgA	Immunoglobulin A
IgAD	IgA deficiency
IL	Interleukin
IL2Rγ	Interleukin (IL)-2 receptor γ gene
ILCs	Innate lymphoid cells
ILFs	Isolated lymphoid follicles
iNKT	Invariant natural killer T cells
iNOS	Inducible nitric oxide synthase
IPEX	Immunodysregulation, polyendocrinopathy and enteropathy, X linked

JAK	Janus kinase
LP	Lamina propria
LPS	Lipopolysaccharide
M cells	Microfold cells
MADCAM-1	Mucosal vascular addressin cell adhesion molecule 1
MFI	Mean fluorescence intensity
MHCII	Major histocompatibility complex class II
MLN	Mesenteric lymph nodes
MM	Memory mutant mice
MMPs	Metalloproteinases
MS	Multiple sclerosis
mTECs	Medullary thymic epithelial cells
MUC2	Mucin-2
MUD	Matched unrelated donors
MyD88	Myeloid differentiation primary response 88
NADPH	Nicotinamide adenine dinucleotide phosphate
NHEJ	Non-homologous end-joining
NK	Natural killer
NLRs	NOD-like receptors
NO	Nitric oxide
NOD	Non-obese diabetic
NSG	Next generation sequencing
OS	Omenn Syndrome
OVA	Ovalbumin
pDC	Plasmacytoid DCs
PHA	Phytohemagglutinin

PID	Primary immunodeficiency
pIgR	Polymeric immunoglobulin receptor
PMN	Polymorphonuclear leucocytes
PPs	Peyer's patches
PRRs	Pattern recognition receptors
PSA	Polysaccharide A
RA	Retinoic acid
RA	Rheumatoid arthritis
RAG	Recombination-activating gene
Reg3	Regenerating islet-derived 3
RLRs	Retinoic acid inducible gene 1 (RIG-1) like receptors
RMRP	RNA component of mitochondrial RNA-processing endoribonuclease
RSSs	Recombination signal sequences
RT-PCR	Real time PCR
S1PR1	Sphingosine-1-phospate receptor 1
SCFAs	Short chain fatty acids
SCID	Severe combined immunodeficiency
SCID-X1	X-linked SCID
SFB	Segmented filamentous bacteria
SH2D1A	SH2 domain containing protein 1A
SHM	Somatic hypermutation
SI	Small intestine
SIgA	Secreted IgA
SP	Single positive
SSC	Side scatter
STAT1	Signal transducer and activator of transcription 1

T1D	Type 1 Diabetes
TACI	Transmembrane activator and calcium-modulating cyclophilin-ligand interactor
TCR	T cell receptor
TDT	Terminal deoxynucleotidyl transferase
TECs	Thymic epithelial cells
TEM	T effector memory cells
TFH	T-follicular helper cells
TGFβ	Transforming growth factor-beta
Th	T helper
TJ	Tight junction
TLR	Toll-Like Receptor
TNF	Tumor Necrosis Factor
TRAs	Tissue restricted antigens
Treg	T regulatory
TRM	Tissue resident memory T cells
TSLP	Thymic stromal lymphopoietin
UC	Ulcerative colitis
UEA-1	Ulex europaeus agglutinin-1
V(D)J	Variable (V), diversity (D) and joining (J)
VEGF-A	Vascular endothelial growth factor A
WAS	Whiskott-Aldrich syndrome
WES	Whole exome sequencing
WSG	Whole genome sequencing
XLA	X-linked agammaglobulinaemia
γc	γ chain

6. INTRODUCTION

6.1 Primary immunodeficiency disorders

Primary immunodeficiency disorders (PIDs) refer to a heterogeneous group of disorders characterized by a poor or absent function of one or more components of the immune system. Over 130 different disorders have been identified to date, and new disorders are continually being discovered [1]. Most PIDs are associated to inherited defects in the immune system development and function, but some acquired forms are also reported [2]. Moreover, PIDs are different from secondary immunodeficiency that may result from other causes, such as viral and bacterial infections, malnutrition and treatment with drugs that induce immunosuppression. PIDs are rare and, particularly, the estimate prevalence in the United States is about 1 in 10,000 live births. They are broadly classified according to the components of the immune system that are affected: innate or adaptive immunity. Defects of innate immune compartment include disorders of phagocytes, Toll-like receptor (TLR)-mediated signalling, and complement. Defects of the adaptive immune responses include antibody deficiency syndromes and combined immunodeficiencies (CIDs).

6.1.1 Innate Immunodeficiency

Innate immunodeficiencies include a group of disorders characterized by defects in the development and function of innate immune components. Chronic granulomatous disease (CGD) is a common phagocyte disease caused by defects in the reduced nicotinamide adenine dinucleotide phosphate (NADPH) oxidase complex, resulting in an inability to produce the superoxide anion necessary for bacteria and fungi killing. Patients with CGD are at high risk of severe infections (skin, liver and perirectal abscesses, pneumonia, and lymphadenitis) [3]. In humans, mutations in genes involved in TLR-mediated signalling result in a selective susceptibility to pathogens. Moreover, a large variety of inherited defects of complement components have been described. In particular, deficiency of early components of the classical pathway (C1q, C1r, C1s, C4, C2 and C3) causes autoimmune manifestations resembling systemic lupus

erythematosus. Defects of the late complement components (C5-C9) are associated with severe neisserial infections [4].

6.1.2 Adaptive Immunodeficiency

Deficiencies in antibody production and function represent the hallmark of PIDs that involve B cells. B-cell defects show increased susceptibility to bacterial infections, involving particularly the respiratory tract. Abscesses in the skin and in other organs, meningitis and urinary tract defects are also described in patients [2].

CIDs include a heterogeneous group of disorders with impaired development, function, or both of T cells, associated with a defective antibody response [5]. In most severe forms of CIDs, also known as severe combined immunodeficiency (SCID), there is a complete lack of T lymphocytes. SCID defects are classified based on the immunological features and are divided in: (1) SCID with absence of T lymphocytes (T^-B^+SCID) or (2) SCID with absence of both T and B lymphocytes (T^-B^- SCID). Patients with SCID present similar features, including early-onset severe respiratory tract infections, chronic diarrhoea, and failure to thrive.

6.1.2.1 Antibody Deficiency

Antibody deficiencies might depend on a variety of defects interfering with B cell development and functions [6]. Several forms of agammaglobulinaemia are characterized by a B cell defect and intact T cell function. Among all the forms, X-linked agammaglobulinaemia (XLA) provides the prototypical clinical description. It results from a mutation in the gene encoding Bruton's tyrosine kinase (BTK), which has a crucial role in B cell development [7]. Indeed, patients present a low number of circulating B cells and extremely low levels of all serum immunoglobulin. The Common Variable Immunodeficiency (CVID) is characterized by a defect in antibody production. In particular, the level of circulating B cells is reduced or normal, and these cells respond and proliferate normally to antigens. However, they fail to terminally differentiate to plasma cells, which secrete antibodies [8]. The classical mutated genes include the inducible T cell co-stimulator (ICOS) and SH2 domain containing protein 1A (SH2D1A). Recently, three additional genes have been associated to the disease: CD19, B cell-activating factor receptor (BAFFR) and transmembrane activator and calcium-modulating cyclophilin-ligand interactor (TACI). Patients with CVID present

increased risk of developing infections, autoimmune diseases, gastrointestinal and pulmonary conditions, and malignancies. Selective IgA Deficiency (IgAD) represents the most common PID [9]. The molecular defect, leading to the absence of IgA class switching, is unknown in most cases. Recurrent pyogenic sinopulmonary infections are associated with IgAD. In addition, hyper-IgM syndromes (HIGMs) represent a group of molecular defects characterized by impaired immunoglobulin class switch recombination (CSR) and somatic hypermutation (SHM) or by impaired SHM alone. Patients with these syndromes have recurrent bacterial infections and, often, lymphoid hyperplasia. Moreover, they have normal number of peripheral B cells but few memory B cells, resulting in normal or increased levels of serum IgM and low or absent levels of serum IgG, IgA and IgE. Several genetic defects have been identified associated to the disease, including defects in CD40 ligand (CD40L), activation-induced cytidine deaminase (AID) and CD40.

6.1.2.2 T Cell-Deficiency

The pathogenesis of SCID affects several steps in T cell development [5]. Adenosine deaminase (ADA) deficiency showed impaired survival of lymphocyte precursors. In particular, ADA is an enzyme of the purine salvage pathway that induces the conversion of adenosine (and deoxyadenosine) to inosine. In the absence of ADA, the apoptosis of lymphoid precursors in the bone marrow and in the thymus is caused by high intracellular levels of toxic phosphorylated metabolites of adenosine and deoxyadenosine [10]. ADA deficiency accounts for 10%-15% of all forms of SCID. Clinical manifestations in ADA patients extend beyond the immune system, ranging from deafness, behavioural problems, costochondral abnormalities and liver toxicity. Defects of cytokine-mediated signalling are responsible for the majority of SCID in humans. SCID-X1 (X-linked SCID) is caused by mutations of the interleukin (IL)-2 receptor γ gene (IL2Rγ), which encodes for the γ chain (γc) shared by cytokine receptors for IL-2, IL-4, IL-7, IL-9, IL-15, IL-21. Patients with SCID-X1 lack both T and natural killer (NK) cells, whereas they have normal number of circulating B lymphocytes [11]. The γc is physically and functionally coupled to the intracellular tyrosine kinase Janus kinase (JAK) 3, which delivers γc-mediated intracellular pathways. Indeed, defects of JAK3 present an immunologic phenotype indistinguishable from that of SCID-X1 [12]. Moreover, mutations in the IL7R (IL-7 receptor) gene,

which encodes for the α chain of the IL-7R, abrogate T cell development but NK and B cell development remains normal [13]. Defective expression of MHC class II (MHCII) molecules is also reported in patients. The disease is characterized by $CD4^+$ T cell lymphopenia with a severe clinical course [14]. Moreover, hypomorphic mutations in RAG genes, which allow residual T cell development, are typically associated with SCID [2]. Other T cell-immunodeficiencies caused by thymic defects have been described, including DiGeorge syndrome (DGS) and Forkhead box N1 (FOXN1) deficiency [15].

6.1.2.3 PIDs associated to V(D)J recombination process

A variety of genetic mutations associated to PIDs result in defects of the protein machinery required for the variable (V), diversity (D) and joining (J) recombination process, critical for producing the diverse repertoire of the developing T- and B- cells. Defects in V(D)J recombination process account for about 30% of human SCID cases and lead to an early arrest of both T and B cell development. This process is carried out by different molecules, including the recombination activating genes, RAG1 and RAG2. Approximately in 70% of SCID patients, mutations are found in the RAG1 and RAG2 genes [16]. Hypomorphic mutations in RAG genes that support partial recombination activity were identified in infants with Omenn Syndrome (OS), a disease characterized by immune dysregulation and the presence of residual oligoclonal, activated T cells infiltrating multiple organs [17-19].

6.1.2.3.1 V(D)J Recombination Process

To obtain the necessary level of diversity, B and T cell receptors are created by recombination of the pre-existing encoding gene segments. These V(D)J gene segments are found as multiple copies that lie upstream of a constant (C) region; these segments are rearranged to yield a contiguous V(D)J region and assemble a single functional receptor in a process defined V(D)J recombination process. This process takes place in the bone marrow or in the thymus and is crucial for the production of mature B and T cells, respectively. Schematically, the V(D)J recombination process can be divided into three steps (**Figure 1**). In the first phase, two recombination activating proteins RAG1 and RAG2 recognize and bind to recombination signal sequences (RSSs) that flank all V and J segments and introduce a double strand-break at the border of RSS. On the

chromosome, coding ends are left as hairpin-sealed structures, whereas signal ends, which are excised from the chromosome, are blunt and 5' phosphorylated. The second steps are taken care by the DNA-repair machinery of the non-homologous end-joining (NHEJ) apparatus. The double strand-break is first recognized by the DNA-dependent protein kinase (DNA-PK) complex formed by the Ku70-Ku80 heterodimer, which binds to DNA ends, and the DNA-PK catalytic subunit (DNA-PKcs). Before re-ligation, the hairpins at the coding ends are first opened, presumably by the Artemis-DNA-PKcs complex. During the third step of the V(D)J recombination, the lymphoid-specific terminal deoxynucleotidyl transferase (TDT) enzyme further increases joining diversity by adding non-templated nucleotides to processed coding ends. Finally, the XRCCA/DNA ligase IV/Cernunnos complex catalyses the ligation step.

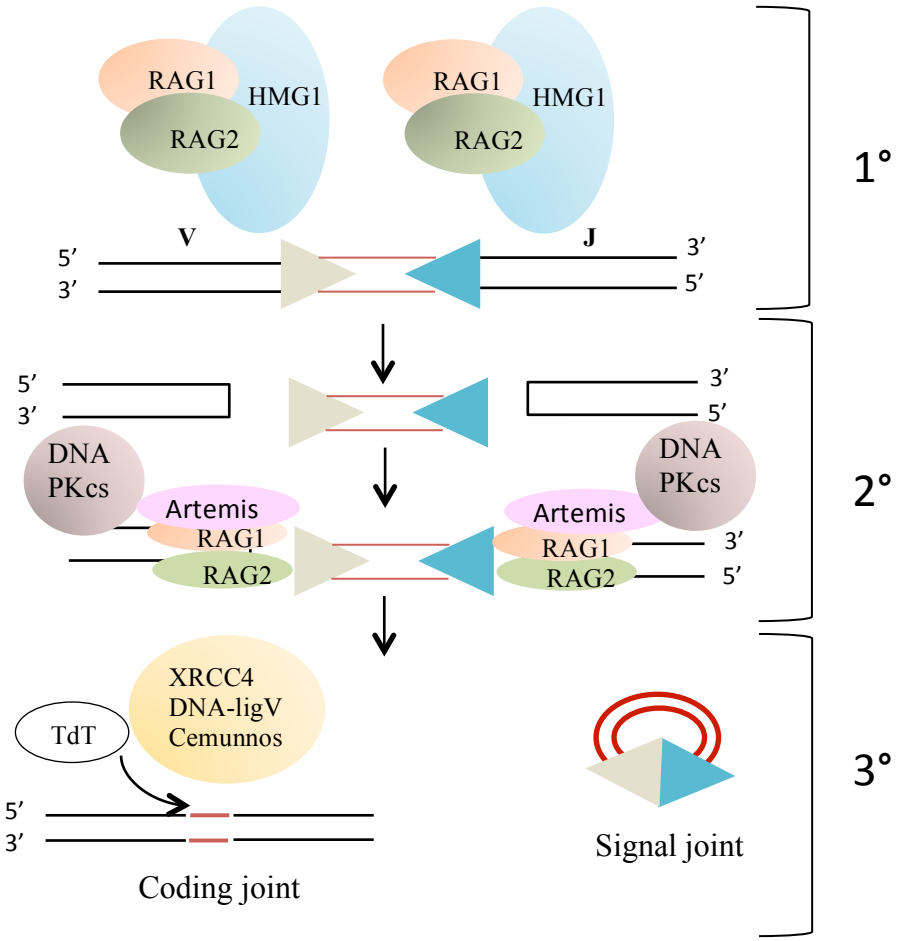

Figure 1: The V(D)J recombination process. *It can be divided into three steps: (A) The RAG1/2 genes recognize the RSS and introduce a double strand break. (B) Artemis, which is recruited and phosphorylated by Ku/DNA-PK complex, opens the hairpins through its endonuclease activity. (C) The XRCC4/DNA ligase IV/Cernunnos complex seals coding and signal joins (Adapted from [20]).*

6.1.2.4 Defects in V(D)J components other than RAG

Mutations in other V(D)J recombination components have been reported in patients, including Artemis, DNA ligase IV and DNA PKcs genes. Affected patients show increased sensitivity to ionizing radiation. The Artemis protein, in complex with DNA-PKcs, performs the crucial NHEJ function of opening the DNA hairpins created by the RAG complex, and then acts to nucleotycally trim the ends to variable extents. Mutations in the Artemis gene represent the most common cause of radiosensitive SCID [21]. DNA-ligase IV is an enzyme in the final DNA re-joining step of NHEJ. Studies showed the embryonic lethality of mice that are deficient in DNA ligase IV and

XRCC4, underlying the crucial role of these factors for viability [22]. DNA-PKcs is the partner of Artemis in DNA hairpin-opening complex. *Van der Burg et al.* described the first human case of DNA-PKcs, showing that residual DNA-PKcs activity is indispensable in humans [23].

6.2 The Omenn Syndrome

Omenn syndrome is an autosomal recessive disease associated to early onset erythroderma, lymphadenopathy, eosinophilia and severe immunodeficiency. Affected patients display a unique combination of clinical and laboratory findings typical of severe immunodeficiency and autoimmune conditions [19]. The association between immunodeficiency and autoimmunity may represent a paradox in OS pathogenesis. The genetic defects that affect T and B development compromise not just the ability to generate a diversified repertoire capable to recognise foreign antigens, but also impinge on central and peripheral tolerance, thus favouring autoimmune manifestations [24].

6.2.1 Molecular bases

The vast majority of OS cases relies on hypomorphic mutations in RAG1 and RAG2 genes, which impair but not abolish the V(D)J recombination process. The biochemical studies of RAG1 and RAG2 mutants revealed the fundamental role of the different RAG gene domains, essential for the catalytic activities of the proteins [25]. Frequently, RAG1 mutations map to domains involved in the recognition of DNA binding and in particular, regions that recognize and bind the RSS flanking the T and B cell receptor gene sequences [26]. Other mutations map to domains involved in the recruitment of the RAG2 protein, leading to a stable complex for DNA bending and cleavage. In addition, the majority of the mutations found in OS cause changes in amino acids, impairing the activity of RAG proteins. Deletions at the N-terminus of RAG1 have been also described. OS was also identified in patients with mutations in *DCLRE1C* gene, encoding for Artemis, which mediates hairpin coding end opening during the V(D)J recombination process [27]. In addition, mutations in RMRP gene (RNA component of mitochondrial RNA-processing endoribonuclease) have been discovered as a possible cause of OS [28]. Furthermore, homozygosity for a missense (C118Y) mutation in the IL7R gene, encoding the α chain of the IL7R and essential for T cell development, has been found as a rare cause of OS, with a normal number of circulating B cells [29]. Recently, patients with OS associated to ADA deficiency have been described [30]. Interestingly, patients with DiGeorge syndrome [31] or leaky SCID with hypomorphic mutations in the IL-2R γ [32], IL-7R α [29], chromodomain helicase DNA binding protein 7 (CHD7) [33] or DNA ligase 4 [34] presented with OS. Based on these

observations, OS is not characterized by a specific genetic defect, but it could be defined as a combination of aberrant inflammatory conditions and multiple genetic defects that abrogate, but not abolish, T-cell development in the thymus.

6.2.2 Clinical presentation

A peculiar clinical spectrum characterizes OS, which was first described in 1965 (**Table 1**) [35]. OS has been defined as a SCID with erythroderma, hepatosplenomegaly, failure to thrive, susceptibility to infections, chronic diarrhoea, and a fatal outcome unless treated with hematopoietic stem cell transplantation (HSCT). Several cases of pneumonitis were also reported in OS, generally caused by *Pneumocystis jiroveci* or virus such as cytomegalovirus or parainfluenza [19]. Besides erythroderma, other skin manifestations are described in OS patients: psoriasis and alopecia are common features, while vitiligo has been recently reported as a unique clinical sign in the absence of over immunological defects [36]. Rash may be present at birth or evolve over the first few weeks of life. Furthermore, a significant protein loss thought the skin and the gut is reported in OS patients, leading to generalized edema and metabolic disorders. Interestingly, OS disease has been also recently associated with a novel phenotype characterized by granuloma formation, Epstein Barr virus (EBV)-related lymphoma and survival into late childhood [37]. Importantly, symptoms of OS patients can evolve with time and may not appear simultaneously. Moreover, several patients present some but not all signs consistent with the disease and are commonly known as affected by atypical form of OS [25]

Classical SCID	**Omenn Syndrome (OS)**
Present in infancy	Present in infancy
Persistent viral respiratory +/- gastrointestinal infections	Erythroderma
Pneumocystis jiroveci pneumonitis	Alopecia
Disseminated BCG infection	Hepatosplenomegaly
Failure to thrive	Massive lymphadenopathy
Superficial candidiasis	Inflammatory pneumonitis/enteritis
Maternofetal GVHD	Hyper-IgE
Absent lymphoid tissue	Eosinophilia
Absent immunoglobulins	Lymphocytosis
Absent T cells	

Table 1: Main features of classical SCID and Omenn Syndrome *(Adapted from [38]).*

6.2.3 Immunological Features

Hypomorphic mutations in RAG genes allow the development of a normal or elevated number of T lymphocytes with limited repertoire diversity. These T cells are highly activated, oligoclonally expanded and commonly present a Th2 phenotype [25]. Such T cells infiltrate several organs, including skin, gut, spleen and liver, resulting in profound tissue damage [39]. Abnormalities of thymic architecture, with a loss a cortico-medullary demarcation and absence of Hassall bodies were reported in OS patients. In addition, the lack of *Aire* (AutoImmune REgulator) expression and of *Aire*-dependent tissue restricted antigens (TRAs) is severely reduced [40]. Moreover, T regulatory (Treg) impairment has been demonstrated in the thymus of patients [41]. In addition, reduced suppressive activity and abnormal phenotype ($CCR7^{-}CD45RA^{-}$) characterizes the Treg population in OS [42]. All these findings suggest an impairment of both central and peripheral tolerance that actively contributes to autoimmunity, typical of OS [42, 43].

In contrast to T cells, circulating B cells are typically reduced or absent, but plasma cells ($Blimp1^{+}CD138^{+}$) can be detected in lymphoid organs and are responsible for the low levels of immunoglobulin, with the exception of IgE, which are often increased [44, 45]. Remarkably, a broad range of autoantibodies has been detected in patients [46], indicating that B cell tolerance is also disrupted in OS. Increased levels of serum BAFF, found in RAG deficient patients and reflecting B cell lymphopenia and inflammation [44], are likely responsible for the survival of autoreactive B cells. Interestingly, activated T cells and ectopic distribution of Langerhans cells characterized the OS biopsies [47]. Finally, defects of invariant natural killer T cells (iNKT) contribute to the immune dysregulation in OS [48].

6.2.4 Treatment and management

If untreated, patients with OS have a fatal prognosis. In particular, skin inflammation worsens over time, leading to higher susceptibility to bacterial and fungal infections. The treatment with drugs including prednisone and cyclosporin A proved effective in

suppressing the expansion of T cell clones and organs infiltration [49]. However, in absence of HSCT, OS remains a fatal disease due to current infections and high mortality early in life. Transplantation of HSC represents instead a permanent cure [50]. Satisfactory results were obtained mostly with HSCT from human leucocyte antigen (HLA)-match family donors. In this case, pharmacological suppression of abnormal and activated autologous T cell clones seems to facilitate the engraftment of bone marrow cells. In contrast, lower survival rate was observed with HSCT from mismatched family donors or matched unrelated donors (MUD). However, the use of myeloablative regimens with busulfan and cyclophosphamide has dramatically improved the outcome of patients treated with HSCT from matched unrelated donors (>80% survival rate) [51].

Overall these data suggested the necessity to develop an alternative form of treatment for patients with RAG deficiency lacking HLA-matched donors.

Gene therapy (GT) approach was successfully used to treat X-linked SCID [52] and ADA deficiency (**Figure 2**) [53, 54]. In both cases, a strong selective advantage for gene corrected-cells has been found in T cell lineage. Importantly, a study described the transplantation of *Rag1*$^{-/-}$ bone barrow progenitor cells transduced with a Moloney murine leukaemia virus carrying the human RAG1 transgene in recipient *Rag1*$^{-/-}$ mice. By this approach, GT-treated mice had lower-than-normal B cells [55]. This indicated that gene-corrected lymphoid progenitors have only a small selective advantage in the thymus and in the bone marrow of *Rag1*$^{-/-}$ mice. Remarkably, relatively inefficient expression of the gene was detected. To overcome this problem, self-inactivating lentiviral vectors expressing codon-optimized human RAG1 under the control of several regulatory elements have been developed. By this approach, partial reconstitution of T cell immunity and antibody response was reported although the number of B cells remained suboptimal [56]. By contrast, another study reported a modest reconstitution of both T and B cells using the same vectors. However, about 50% of GT-treated mice developed an OS phenotype [57].

Promising preclinical studies were obtained with GT for RAG2 deficiency [57]. Significant improvement of peripheral T and B immunity, even at a relatively low copy number, was obtained using the vectors expressing codon-optimized human RAG2 and containing other modifications to reduce the risk of silencing of the RAG2 transgene.

These data offer hope for the development of GT approach to cure human RAG2 deficiency. Whether this approach could be useful for treating hypomorphic mutations, where competition between endogenous cells and gene-transduced cells might affect the immune reconstitution, remains to be demonstrated.

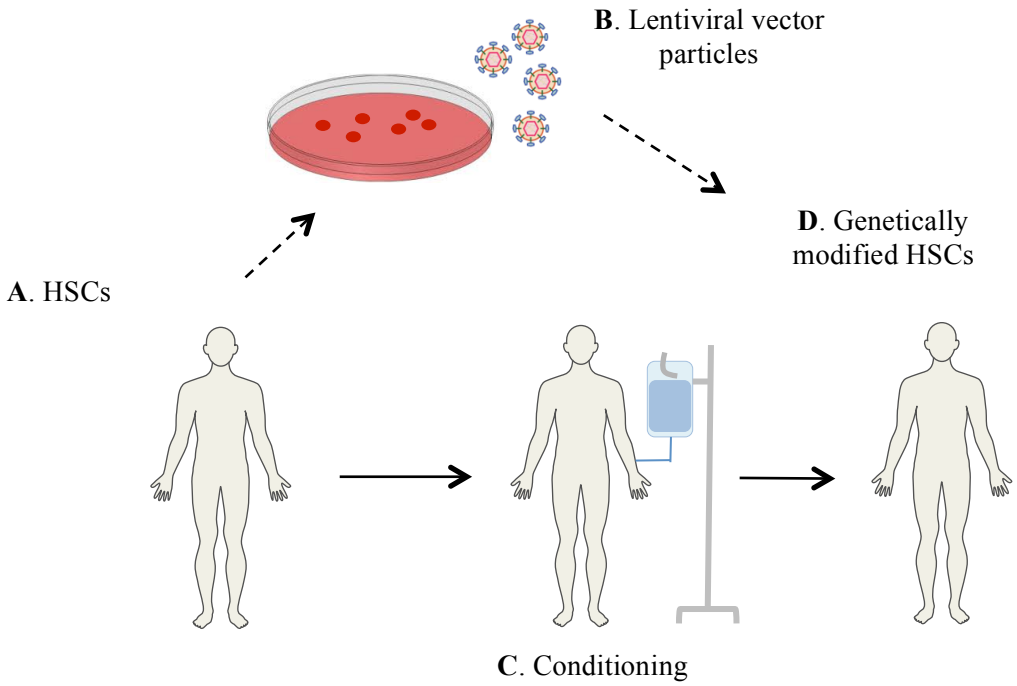

Figure 2: GT procedure. *(A) HSC were collected from bone marrow of a patients. (B) Lentiviral-vector particles containing a functional gene were introduced in HSC. (C) To eradicate the patient's remaining HSCs and make room for the genetically modified cells, the patient underwent chemotherapy. (D) The genetically modified HSCs were then transplanted into the patient (Adapted from [58]).*

6.2.5 Diagnosis

For patients with SCID without detectable enzyme deficiencies, prenatal diagnosis has been possible through the evaluation of lymphocyte populations and phytohemagglutinin (PHA)-induced lymphocyte proliferation in fetal cord blood samples [59]. However, cordocentesis can only be performed relatively late in pregnancy, between 18 and 20 weeks of gestation with abortion risk [60]. Furthermore, prenatal diagnosis of OS based on fetal blood samples leads to diagnostic errors due to the variable numbers of circulating T cells exhibiting residual *in vitro* proliferation in response to PHA. Currently, a safer and more accurate diagnosis for SCID and OS cases is obtained through genome sequencing of the complete coding regions of both RAG1

and RAG2 from the proband and the parents [61]. From 2010 onward, next generation sequencing (NSG) approach is being increasingly used in the PID field [62]. Specifically, NSG approach is a sequencing method in which hundreds of millions of small DNA fragments are sequenced in parallel. Indeed, NSG can be used to sequence entire genome (whole genome sequencing, WSG) or targeted panel of genes, ranging from a small number of genes to the whole exome (WES). In the PIDs field, NSG is being increasingly used for the molecular diagnosis of PIDs and for the discovery of novel disease-causing genes [63].

6.3 The mouse models of Omenn Syndrome

6.3.1 The Rag1(R972Q) mice

Animal models that recapitulate key features of human OS have been described [64-66]. In particular, *Khiong et al.* developed the memory mutant mice (MM), so called for the unusual high percentage of memory phenotype T cells [64]. The MM phenotype was caused by a spontaneous point mutation in RAG1 gene (R972Q), which affects the V(D)J recombination process. The MM mice present several immunological features in common with OS patients, such as skin redness, hepatosplenomegaly, eosinophilia and increased IgE levels. In particular, spleen, lymph nodes and the thymus were characterized by low cellularity and abnormal morphology. Analysis of T cell development in the thymus revealed a partial block at the double negative 3 (DN3) stage ($CD4^-$ $CD8^-$ $CD44^-$ $CD25^+$). In addition, $CD4^+$ $CD8^+$ double positive (DP) cells were decreased as number. Similar to human disease, T cells presented an oligoclonal T cell receptor (TCR). Moreover, MM mice developed a distinctive B cell defect. In bone marrow, MM mice showed a partial block in B cell development at the pro-B cell stage and in the spleen mainly at pre-B stage. Interestingly, mutant mice developed increased IgM, IgG2a and IgG2b levels. In contrast to OS features, T cell infiltration was not reported in tissues as well as autoimmune manifestations, such as erythroderma or colitis.

6.3.2 The Rag1 (S723C) mice

Another mouse model was generated by *Giblin et al*, carrying a homozygous mutation in the RAG1 gene (S723C) [66].

In particular, the $Rag1^{S723C/S723C}$ mutation reduced the V(D)J recombination process and determine impaired T cell development. Activated-oligoclonal T cells, reduced circulating B cells but significant levels of immunoglobulin were reported in the mutant mice. However, only a minority of mice presents signs of autoimmunity, including tissue infiltration and autoantibodies.

6.3.3 The Rag2(R229Q) mice

Our group developed an engineered mouse model, introducing a hypomorphic mutation in the RAG2 core domain-coding region by homologous recombination (**Figure 3**). The *Rag2*$^{R229Q/R229Q}$ mice recapitulate most of the clinical and immunological features of human pathology [44, 47, 65, 67].

At 3 months of age, the *Rag2*$^{R229Q/R229Q}$ mice started to develop several skin manifestations, including erythroderma and alopecia, wasting syndrome and colitis. Oligoclonal self-reactive T cells infiltrate target organs such as skin, liver, lung, kidney and gut. Immune dysregulation was described in the thymus of *Rag2*$^{R229Q/R229Q}$ mice. Indeed, marked thymic abnormalities, with lack of corticomedullary demarcation (CMD) and impaired maturation of thymic epithelial cells (TECs) were described. In addition, the mutant thymus showed severe depletion of Ulex Europeus Agglutinin-1 (UEA-1) positive medullary thymic epithelial cells (mTECs), homogeneously distributed in normal thymus.

Rag2$^{R229Q/R229Q}$ mice also show impairment of central and peripheral tolerance. In particular, reduced *Aire* expression was observed in the thymus, as reported in the OS patients. In addition, strong reduction in the frequency and the absolute number of Treg subset was found in hematopoietic organs.

Furthermore, analysis of T cell development in the thymus showed an arrest at the DN3 stage ($CD44^{-}CD25^{+}$) with absence of DP cells and reduced number of single positive (SP) cells. The few SP cells generated expressed TCRα/β at the cell surface and were exported to the periphery, where they infiltrated target organs.

B cell differentiation was also affected in *Rag2*$^{R229Q/R229Q}$ mice, with a predominant block at the pre-B cell stage in the bone marrow. This resulted in a prominent reduction of circulating B cells and a marked hypogammaglobulinemia, despite elevated IgE serum levels. A larger expansion of the immunoglobulin secreting cell population could be detected mainly within the secondary lymphoid organs, and associated with upregulation of the B lymphocyte-induced maturation protein 1 (Blimp1), and consequent transcriptional repression of B cell lymphoma 6 protein (Bcl-6) and c-Myc. Furthermore, BAFF abundance was found in the serum of mutant mice. In the liver, complete absence of iNKT cells was observed, as described in OS patients [48]. Interestingly, skin infiltrate showed activated oligoclonal T cells and ectopic

distribution of Langerhans cells (LCs), similarity to the human disease. The abundant presence of LCs in the dermis, instead of the normal distribution in the epidermis, could potentially contribute to the initiation of the skin manifestations in OS [47].

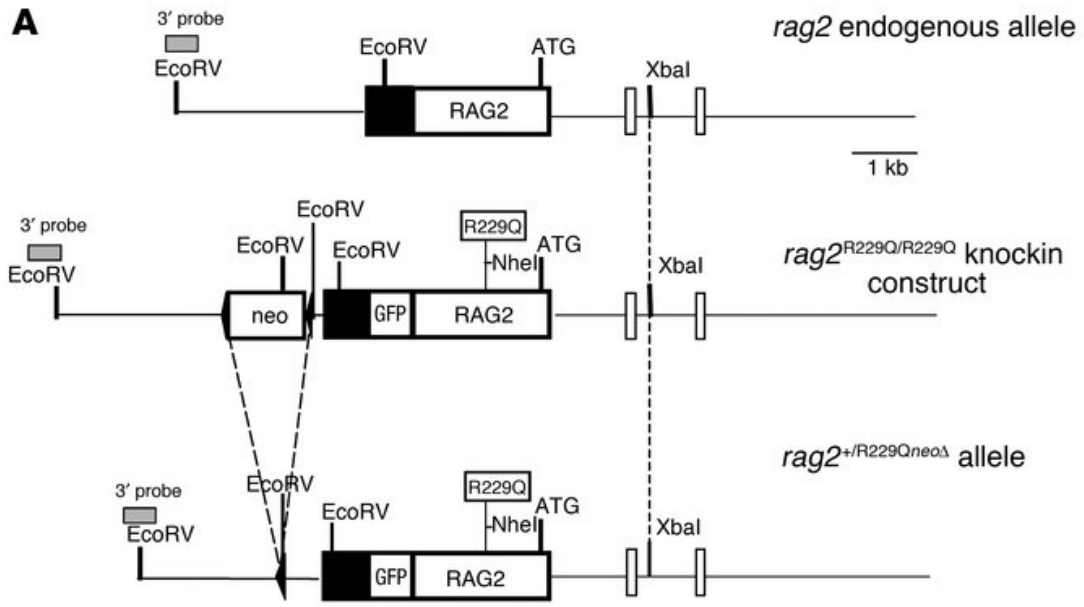

Figure 3: Scheme of the Rag2GFP targeting vector used for the generation of Rag2$^{R229Q/R229Q}$ mice. *Specifically, a targeting vector was designed to replace endogenous Rag2 with the gene carrying the R229Q substitution and an NheI restriction site. GFP was fused in frame with the Rag2 neo cassette flanked by loxP sites (arrows) (Adapted from [65]).*

6.4 The gastrointestinal (GI) tract

6.4.1 Intestinal manifestations in PIDs

Patients with PIDs can present IBD-like gastrointestinal pathology, manifesting in the 25% of cases during the childhood. In several PIDs, intestinal manifestations due to immune dysregulation are the initial or the leading symptom and may manifest before other characteristics of PIDs. In other cases, gastrointestinal pathology is the result of an increased susceptibility to infections.

Intestinal granulomas are detected in nearly 50% of CGD patients and up to 17% of these patients develop colitis [68]. Moreover, patients with mutation in IL-10 receptor and IL-10 genes can develop early onset enterocolitis [69]. Gastrointestinal disease can also be present in other PIDs, including Whiskott-Aldrich syndrome (WAS), immunodysregulation, polyendocrinopathy and enteropathy, X linked (IPEX) syndrome and NF-kB essential modulator defects. Intestinal disorders affect also SCID patients. Severe diarrhea and malabsorption early in life are found in these patients. Frequent cytomegalovirus, rotavirus and adenovirus infections have been reported. Moreover, patients with SCID who receive blood transfusions and allogenic HSCT are susceptible to graft-versus-host disease (GVHD), a severe condition affecting both small and large intestine [70]. Patients with OS developed severe IBD-like immunopathology [71]. CVID is also associated with intestinal inflammation, favored by the dysregulation of the T-cell mediated cytokine production [72]. IBD-like phenotype was also observed in patients with hyper-IgM and in patients with agammaglobulinemia [73].

Genomics studies have recently provided important insights into the pathogenesis of PIDs and inflammatory bowel disease. In particular, genome-wide association studies (GWAS) revealed that known IBD risk loci are particularly enriched for genes involved in PIDs, including those linked to reduced levels of circulating T cells (ADA, CD40, TAP1, TAP2, NBS1, BLM, DNMT3B), and to T-helper cells responsible for producing IL-17, memory (STAT3, SP110), and regulatory T cells (STAT5B).

6.4.2 Anatomy and physiology of GI tract

The gastrointestinal tract (GI) hosts the largest compartment of the immune system. It is continually exposed to a wide range of antigens and potential immune stimuli derived from the diet and the commensal bacteria. The GI tract is a large and muscular tube, which extends from the mouth to the anus. It consists of the esophagus, stomach and intestines, divided in small and large (**Figure 4**).

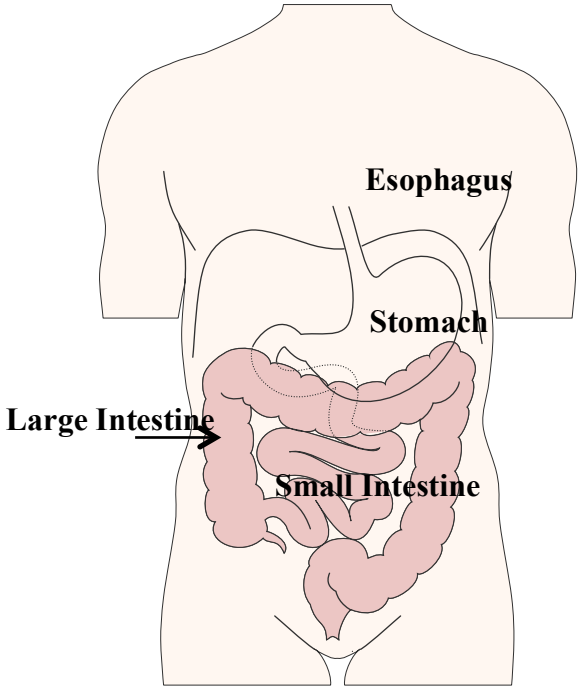

Figure 4: Anatomy of the human GI tract.

The small and the large intestines form a continuous tube that is lined internally by a single layer of columnar epithelium and extends from the stomach to the anus. The small intestine (SI) begins at the pylorus and ends at the ileocaecal valve, which is the entry point into the large intestine. Three segments compose the small intestine: the duodenum, the jejunum and the ileum. As to the large intestine, it begins at the caecum, followed by the ascending, the transverse, the descending colon and the rectum, terminating at the anus. Differences in size characterize the small and large intestines; the small intestine consists of multiple coins amounting to 6-7 meters in length; the colon is wider in diameter and shorter (1.5 meters). The small intestine is characterized

by finger-like projections know as villi, which extend into the lumen (**Figure 5**). In contrast, villi are not present in the caecum and in the colon [74]. The main role of small intestine consists in the nutrient uptake from the intestinal lumen and the distribution in the blood circulation. On the contrary, the reabsorption of water and the elimination of undigested foodstuffs represent the main functions of large intestine. Interspersed throughout the intestine are gut-associated lymphoid tissues (GALT), including Peyer's patches (PPs) in the small intestine and isolated lymphoid follicles (ILFs) in the colon.

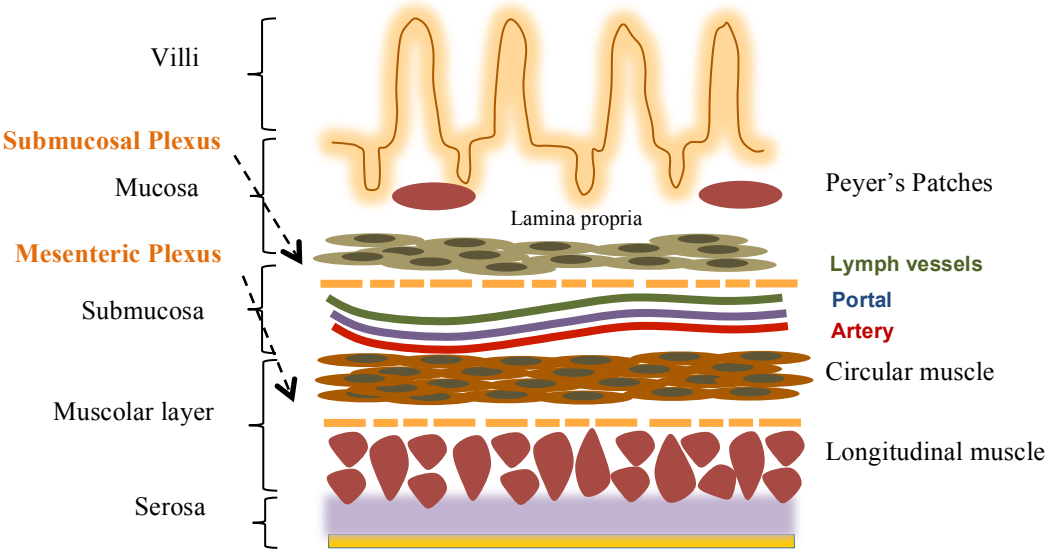

Figure 5: Anatomy of the human small intestine. *The GI tract is throughout divided into four layers: the mucosa (epithelium, LP, muscularis mucosae), submucosa, muscular layer and the serosa.*

6.4.3 Intestinal microbiota

The microbiota that colonizes the intestine contains about 10^{14} microorganisms. The number of bacteria increases going down the intestine, ranging from 10^{5} per ml in the upper small intestine and up to 10^{12} in the large intestine (**Figure 6**). Approximately 500-1000 species belong to the major phyla. The relative number of these varies among individuals but the Firmicutes, Bacteroidetes, Proteobacteria and Actinobacteria are the most prevalent taxa. Members of Archaea kingdom are also present [74].

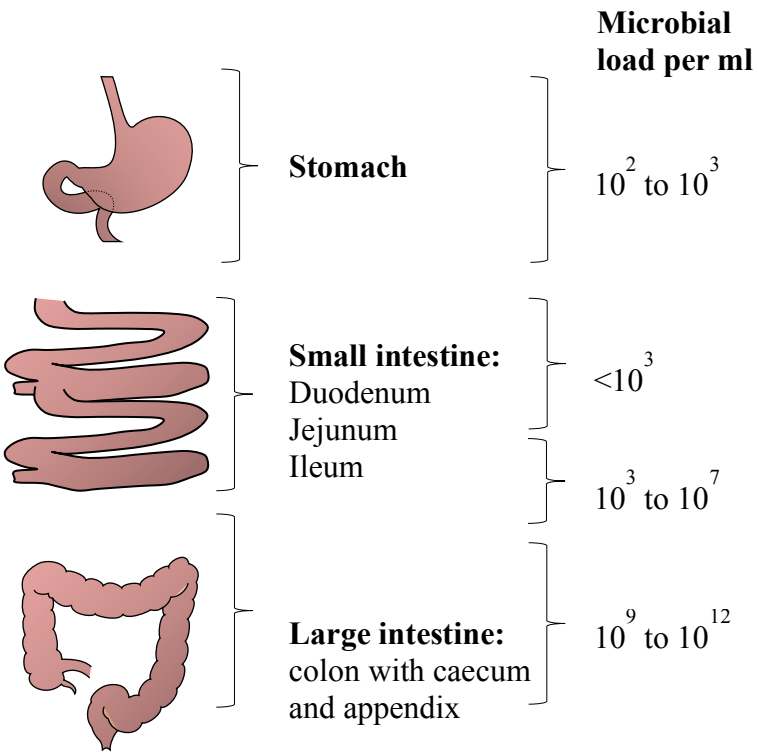

Figure 6: Anatomy of the GI tract and distribution of commensal microbes along the length of the intestine *(Adapted from [74]).*

6.4.4 Intestinal innate immune defenses: physical and chemical barrier

In the GI tract, highly specialized defense barriers have evolved to confine the microbiota and to resist to invading harmful organisms. To this aim, intestinal epithelial cells (IECs) generate various types of barriers: physical and chemical barriers (**Figure 7**). Physical barrier includes the mucus layer covering the intestinal mucosa, the glycocalyx on the microvilli of absorptive IECs, and the cell junctions firmly linking IECs. The mucus is a viscous fluid secreted by goblet cells that is enriched in mucin glycoproteins. The number of goblet cells in the large intestine is much higher compared to small intestine. In fact, the mucus is very thick in the large intestine. Two layers compose the mucus: the inner, firm mucus layer and the outer, loose mucus layer. Both mucus layers are organized by gel forming mucin-2 (MUC2), which is highly O-glycosylated protein produced by goblet cells. The inner mucus layer is a stratified mucus layer anchored to the intestinal epithelia and does not allow bacteria to invade the epithelium. On the contrary, the outer mucus layer is inhabited by a large amount of intestinal bacteria. Moreover, various antimicrobial molecules, including the defensin

family of proteins, secreted by IECs, and the immunoglobulin A (IgA), are involved in the protection against bacterial invasion of the mucus inner layer. The glycocalyx, a meshwork of carbohydrate moieties of glycolipids and glycoproteins, protect the intestinal mucosa from invading bacteria. In addition, cell junctions, such as tight and adhesion junctions linking epithelial cells hamper the microbial invasion through the paracellular pathways [75]. Chemical barriers, including antimicrobial peptides (AMPs) and the regenerating islet-derived 3 (Reg3) family of proteins produced by IECs, have a crucial role in the segregation of intestinal bacteria and epithelial cells [76]. AMPs include the defensin family (α-, β- and θ-defensins) and the cathelicidins, both of which interact with the negatively charged microbial cell membrane and cause membrane disruption by forming pore-like structures [77]. The Reg3 family of proteins includes many antimicrobial proteins mainly produced by Paneth cells. In particular, Reg3γ is active against Gram-positive bacteria and has a critical role in the spatial separation of the intestinal bacteria and the epithelium of the small intestine [76].

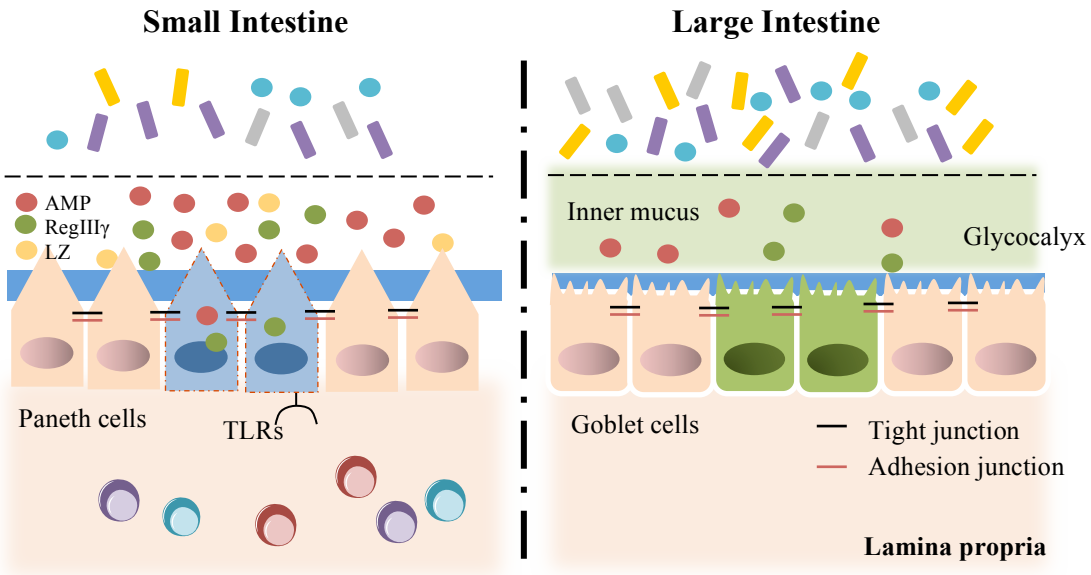

Figure 7: Physical and chemical barrier in the intestine. *In the small intestine, chemical barriers, including AMPs and Reg3γ, have an important role in the segregation between intestinal microbiota and IECs. In the large intestine, the inner mucus promotes the segregation between microbiota-IECs. Tight and adhesion junctions limit the microbial penetration (Adapted from [75]).*

6.4.4.1 Intestinal epithelial cell functions

IECs express pattern recognition receptors (PRRs) and act as sensors of the microbial environment. Members of the TLR, NOD-like receptor (NLR) and retinoic acid inducible gene-1 (RIG-1)-like receptor (RLR) families provide distinct pathways for the recognition of microbial ligands at the intestinal level. Moreover, another function of IECs regards the transport of secretory immunoglobulins across the epithelial barrier. In particular, dimeric IgA complexes, produced by plasma cells in the lamina propria (LP), are bound by the polymeric immunoglobulin receptor (pIgR) on the basolateral membrane of IECs and are actively transcytosed into the intestinal lumen [78]. In addition, specialized IECs called microfold cells (M cells), mediate the sampling of luminal antigens and intact microorganisms for presentation to the mucosal immune system [79].

6.4.5 Intestinal immune cells

The LP and epithelium represent the effect sites of the mucosal immune system. Indeed, LP contains B cells, T cells and other populations, including dendritic cells (DCs), macrophages, eosinophils and mast cells, whereas the epithelium contains mainly T cells.

6.4.5.1 Dendritic cells

DCs are positioned within the LP and in organized lymphoid structures and exhibit a dual role in tolerance and immunity in the gut. In particular, intestinal DCs transport bacterial antigens from the LP into the mesenteric lymph nodes (MLN) and are crucial for inducing oral tolerance to food antigens. Two major $CD11C^+$ $MHCII^+$ DCs subsets have been identified in the intestine: a $CD103^-CD11b^+CXCR1^+$ subset that resides adjacent to the epithelium where they use the trans-epithelial dendrites to acquire luminal antigens, and a $CD103^+CX3CR1^-$ subset that reside within the LP. Intestinal $CD103^+$DCs are migratory and travel to the MLN via the afferent lymph. At steady state, the migration of $CD103^+$DCs from the LP to the MLN establishes T cell responses specific for harmless luminal antigens, representing an important process for oral tolerance. Several DC subsets contribute also to T regulatory generation. In particular, the $CD8a^+$ DC subset, promoting Treg generation in the presence of Transforming Growth Factor (TGF) β, and the $CD103^+$ DCs.

6.4.5.1.1 DCs and gut-homing imprinting on T cells

An important function of DCs is the ability to imprint homing properties on T cells, in order to localize immune responses to a specific tissue. Indeed, T cells activated by intestinal DCs but not from splenic or skin-draining LN, acquire the α4β7 integrin and CCR9 chemokine expression and home to the intestine [80, 81].

In particular, only the CD103-expressing DCs have the capacity to induce gut-homing molecules on T cells, targeting lymphocytes to intestinal tissue (**Figure 8**).

Iwata et al. identified Retinoic Acid (RA), the active metabolite of Vitamin A, as a factor capable of instructing the expression of gut-homing receptors during T cell priming. The ability of intestinal $CD103^+$ DCs to produce RA is conferred by their expression on the RALDH enzymes that oxidize retinal into the active RA. Among the classes of RALDH enzymes, RALDH-2 (encoded by *aldh1a2*) seems to be the most predominant enzyme expressed by $CD103^+$ DC of the intestine, MLN and PP [82]. The distribution of RALDH-positive DCs correlates with the presence of retinol or RA within the body. In agreement, retinol is abundant in the small intestine and the MLN compared to the colon and spleen, corresponding to the high frequency of RALDH-positive DCs in these sites [83].

T cells that migrate to the small intestine LP express the integrin α4β7 [84] and the chemokine receptor CCR9 [85]. The main α4β7 ligand, the mucosal addressin cell adhesion molecule-1 (MAdCAM-1), is expressed on intestinal LP venules and the CCR9 ligand CCL25/TECK is strongly expressed by epithelial cells in the small intestine and in the LP venules. The integrin α4β7 is also critical for T cell migration into the colon, even during inflammation. On the contrary, the colon is devoid of $CCR9^+$ cells, and particularly, its ligand CCL25 is not expressed.

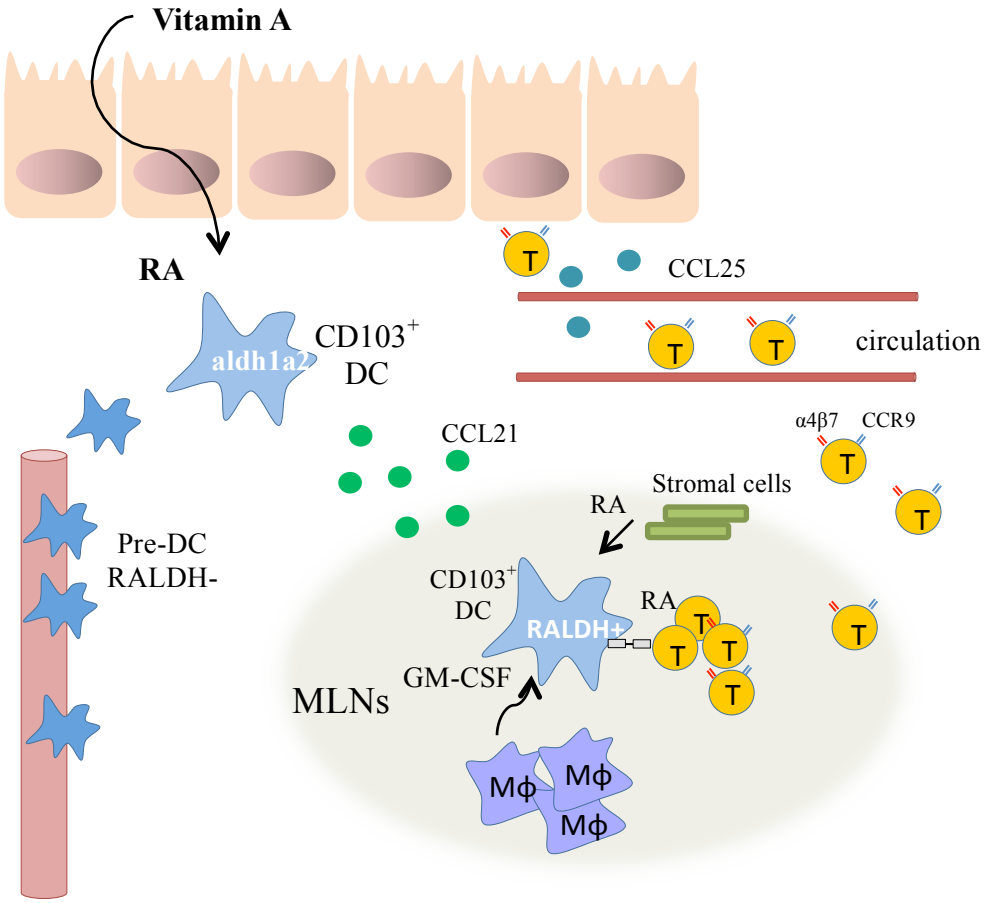

Figure 8: Intestinal DCs imprint gut homing receptors on T cells. *Migratory CD103$^+$ DCs migrate to the MLN and are exposed to stromal derived-RA and macrophage-derived GM-CSF, inducing increased expression of DC RALDH-2. In the MLN, RA produce by CD103$^+$ DCs induce expression of gut homing receptors, directing T cell migration to the small intestine (Adapted from [86]).*

6.4.5.2 Intraepithelial lymphocytes

The intestinal epithelium contains numerous T cells that are located at the basement membrane between enterocytes at a frequency of up to 10-15 intraepithelial lymphocytes (IELs) per 100 epithelial cells. They provide the first line of defense against infections, preserving the barrier integrity.

The majority of IELs express the CD8αα glycoprotein that binds to the MHC class I (MHC-I) molecule. Intestinal IELs can be divided in two subsets based on TCR receptor: αβ TCR or γδ TCR heterodimers. About 50% of IELs express γδ in the small intestine, while 40% are positive in the colon [87]. Interestingly, *Ismail et al.* demonstrated that γδ IELs induce the production of innate antimicrobial peptides via the

Myeloid Differentiation Primary Response Gene 88 (MyD88) pathway in response to harmful pathobionts that penetrate the intestinal epithelium [88].

6.4.5.3 Lamina propria T cells

Both $CD4^+$ T cells and $CD8^+$ T cells are found in the intestines, at the approximate ratio of 2/1. They may derive from conventional T cells that have been primed in secondary lymphoid organs. Indeed, majority of $CD4^+$ and $CD8^+$ T cells display an effector memory phenotype in the intestine. Intestinal $CD4^+$ T cells are mostly located in the LP. Upon stimulation, naïve T cell can differentiate into four major subtypes: T helper 1 (Th1), Th2, Th17 or Treg cells [74]. These various $CD4^+$ T cell subsets are distinguished by the expression of different transcription factors and cytokines. Several studies highlight the important role of gut microbiota in the development of $CD4^+$ T cells, within and outside the intestine. Indeed, reduced number of LP $CD4^+$ T cells was found in GF mice. Moreover, the spleen and the MLNs of GF mice exhibit defects, as lymphocyte zone are absent [89].

6.4.5.3.1 T-helper1 cells

Th1 cells are critically required for appropriate responses to intracellular bacteria and viruses. Th1 cells develop via a molecular pathway involving activation of signal transducer and activator of transcription 1 (STAT1) and STAT4 by IFNγ and IL-12, respectively, which leads to the induction of Tbet, essential transcription factor for the development of Th1 cells. Interferons (IFN) are a large family of proteins, which include: type I IFN (multiple IFN-α and one IFN-β) responsible for antiviral immunity; type II IFN, known as IFNγ, promotes the response to intracellular bacteria; the novel family type III IFN (IFN-λ1, IFN-λ2, IFN-λ3 and IFN-λ4) is induced by viral infection and shows antiviral activity. Several studies demonstrate that exposure to commensal bacteria contributes to drive physiological Th1 development. In agreement, GF mice have reduced number of Th1 cells in both mucosal and systemic compartments. This reduction in Th1 immunity results in augmented susceptibility to infection with different pathogens, such as *Shigella flexneri* and *Listeria monocytogenes* [90]. Moreover, *Bacteriodetes fragilis* was shown to induce the development of a systemic Th1 response through Polysaccharide A (PSA) molecules [89].

6.4.5.3.2 T-helper 17 cells

Th17 cells are crucial for host defense and have a role in the development of autoimmune diseases by producing the proinflammatory cytokines IL-17A, IL-17F and IL-22. The development of Th17 cells in mice requires the combination of signals via the TCR and from TGF-β1, IL-1β, and STAT3 activating cytokine, such as IL-6 and IL-21. Unlike other $CD4^+$ T cell subsets, Th17 preferentially accumulate in the intestine, indicating that the development of Th17 might be regulated by gut-intrinsic mechanisms. Indeed, mice treated with antibiotics and GF mice present reduced intestinal Th17 cells [91]. Studies revealed that a particular species of *Clostridia*-related bacteria, called segmented filamentous bacteria (SFB), promotes the generation of Th17 cells in the small intestine (**Figure 9**) [92]. In particular, SFB drive Th17 accumulation via a serum amyloid A protein-dependent effect, resulting in IL-6 and IL-23 production from DCs. Th17 induction by SFB is not entirely benign, because mono-association of mice with SFB induced Th17-mediated inflammatory arthritis [93] and multiple sclerosis-like symptoms in the experimental autoimmune encephalomyelitis (EAE) [94]. Another mechanism described for the generation of Th17 cells involved the luminal adenosine triphosphate (ATP), which is provided by commensal bacteria [95]. Moreover, the reconstitution of GF mice with the intestinal microbiota of conventional mice promotes the development of intestinal Th17 [96]. All these studies highlight the critical role of components of the microbiota in the generation of Th17 cells.

6.4.5.3.3 T Regulatory cells

T Regulatory Cells (Tregs) accumulate in the intestine and are essential for maintaining the gut homeostasis by preventing inappropriate innate and adaptive immune responses. Regulatory $CD4^+$ T cells include subsets distinguishable on the basis of their expression of the transcription factor Foxp3: $Foxp3^+$(Treg) or $Foxp3^-$ (T regulatory cells 1 (Tr1)). Most $CD4^+Foxp3^+$ Treg cells originate in the thymus under the influence of adequate TCR stimulation. Further development requires signals from the costimulatory molecule CD28 and common γ chain cytokines, including IL-2 and IL-15, to activate STAT5 and induce Foxp3 expression [97]. After exiting the thymus, some Treg cells migrate to the intestine, where they recognize intestinal antigens and prevent inappropriate immune responses. However, the intestine contains a large number of non-thymically derived

Foxp3$^+$ iTreg cells. Indeed, naïve CD4$^+$ T cells can differentiate into induced Foxp3$^+$ Treg (iTreg) cells when activated by transient TCR stimulation or TCR stimulation in the presence of TGF-β and IL-2. IL-10 represents the immunosuppressive cytokine crucial for the regulatory properties of Treg cells. In the colon, Foxp3$^+$Treg cells are the almost exclusive T cell source of IL-10 while in the small intestine, both Foxp3$^+$ Treg and Tr-1 cells produce IL-10. Importantly, Tr1 cells display their suppressive function via the production of IL-10 and TGF-β. Moreover, the maintenance of the Treg population is also different in the large and small intestine. Indeed, Treg cells are maintained in the small intestine of GF mice [98]. On the contrary, the presence of Treg cells in the colon is highly dependent on the presence of the gut microbiota, being significantly reduced in GF conditions and by antibiotic-treatment. Specific populations of commensal bacteria have been found to expand Treg cells in the colon (**Figure 9**). In particular, the Treg accumulation is promoted by the colonization of GF mice by one of these bacterial populations: a mixture of 46 *Clostridium* spp. Cluster IV and XIVa strains [99]; altered Schaedler flora (ASF) consisting in a mixture of eight commensal bacteria [100] and the human commensal bacteria *B. fragilis* [101]. Moreover, several studies highlight the important role of short-chain fatty acids (SCFAs) derived from gut commensals metabolism in inducing Treg differentiation and accumulation. In particular, *Garret et al.* demonstrated that oral administration of SCFAs (including butyrate, acetate and proprionate) in GF mice increases Treg number in the colon, but not in other lymphoid organs [102]. Further studies showed that butyrate could downregulate the production of proinflammatory mediators (including IL-6, nitric oxide (NO) and IL-12) from LP macrophages, via inhibiting histone deacetylases, underlying the importance of butyrate in the maintenance of tolerance to microbiota [103]. Importantly, *Kawamoto et al.* showed that Foxp3 cells contributed to the diversification of the gut microbiota. In particular, Treg cells repress inflammation and support IgA selection in the germinal centers (GCs) of PPs. Indeed, diversified and selective IgAs are crucial for the maintenance of balanced intestinal microbiota [104].

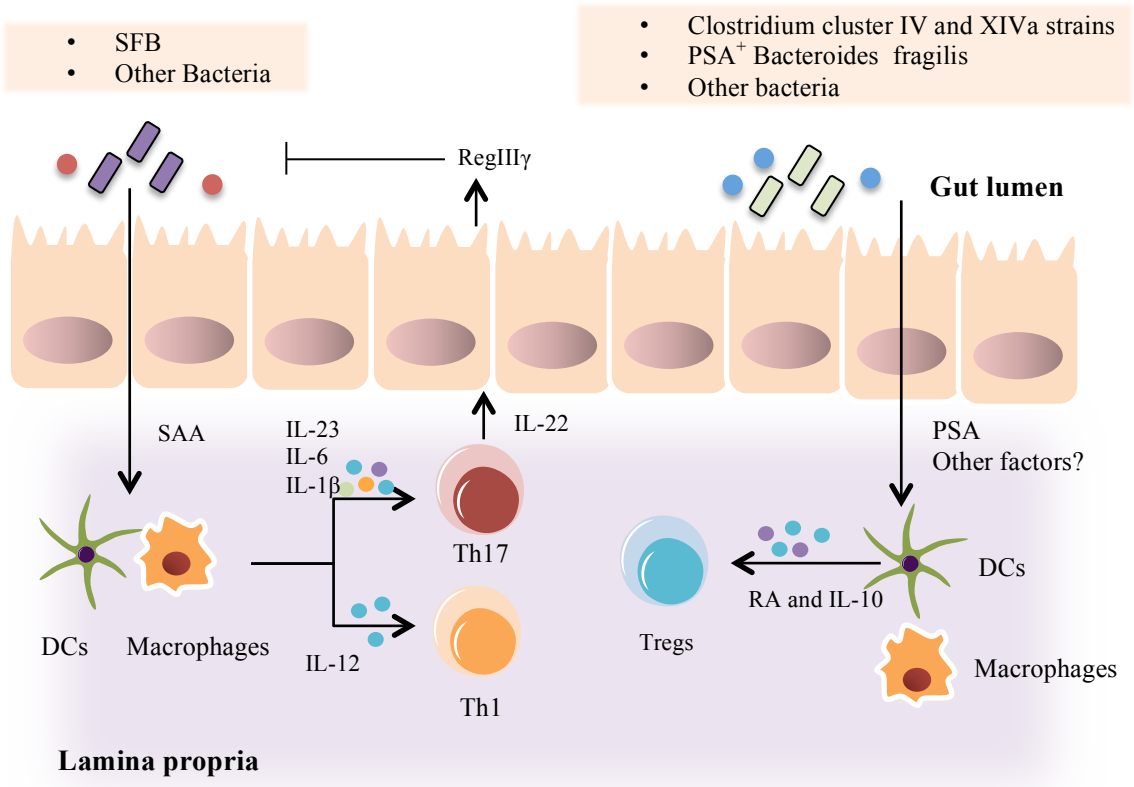

Figure 9: Intestinal microbiota shapes T cell immunity. *SFB and other commensal bacteria activate LP DCs and macrophages to induce Th17 and Th1 cells thought the production of several chemokines (IL-6, IL-1β and IL-23). Clostridium spp. clusters IV and XIVa, PSA+ B. fragilis and other commensal bacteria stimulate the generation of Treg cells (Adapted from [105]).*

6.4.5.4 IgA-producing B cells and plasma cells

IgA is the major class of immunoglobulins produced in mucosal tissue, including the intestine. In the intestinal lumen, IgA is produced as polymeric IgA at high concentrations. Polymeric IgA is transported via pIgR that is expressed on intestinal epithelial cells and is released into the intestinal lumen as secreted IgA (SIgA). Remarkably, SIgA coat commensal bacteria and soluble antigens, inhibiting their binding to the intestinal epithelium and their penetration into the LP, and neutralize toxin and pathogens without causing inflammation due to its ability to inactivate the complement cascade [106]. In addition, SIgA promote the establishment of a mutualistic host-microbe relationship, by downregulation of proinflammatory epitopes by microbes. Moreover, SIgA neutralizes microbial compounds with proinflammatory activity (such as Lipopolysaccharide, LPS) and facilitates the formation of a biofilm that favors the growth of commensals while attenuating that of pathogens. Intestinal plasma

cells that produce IgA can be generated by both T-dependent and T-independent mechanisms (**Figure 10**):

T cell dependent induction of IgA^+ B cells: IgA^+ B cells are mostly generated in the GCs of PPs by activation of B cells and induction AID, a key enzyme required for CSR and SHM. Mechanistically, DCs uptake luminal antigens and migrate to the T cell-zone, where they induce the differentiation of CD4-expressing T cells in T-follicular helper cells (TFH). CD40L and IL-21 by TFH induce the expression of AID in B cells and promote the IgA-CSR. Then, IgA^+ plasmablasts migrate from the PPs to the gut LP where they further differentiate into IgA plasmacells that secrete IgAs [107].

T cell independent induction of IgA^+ B cells: Unlike in PPs, the generation of IgA^+ cells in the LP and in ILFs does not require T cells or the GC formation. Many DCs, possibly CX_3CR1^+ DCs, take up luminal antigens and activate B cells. Several factors released by DC and macrophages facilitate the class switching of B cells to IgA^+ B cells. In particular, Tumor Necrosis Factor (TNF) α induces the expression of metalloproteinases (MMPs), which mediate the conversion of TGF-β1 from inactive to active form. Together with BAFF and a proliferation inducing ligand (APRIL), active TGF-β1 facilitates the CSR to IgA [107].

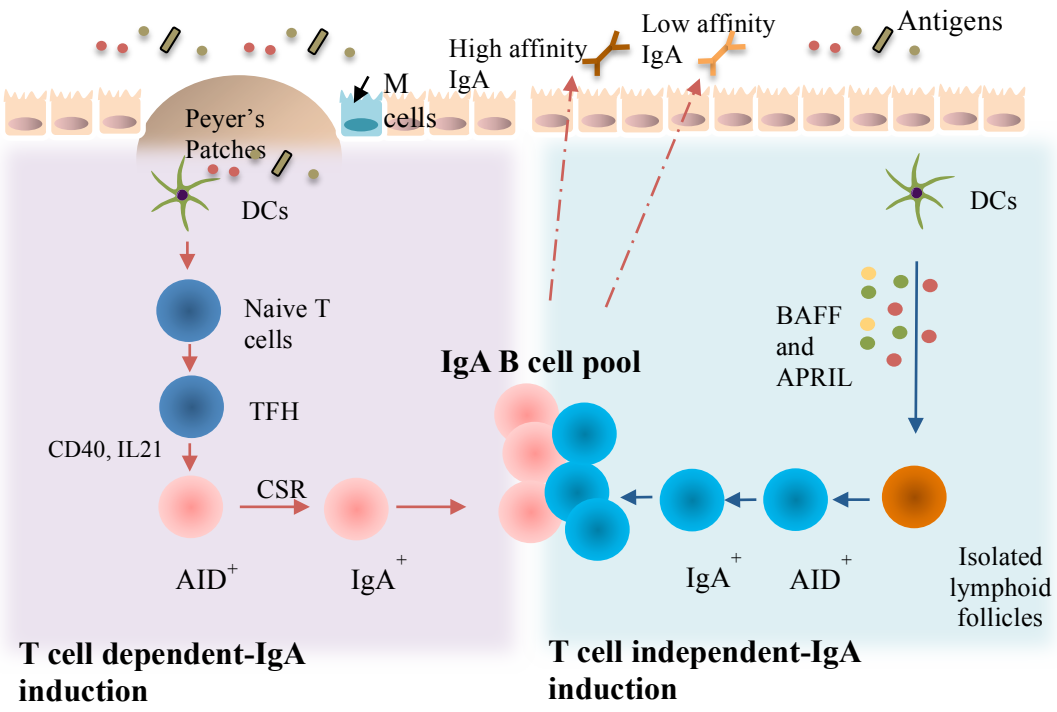

Figure 10: Intestinal plasma cells that produce IgA can be generated by both T-dependent and T-independent mechanism. *(A) In T cell dependent IgA production, DCs induce the differentiation of naïve T cells to TFH. B cells, which are stimulated by activated T cells, express CD40L and several cytokines necessary for the induction of AID and CSR. (B) On the contrary, in T cell independent IgA production, AID is induce by innate mechanisms, including TLR signaling, APRIL and BAFF, which are produced by DCs (Adapted from [108]).*

IgA has been shown to regulate the composition and the function of the gut microbiota. Dysfunction in the IgA compartment as a result of deficiency in AID, leads to alteration in the composition of the intestinal microbiota. The gut microbiota also regulates IgA production, as demonstrated by the reduction of IgA number in GF mice. Moreover, commensal bacteria instruct LP DCs to induce the differentiation of IgA-producing B cells. In particular, bacterial-derived flagellin promotes the synthesis of RA, which is an essential molecule that facilitates the differentiation of IgA-producing B cells by intestinal DCs. In addition, gut microbiota promotes the expression of factors that are involved in the induction of IgA^+ B cells, such as TNF, inducible nitric oxide synthase (iNOS), BAFF and APRIL in LP DCs (**Figure 11**). Moreover, intestinal plasma cells express TNF and iNOS after microbial exposure and promote the IgA secretory function of B cells [109].

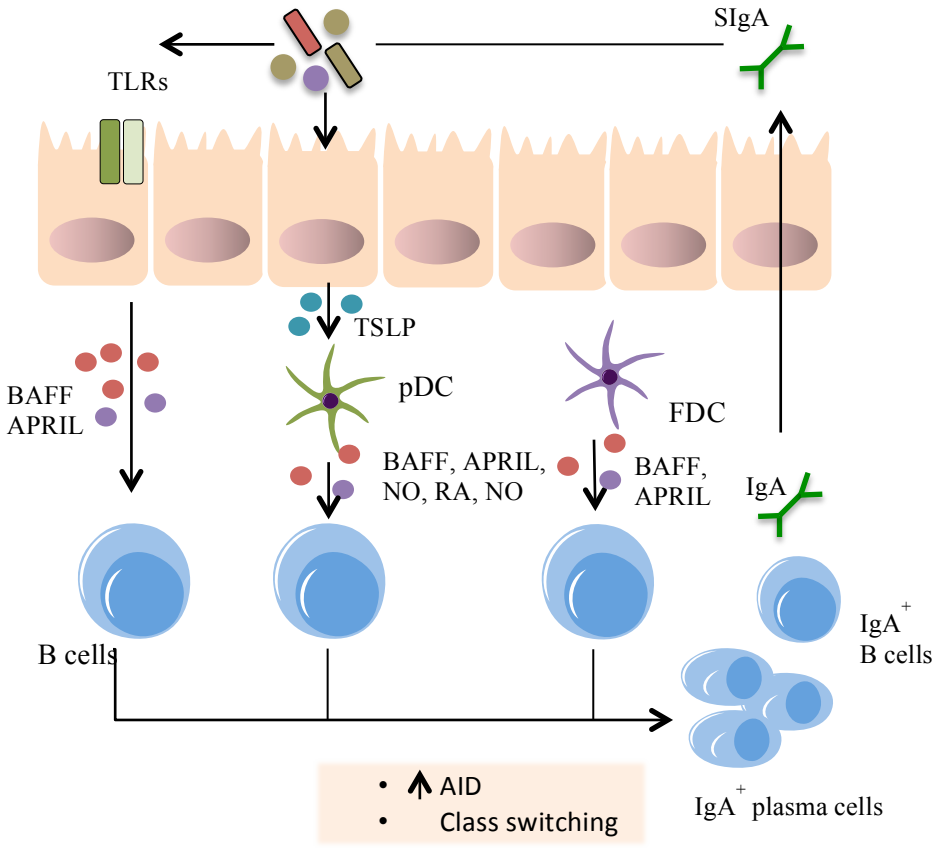

Figure 11: Intestinal microbiota promote the generation of IgA-producing B cells and plasma cells. *TLR activation on IECs induces the production of BAFF and APRIL, promoting the differentiation of IgA-producing plasma cells. IECs also produce thymic stromal lymphopoietin (TSLP) to promote BAFF and APRIL expression by DCs. Various types of DCs secrete BAFF, APRIL, NO, RA and TNF to facilitate the expression of AID and IgA class switching in B cells (Adapted from [105]).*

6.4.6 Role of intestinal microbiota in IBD

In the GI tract, several immunoregulatory mechanisms prevent the unnecessary activation of the immune system against innocuous antigens including those expressed by commensal bacteria. A breakdown of these regulatory mechanisms results in a set of chronic inflammatory conditions, known as Inflammatory Bowel Disease (IBD), encompassing Crohn Disease (CD) and Ulcerative Colitis (UC) (**Figure 12**). A mixture of genetic factors, the host immune system, environmental factors as well as the microbiota contribute to the etiology of the disease. IBD is associated to important changes of the intestinal microbiota; in particular, several studies have shown that both CD and UC are associated to reduced complexity of the gut microbiota and consistent shifts to dysbiotic conditions. Both CD and UC are characterized by an expansion of the phyla *Proteobacteria* and in particular of the *Enterobacteriaceae* family [110]. Moreover, several inflammatory commensals, such as adherent-invasive *Escherichia coli*, *Yersinia* and *Clostridium difficile*, are much more common in patients with CD compared to healthy individuals [111]. Furthermore, several commensal bacteria that are typically found in low abundance, can acquire pathogenic properties. Indeed, *E.coli*, which is innocuous at steady state condition, is able to use inflammatory NO generated by immune responses as an energy source, acquiring a significant growth advantage [112]. Other bacteria, called *Bilophila wadsworthia*, take advantage of dietary induced bile acids to dominate the intestine, contributing to the intestinal disease [113]. Studies revealed also the capacity of the intestinal flora in influencing IBD. In fact, mice deficient in both Tbet and adaptive immunity develop a spontaneous and transferrable form of ulcerative colitis (TRUC mice) [114]. The transfer of the microbiota from TRUC mice to *wild-type* mice recipients also transfers the colitis. In particular, several species of commensal bacteria such as *Proteus mirabilis*, *Klesbiella pneumoniae* or *Helicobacter typhlonius* are increased in the intestine of TRUC mice and can transfer the colitis to *wild-type* mice [115, 116]. Another important factor in the induction of IBD is the loss of symbiotic commensal bacteria that rely upon fermentation as their energy source. Studies revealed that the bacteria of the phylum Firmicutes and in particular the class *Clostridia* are reduced in patients with IBD [110]. In fact, Clostridia are essential bacteria to generate colonic Tregs, that can oppose colitis induction [99]. Moreover, the diet has an important effect on the microbiota composition, leading to the

expansion of pathobionts. For instance, a diet rich in saturated milk fats induces dysbiosis and the expansion of *Bilophila wadsworthia,* promoting Th1 immune response and exacerbating colitis in *Il10*$^{-/-}$ mice but not in *wild-type* mice [113]. Taken together, these observations suggest that the intestinal immune system is shaped by commensal dysbiosis in two different ways. First, by the outgrowth of opportunistic bacteria that drive intestinal inflammation, and second, by the loss of benign fermenting bacteria which produce essential metabolites for immunoregulatory functions.

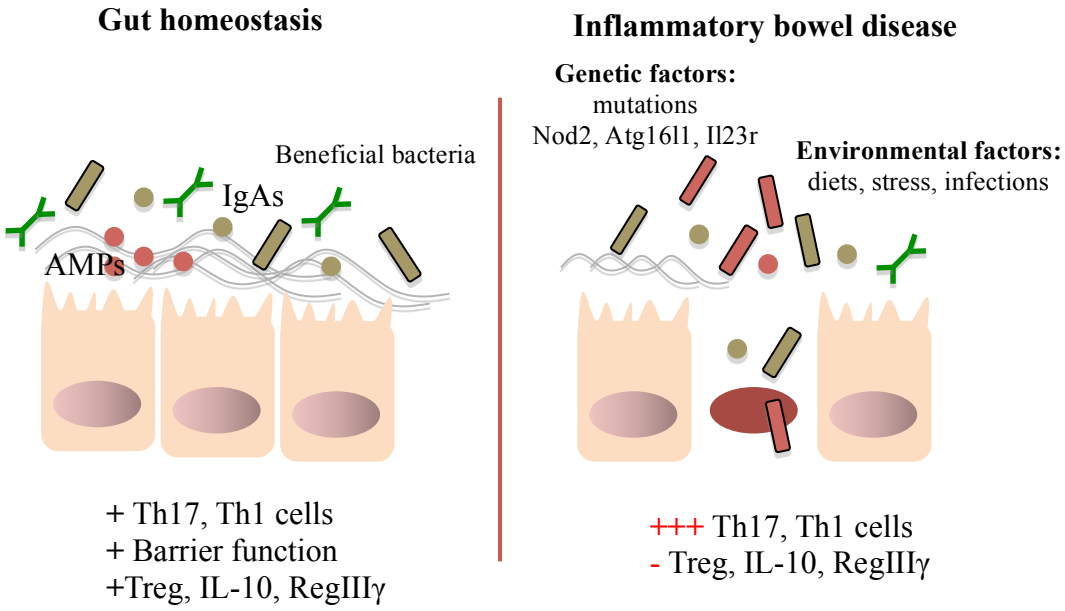

Figure 12: Inflammatory and anti-inflammatory properties of intestinal microbiota in IBD. *Beneficial commensal microbiota protects the intestinal mucosa thought the induction of Treg cells, IL-10 and the antimicrobial peptide Reg3γ. In IBD, a combination of genetic and environmental factors results in a disruption of the microbial community, leading to dysbiosis. This condition causes a loss of beneficial bacteria and/or accumulation of pathogenic bacteria, leading to chronic inflammation mediate by Th1/Th17 cells (Adapted from [105]).*

6.4.7 Microbiota and extra-intestinal diseases

The microbiota may also contribute to autoimmune diseases at extra-intestinal sites (**Figure 13**). Studies in animal models suggested that host immune responses are Th2-biased under GF conditions. In particular, GF mice or antibiotic-treated mice show an expansion of basophils in the peripheral blood and increased serum IgE levels. Cystic fibrosis (CF) is also modulated by gut microbiota. The pathogenesis of Rheumatoid Arthritis (RA) is influenced by the intestinal microbiota. Studies in animal models indicated that gut microbiota contributes to disease symptoms. In fact, arthritis symptoms are reduced in K/BxN transgenic mice in GF condition. Moreover, Th17 cell response are implicated in promoting disease, and SFB-mediated enhancement of the Th17 cell immunity, stimulating autoantibody production by B cells, promote the disease [93]. In addition, analysis of the microbiome in patients suffering RA confirmed a correlation between the disease and the pro-inflammatory members of *Prevotellaceae* family [117]. Furthermore, the impact of the microbiota in inducing Multiple Sclerosis (MS) has been largely investigated. In particular, the incidence of disease in the mouse model of Experimental Autoimmune Encephalitis (EAE) is also dependent on the commensal microbiota. Accordantly, the development of the disease varied among genetically identical mice housed in different animal facilities. Furthermore, studies showed that the activation of myelin-specific B cells and the invasions of the neurons by T cells require intestinal microbiota [118]. By contrast, several commensal bacteria are capable of attenuating inflammation in the central nervous system (CNS). For example, PSA^+ *B. fragilis* can prevent EAE symptoms, inducing Treg cell differentiation [119]. The intestinal microbiota can also provide protection against some inflammatory diseases. For example, the incidence of disease in the Non-Obese Diabetic (NOD) mouse model of Type 1 Diabetes (T1D) is high in GF mice and the presence of SFB induces protection from the disease [120].

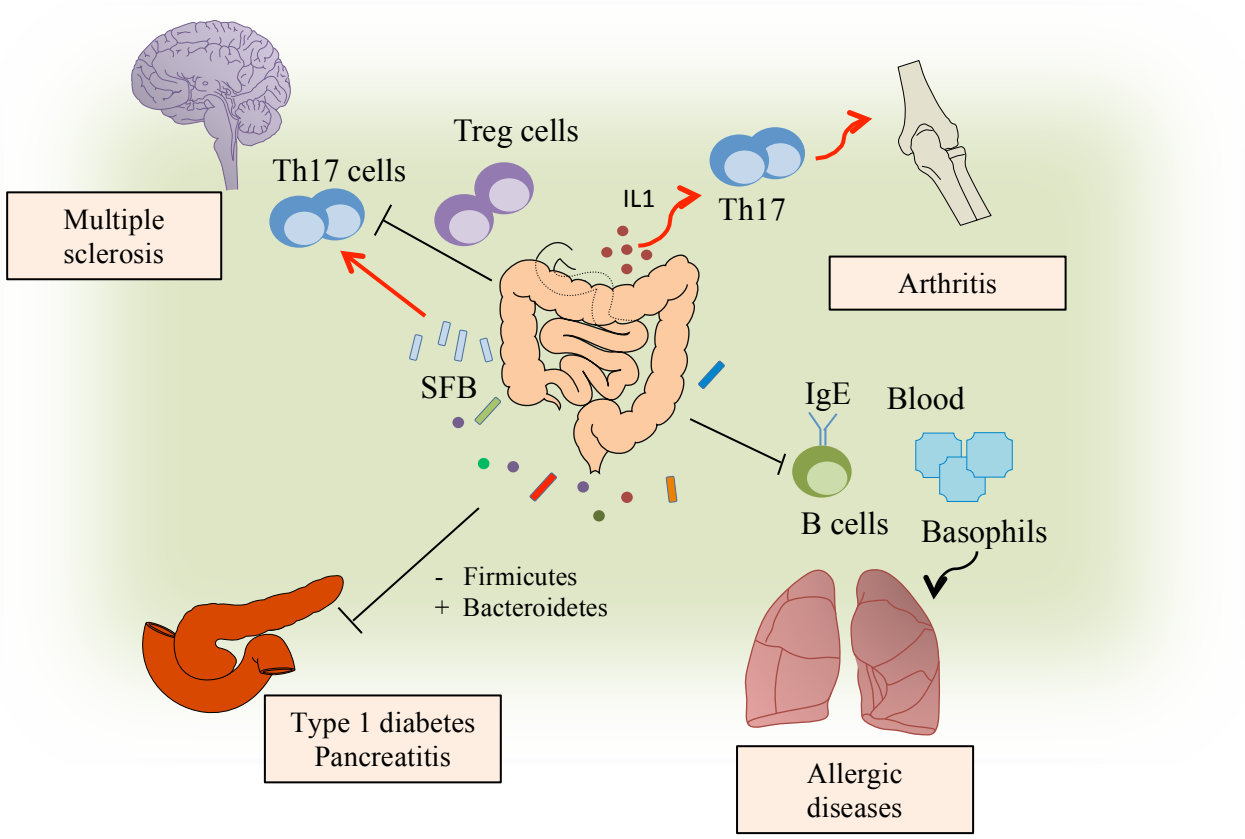

Figure 13: Intestinal microbiota affects autoimmune diseases at extra-intestinal sites. *Increased intestinal Th17 promote the expansion of pathogenic autoantigen-specific T cells, causing inflammation in the CNS. On the contrary, beneficial commensal bacteria can attenuate CNS inflammation, inducing Tregs generation. Moreover, microbiota-induced IL-1β signaling participates to the development of RA through the induction of Th17 cells. In addition, attenuated risk of T1D is associated to decreased Firmicutes/Bacteroidetes ratio as well as deficiency in MyD88 signaling in non-obese diabetic mice. Finally, microbial compounds stimulate peripheral B cells, inhibiting IgE production. Decreased IgE levels result in reduced number of basophils and consequently, attenuated risk of allergic airway inflammation (Adapted from [105]).*

6.5 The Skin compartment

6.5.1 Skin manifestations in PIDs

Cutaneous manifestations are common in PIDs, affecting between 40% and 70% of patients with diagnosed PIDs. Skin infections characterize several PIDs, but more frequently noninfectious cutaneous manifestations have been found in many of these disorders, including cutaneous granuloma, dysplasia of skin, hair, and nails, eczematous lesions, autoimmune conditions and frank vasculitis [121].

Skin infections involving bacteria include folliculitis, abscesses, furunculosis, impetigo, or pyoderma gangrenosum. Among disorders of phagocytosis, CGD present frequent bacterial infections, with suppurative adenitis in 53% of patients and subcutaneous as well as liver abscess due to *Staphylococcus* being the most common [122]. Bacterial skin infections are also a prominent feature of the hyper-IgE syndrome, due to a STAT3 deficiency, or the dedicator of cytokinesis protein 8 (DOCK8) deficiency. Severe recurrent abscesses with *Staphylococcus aureus* particularly localized on the scalp, face and neck, characterized the disease [123]. Atopic dermatitis or eczematous lesions seems to be the second most common presentation in PIDs. In particular, eczema occurs in 71% of patients with WAS [124]. Moreover, the erythematous rash in OS is often described as erythroderma and patients tend to have alopecia with loss of eyebrows and eyelashes [25]. Other skin manifestations are often reported in PIDs. Particularly, the skin may also be a site of the granulomatous lesions in CGD [125]. Patients with mutations in the early complement factors (C1, C2, C4) often present photosensitive malar rash and mucocutaneous vasculitis typical of systemic lupus erythematous. Autoimmune dermatomes such as vitiligo and alopecia are present with increased prevalence in several adaptive PIDs, including SCID [126, 127] and IgAD [128]. Moreover, cutaneous autoimmune manifestations such as vitiligo and alopecia characterized the autoimmune polyendocrinopathy-candidiasis-ectodermal dystrophy (APECED), a genetic disorder due to a mutation in *Aire* gene [129].

Recently, *Oh et al.* characterized the bacterial and fungal microbiota of several groups of PID, including hyper-IgE deficiency, WAS syndrome and DOCK8 syndrome. All individuals with these PIDs exhibit skin eczema. The study demonstrated an increased permissivity in the bacterial and fungal colonization of the skin of PID patients, dysbiosis and strong association with skin disease manifestations and severity.

Specifically, these patients present increased representation of fungi that can develop as opportunistic pathogens, including *Candida albicans* and *Aspergillus* sprecies (spp). Based on these results, it has been hypothesized that PIDs increase the host's ability to be colonized by atypical microbiota [130].

6.5.2 Skin anatomy and physiology

The skin is a complex organ that acts as a chemical and physical barrier to protect the body from infection and penetration of toxic agents. The human skin, with its surface area of 1.8 m^2, is composed of the epidermis, attached to basement membrane, underlined by the dermis and a subcutaneous fatty region. Specialized epithelial cells, called keratinocytes, compose the stratified layers of the epidermis. The outermost layer of the epidermis, the stratum corneum, is characterized by dead keratinocytes, called corneocytes, functioning as a barrier to exclude many toxic agents and avoid dehydration. This is followed by the stratum granulosum, containing tight junctions and the stratum spinosum. Lastly, the basal stratum constitutes the bottom layer of the epidermis and is responsible for constantly renewing the cells of the epidermis. This stratum is attached to a complex basement membrane (**Figure 14**). Importantly, the upper layers of the epidermis are composed by keratinocytes in cell division. The progeny of these cells move upwards as they differentiate and eventually die [131].

The epidermis contains dispersed cell type called Merkel cells, which stimulate nervous system [132], and melanocytes, which are important for protection against ultraviolet light damage. Specialized cells of the epidermis include also Langerhans cells, the main skin resident immune cells, and T cells, mainly $CD8^+$ T cells, resident in the stratum basal and stratum spinosum.

The dermis is characterized by a network of fibroblasts that produces a collagen-rich extracellular matrix. In addition, the presence of blood and lymphatic vessels in the dermis allows the trafficking of immune cells. Many specialized cells, including DCs, αβ T cells, γδ T cells and NK cells reside in the dermis.

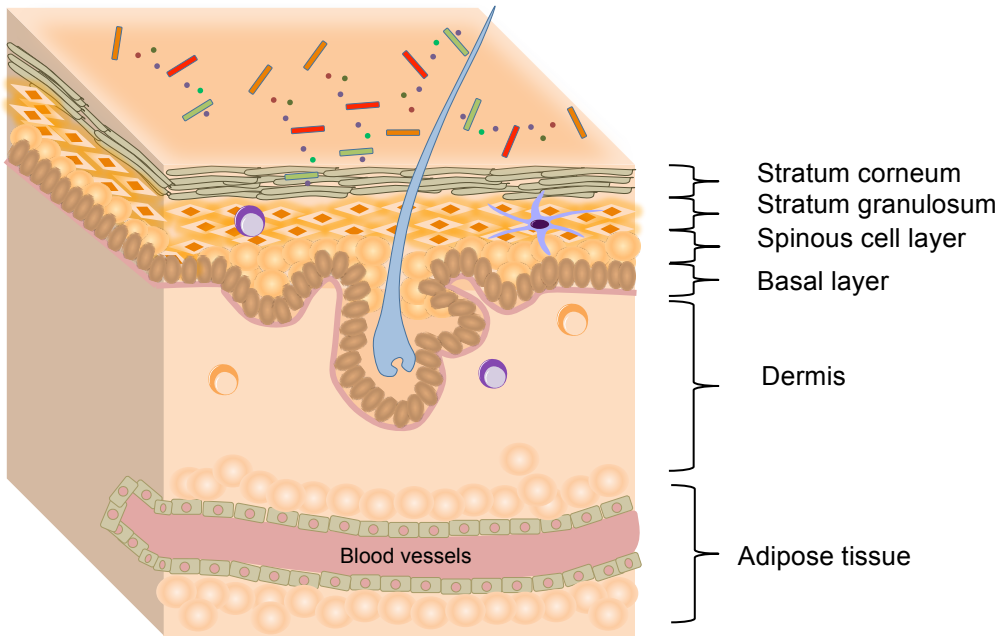

Figure 14: Structure and anatomy of the human skin. *It is composed by two layers: epidermis and dermis. Epidermis is a stratified squamous epithelium which is divided in four layers: stratum corneum, stratum granulosum, stratum spinosum, and stratum basale (Adapted from [133]).*

6.5.3 Skin microbiota

The skin contains about 10^{12} resident bacteria/m^2. Most skin bacteria can be divided in four different phyla: Actinobacteria, Firmicutes, Bacteroidetes and Proteobacteria. Importantly, the skin microbiota is dependent on the body areas (**Figure 15)**; in particular, the colonization of bacteria is dependent on the physiology of the skin site, with specific bacteria being associated with moist, dry and sebaceous environment. Indeed, bacterial diversity seems to be lowest in sebaceous sites and *Propionibacterium* spp are the dominant microorganisms in these areas. On the contrary, *Staphylococcus* and *Corynebacterium* spp are the most abundant in the moist areas, suggesting that these bacteria prefer high humidity environments. Mixed representations from the phyla Actinobacteria, Firmicutes, Bacteroidetes and Proteobacteria colonize the dry areas of the body [134].

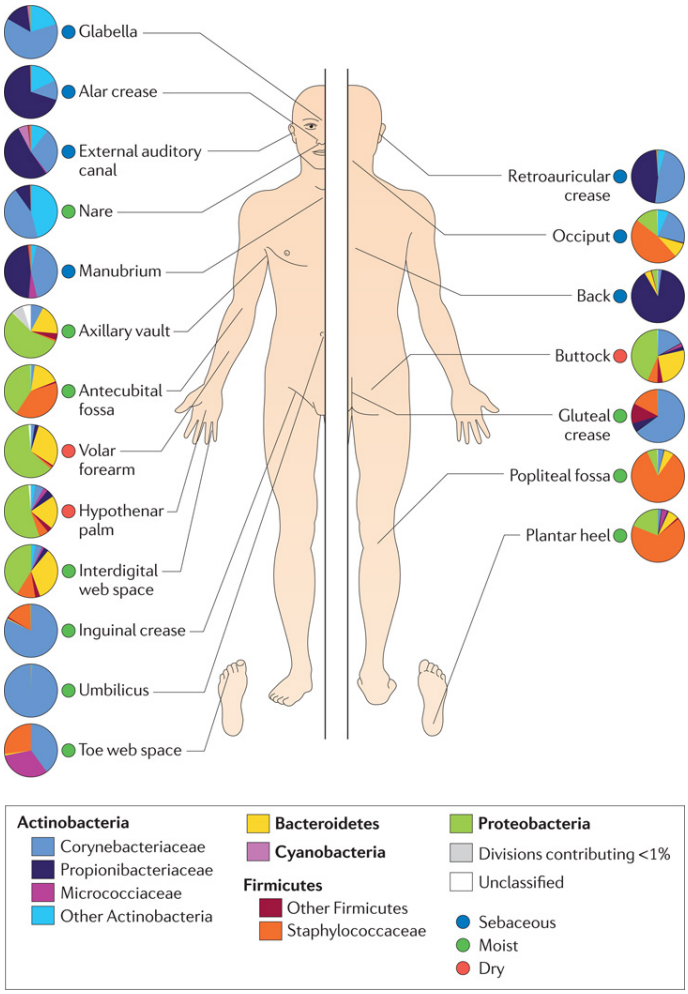

Figure 15: Distribution of bacteria on skin sites. *The skin microbiota diversity is highly dependent on the body areas, divided in moist, dry and sebaceous (Adapted from [134]).*

6.5.4 Innate immune barrier in the skin

In the skin compartment, the physical and biochemical barrier consists in a combination of terminally differentiated keratinocytes and the acidic, hydrophilic composition of the skin, as the results of sebum, lipids and AMPs production [135]. In addition, innate immune cells such as polymorphonuclear leucocytes (PMN), monocytes and macrophages, DCs and NK cells contribute to the cutaneous innate immune defenses.

6.5.4.1 Keratinocytes

Keratinocytes can sense pathogens and discriminate between commensal organisms and harmful bacteria. They represent the major cell type in the epidermis, constituting more than 90% of epithelial cells. They express several pattern recognition receptors, including TLRs recognizing a great variety of pathogens and self-components (**Figure 16**), NLRs, which respond to bacterial peptidoglycan, and NLR pyrin domain-containing proteins that respond to viral, fungal and self-compounds. Moreover, the expression of RLRs allows the response to viral RNA whereas C-type lectins, such as Dectin-1, detect fungal infections.

In response to microbial sensing, keratinocytes can produce several antimicrobial peptides (AMP): LL-37, β-defensins (HBDs), RNAses, and S100 family members. Importantly, during skin infection, the local production of AMPs by keratinocytes can be amplified by T cell-derived cytokines, such as IL-17A and IL-22 [136]. In addition to AMPs, keratinocytes release numerous cytokines, including IL-1, IL-6, IL-10, IL-18 and TNF. Moreover, keratinocytes represent an important source of chemokines and express chemokine receptors, modulating immune responses by attracting several cell types to the skin. By expressing CC-chemokine-ligand 20 (CCL20), CX-chemokine ligand 9 (CXCL9), CXCL10, CXCL11, keratinocytes can attract T cells to the cutaneous compartment. Moreover, keratinocytes regulate the trafficking of Langerhans cell precursors to the epithelium thought the expression of CCL20 [137]. In the epidermis of patients with psoriasis, keratinocytes can also recruit neutrophils by producing CXCL11 and CXCL8 [138].

Importantly, keratinocytes can act also as non-professional antigen presenting cells (APCs). In fact, several studies showed that keratinocytes express MHCII molecules in different skin disorders, especially characterized by T cell infiltrates [139].

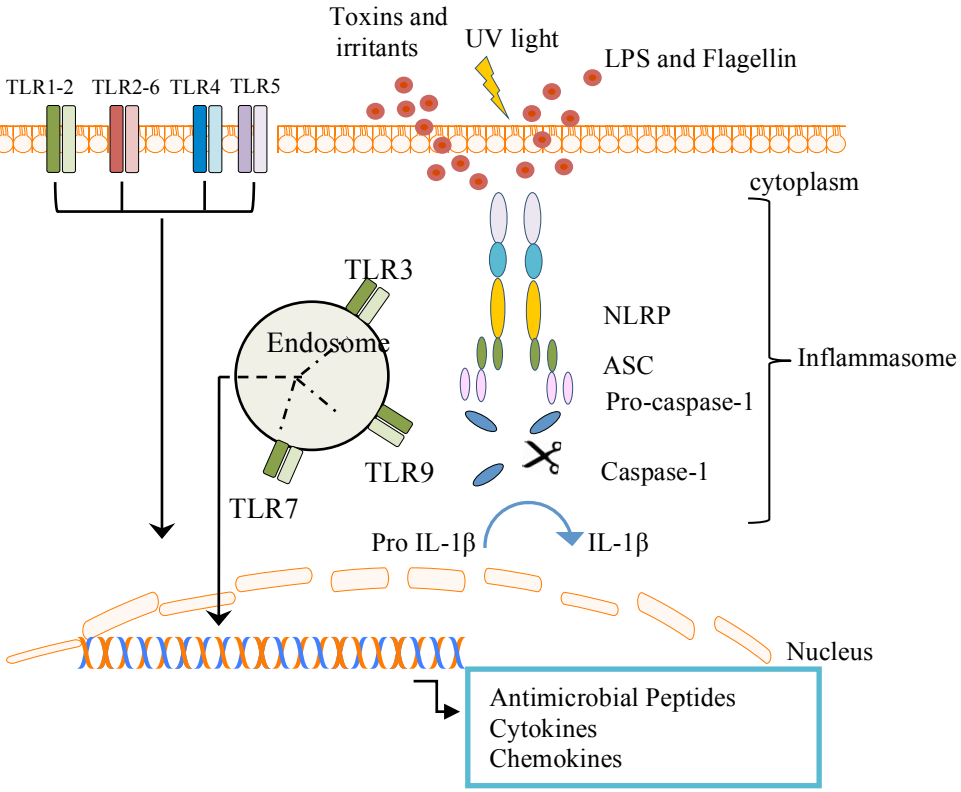

Figure 16: Microbial recognition and activation by keratinocytes. *Keratinocytes recognize foreign and dangerous agents, including irritants and toxins through TLRs and the inflammasome machinery. In particular, microbial recognition by TLRs induces the activation of several cellular pathways, necessary for the release of chemokines, cytokines and antimicrobial peptides. Moreover, following exposure to stimuli, such as UV irradiation, keratinocytes release the active form IL-1β through the activation of the inflammasome (Adapted from [140]).*

6.5.4.2 Antimicrobial peptides

Antimicrobial peptides (AMPs) bind membranes of microbes through their hydrophobic surface and form pores in the membrane, resulting in microbial killing. The most important keratinocyte-derived AMPs in human skin are the β-defensins (HBD)-1, HBD-2 and HBD-3. HBD-1 is constitutively expressed in human epidermis and exhibit antimicrobial activity against Gram-negative bacteria. On the contrary, HBD-2 can be induced by inflammatory mediators such as TNFα, IL-1 and several microbial components and showed efficacy against Gram-negative bacteria. HBD-3, inducible HBD, demonstrated potent bactericidal activity against the Gram-positive pathogens. The cathelicidin LL-37 showed pronounced antibacterial, antifungal and antiviral

activity. LL-37 has a central role also in several skin disorders. In atopic dermatitis, LL-37 levels are reduced, explaining the predisposition of atopic skin to bacterial infections. Moreover, altered processed peptides of cathelicidin are found in rosacea lesions, contributing to cutaneous inflammation. Another important AMP that induces the permeabilization of bacterial membranes is psoriasin (S100A7). It plays a central role in killing *E. coli* and is a potent chemo attractant for $CD4^+$ T cells and neutrophils. Studies revealed that the expression of some AMPs can be controlled by specific members of the microbiota, such as *Prionibacterium* spp.[141].

6.5.4.3 Dendritic cells

Initiation of the adaptive immune responses requires pathogen-derived antigen capture, processing and presentation by DCs. In the skin, DCs are divided in three distinct subsets: Langerhans cells, found in the epidermis, and two dermal populations, $CD11b^+$DCs ($CD1c^+$ DCs in humans) and $CD103^+$ DCs. In particular, $CD103^+$ dermal DCs are members of the $CD8^+$ DC-like group and are important for $CD8^+$ T cell responses and viral immunity. These cells express molecules directed to recognition of viral and other intracellular pathogens, produce IL-12 to drive Th1-cell type immunity and are efficient at cross-presenting antigens for the induction of $CD8^+$ T cell responses. The role of $CD11b^+$ DCs in mouse skin immunity has not been defined, although they have been linked to Th17-mediated immunity in other tissues. Indeed, after skin infection with herpes simplex virus (HSV), $CD11b^+$ DCs present antigens preferentially to $CD4^+$T cells. A study divided the $CD11b^+$ dermal DCs based on the expression of ALDH, demonstrating that $ALDH^+$ DCs may convert retinol to RA that drive Treg cell generation [142]. Langerhans cells are positioned in the epidermis above the basal keratinocytes and project their dendrites upward toward the cornified epithelial layer. These dendrites are able to sample antigens within the cornified layer without damaging the epidermal integrity. Recently, several studies highlighted that Langerhans cells contribute to priming immunity to skin pathogens such as *C. albicans* and *S. aureus*, favoring induction of Th17-mediated responses [143]. In contrast, Langerhans cells have a poor capacity to induce $CD8^+$ T cells, as shown for $CD103^+$ DCs. It was also described the immunosuppressive role of Langerhans cells, by inducing T cell deletion or by activating Treg cells to dampen skin immune responses. Plasmacytoid DCs (pDC) are only moderately efficient presenting cells but represent the major source of type I

IFN. They circulate in the blood and are basically absent from human skin. However, they are recruited during inflammatory conditions such as viral infection, allergy or autoimmunity.

6.5.4.3.1 DCs and skin homing imprinting on T cells

DCs from skin-draining lymph nodes (DLNs) specifically imprint skin homing receptors on activated T cells. The T cell localization in the skin requires the expression of cutaneous lymphocyte associated antigen (CLA). CLA mediates the tethering and the rolling of T cells through the interaction with its endothelial receptor E-selectin, expressed normally on skin post-capillary venules. However, other skin molecules have been implicated in the homing process. For instance, the interaction between CCR4 and its ligand CCL17 (TARC) has been implicated in skin homing of immune cells; in particular, CCR4 is necessary for antigen-driven accumulation of $CD4^+$ T cells under physiological conditions [144]. Moreover, interaction between CCR10 and its ligand CCL27 (CTAK) has also been implicated in skin homing [145]. Recently, vitamin D has been proposed to have a key role in the guidance of memory T cells through the upregulation of the receptor CCR10 [146].

6.5.5 Skin T cells

Lymphocytes are present in significant numbers in human skin, while B cells are rare. Indeed, human healthy skin contains more than $2x10^{10}$ skin resident T cells. Epidermal T cells are mainly distributed at the basal and suprabasal keratinocytes layer, in close contact with Langerhans cells. In the dermis, T cells are preferentially clustered around postcapillary venules and are often situated just beneath the dermal–epidermal junction or adjacent to cutaneous appendages. Conventional T cells, known as αβ T cells, reside in the skin and the majority presents a memory phenotype. Unconventional T cells, called γδ T cells, reside mainly in the epidermis (**Figure 17**).

6.5.5.1 αβ T cells

Human skin contains a large numbers of αβ T cells, with a memory phenotype. These cells consist of both $CD4^+$ and $CD8^+$ subsets, with about 10% of the $CD4^+$ T cells expressing Foxp3, indicating a Treg cell phenotype. $CD8^+$ T cells are predominantly localized in the epidermis while $CD4^+$ T cells in the dermis. Interestingly, the epidermal

$CD8^+$ cells persist for long period in the skin and are known as tissue resident memory T cells (T_{RM}). During cutaneous inflammation or infection, effector $CD8^+$ T cells enter in the dermis from the blood and migrate to the epidermis through the chemokine receptor CXCR3 [147]. Several signals found within the epidermis instruct $CD8^+$ T cells to develop T_{RM} via the upregulation of molecules, such as CD103 and CD69, and the downregulation of sphingosine-1-phospate receptor 1 (S1PR1), required for tissue exit. Notably, $CD8^+$ T_{RM} cells protect mice against skin infection with viruses [148]. In contrast to $CD8^+$ T cells, a proportion of memory $CD4^+$ T cells is able to migrate into the circulation and is known as T effector memory cells (T_{EM} cells) [149]. However, many remain in the skin and express markers of T_{RM} cells, such as CD103 and CD69. In agreement, about a half of the $CD4^+$ T cells in the skin lack the expression of CCR7, a chemokine receptor necessary for the migration to the LN [150].

Three many subsets of $CD4^+$ T cells, such as Th1, Th17 and Th2, have been identified in the skin during inflammatory conditions. The Th1 responses are associated with autoimmunity and immune–mediated diseases, like psoriasis, whereas Th2 responses are linked to allergic diseases, such as atopic dermatitis and acne. Recently, Th17 responses have been described to exert a potential role in the pathogenesis of both psoriasis [151] and atopic dermatitis [152].

6.5.5.2 γδ T cells

The epidermis contains γδ T cells that represent all the epidermal T cells in mice, known as dendritic epidermal T cells (DETCs), while they constitute a minor subset in humans. DECTs express a conserved Vγ5 Vδ1 TCR and are constitutively clustered on dendritis forming polarized anchors at epithelial tight junctions.

DETCs exhibit slow homeostatic division under steady state conditions and need exogenous IL-15 and IL-2Rβ for proliferation and survival. They have been shown to participate in would healing and contribute to inflammation, tumor surveillance, contact hypersensitivity and antibacterial response. Studies demonstrated that wounds without DETCs show impaired keratinocyte proliferation, reduced inflammation and slower closure [153]. Activated DETCs express a large variety of chemokines and cytokines, such as CCL3, CCL4, CCL5 and XCL1, IFNγ, IL-2 and IL-13. In addition to the presence of DETCs in the epidermis, mice present a large Vγ5-Vγ4+ population of γδ T cells in the dermis. The dermal γδ T cells do not require IL-15 for survival but need IL-

7. Moreover, the majority of dermal γδ T cells expresses CCR6 and produce IL-17. In particular, this population has an important role in the imiquinod-induced model of psoriasis. In agreement, psoriatic patients showed increased numbers of IL-17-producing γδ T cells in their skin [154]. Several studies have investigated the possible link between skin microbiota and γδ T cells, underling the reduced ability of these cells to produce IL-17 in mice devoid of live bacteria [155].

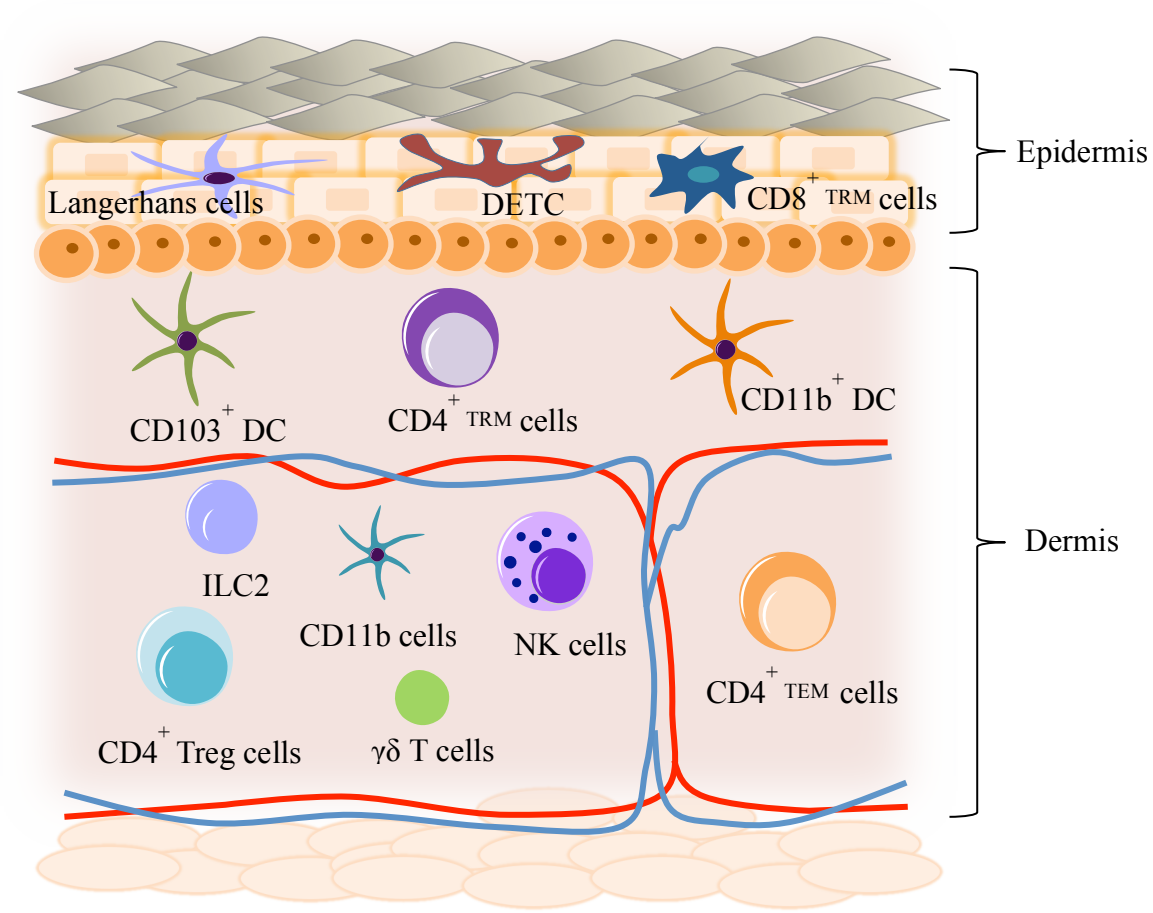

Figure 17: Overview of the main populations located in the skin. *The mouse epidermis is populated by three important immune cell types: Langerhans cells, DETCs and $CD8^+$ T_{RM} cells. The dermis contains: Treg cells, $CD4^+$ T_{RM} cells, $CD4^+$ T_{EM} cells, other γδ T cells, innate lymphoid cells (ILCs) and several DC populations (Adapted from [156]).*

6.5.6 Association of the microbiota with inflammatory skin disorders

The commensal bacteria protect the skin from infections by competing pathogens and contribute to immune homeostasis by modulating cutaneous immune responses in beneficial and harmful ways. On the other side, the immune system releases several antimicrobial peptides to control the microbial colonization of the skin. Cutaneous commensal bacteria can control skin resident T cell function and protective immunity to pathogens. During the infection with the parasite *Leishmania major*, the presence of *S. epidermidis* is necessary for IFNγ and IL-17A production by skin resident T cells and for protective immunity [155].

Moreover, studies reported that skin colonization with *S. aureus* triggers local allergic responses by releasing δ-toxin, which directly induces the degranulation of dermal mast cells, promoting adaptive and innate Th2 immune responses [157]. Skin bacteria can also contribute to the pathogenesis of several skin disorders, such as psoriasis, atopic dermatitis, and acne. Indeed, *S. aureus*, a common cause of skin disease, is frequently found in the skin of patients with atopic dermatitis [158]. More specifically, the relative abundance of *S. aureus* and also the skin commensal *Staphylococcus epidermis* increase with clinical disease activity. *Iwase et al.* suggested that increased abundance of *S. epidermis* reflects a microbial response to *S. aureus* overgrowth [159]. Moreover, increased bacterial diversity end enrichment in *Streptococcus* spp was detected in lesional psoriasis [160]. Additionally, the skin of patients that are affected by acne vulgaris is dominated by a single bacterium, *Propionibacterium acnes* [161]. Studies on the skin of PID patients revealed altered indigenous microbiota composition, with colonization of several microbial species not observed in healthy controls, such as *Clostridium* species and *Serratia marcescens* [130].

However, commensal bacteria are not only the unique source of disease state, but additional triggers, such as genetic predisposition and/or infections could contribute to the development of the disease. In particular, variations of the skin barrier and consequent cutaneous penetration of microbes play an important role in triggering skin diseases. For instance, mutations in the epidermal expressed filaggrin (FLG) gene are associated to atopic dermatitis [162]. Moreover, deficiency in disintegrin and metalloproteinase domain-containing protein 17 (ADAM-17) was sufficient to induce the expansion of *Corynebacterium bovis* and *S. aureus* in mice, contributing to enhance

atopic dermatitis [163]. Finally, in the context of metabolic disorders, chronic inflammatory state and altered nutrient availability could contribute to the emergence of several bacteria that induce local inflammation (**Figure 18**).

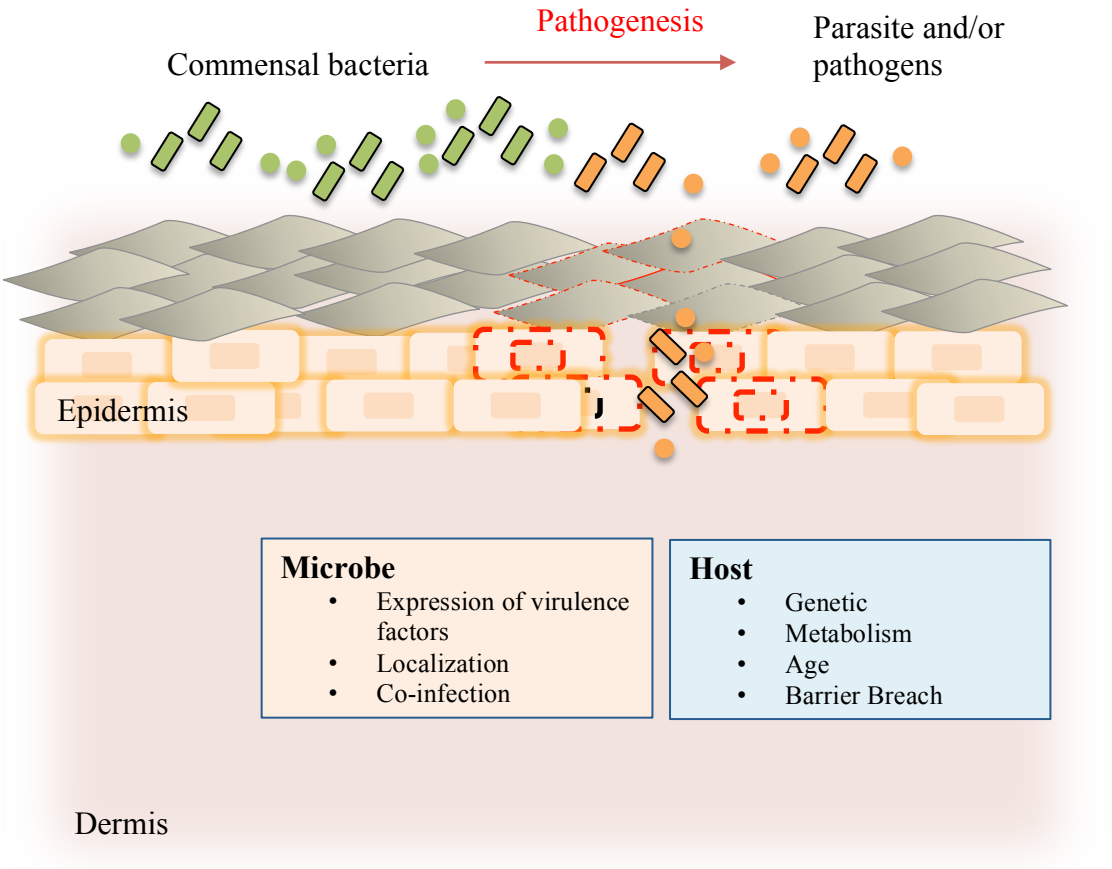

Figure 18: Mechanisms through which skin microbiota might initiate or amplify cutaneous disorders. *The capacity of the skin microbiota to promote disease could depend by host genetic predisposition, metabolic disorders, altered barrier integrity and infections (Adapted from [164]).*

7. AIM OF THE STUDY

Omenn syndrome is a complex disease in which immunodeficiency is associated with autoimmune manifestations that can manifest in the form of an inflammatory bowel disease-like illness and cutaneous degeneration. Although the identification of the molecular bases of OS has allowed the precise diagnosis of the disease, the mechanisms underlying autoimmunity are still puzzling and difficult to explore in OS patients. In literature, compelling evidence indicates the critical role played by the environment (physical insults, toxins, nutrition and microorganisms) in the induction of autoimmune disease. In particular, pathogenic, pathobiotic and commensal microorganisms have been shown to influence the disease progression in genetically susceptible hosts. In this regard, one of the most intriguing and still unsolved question regarding OS disease is whether the source of the (limited) immunophenotypic variation in patients, ranging from leaky forms of severe combined immunodeficiency to full blown forms with severe autoimmunity, depends on defects in the gut-blood barrier, which may render OS patients susceptible to inflammation sustained by endogenous commensal flora, whose antigens might be recognized by homeostatically proliferating peripheral oligoclonal T cells. Moreover, in OS, iatrogenic components altering the commensal microbiota (e.g., prolonged courses of antibiotic) may interfere with immunological tolerance by affecting the development of functional regulatory T cells. Thus, in this thesis I aim to investigate the extent to which alterations in the homeostasis of the intestinal tract, the largest body surface in contact with the external environment and key component of the host defence against pathogens affected by a constant interaction between resident microbes and the immune system, influences the pathogenesis of autoimmune manifestations. Thanks to the availability of the *Rag2*$^{R229Q/R229Q}$ mouse, which faithfully recapitulates the human disease, I plan to define the cellular and molecular bases underlying the intestinal inflammation in OS and to challenge the hypothesis that a dysregulated adaptive and/or innate immune response to the commensal bacterial flora plays a central role in disease pathogenesis, causing both local and systemic autoimmunity, particularly the skin manifestations. To this end, I will pursue the following aims:

Aim 1. To study the intestinal pathology in *Rag2*$^{R229Q/R229Q}$ mice

- To determine the cellular and molecular bases of the altered intestinal immune homeostasis in *Rag2*$^{R229Q/R229Q}$ mice
- To investigate whether T regulatory impairment contributes to intestinal inflammation in OS
- To assess whether B cell compartment could be crucial for maintaining intestinal homeostasis and avoid bacterial translocation
- To explore the role of gut microbiota on intestinal and systemic autoimmunity in the OS pathogenesis

Aim 2. To study the skin degeneration in *Rag2*$^{R229Q\ /R229Q}$mice

- To characterize the cellular and molecular bases of the altered cutaneous homeostasis in *Rag2*$^{R229Q/R229Q}$mice
- To investigate dysfunctions of the skin barrier integrity in OS pathogenesis
- To explore the contribution of altered gut permeability and inflammation in OS skin degeneration

Data obtained in these aims are expected to highlight the pathogenic mechanisms basically involved in the induction of IBD-like and skin disorders in OS; hence, they may have further implications for the development of treatment strategies for this immunodeficiency that may utilize improvement of colitis and skin disease as a measure of clinical efficacy. Moreover, these findings will help to define the extent to which intestinal inflammation may impinge on the overall clinical disease phenotype, with particular attention to the outcome of autoimmune manifestations. I expect to understand if and to what extent an altered composition of intestinal microbiota in the *Rag2*$^{R229Q/R229Q}$ mice directs the type of mucosal and systemic immune responses by affecting the balance between pro-inflammatory and anti-inflammatory cell populations. These findings would help to reveal and recognize a novel and important aspect in the pathogenesis of OS and other forms of immunodeficiency associated with both intestinal and cutaneous diseases. Moreover, results from this thesis will have more broad implication in fundamental immunology contributing to gain insight into the molecular mechanisms underlying the microbiota-mediated fate determination of T

cells. Finally, they will also provide new foundations for the design of novel immuno- or microbe-based therapies.

8. MATERIALS AND METHODS

8.1 Mice used in the study

129Sv/C57BL/6 knock-in *Rag2*$^{R229Q/R229Q}$ mice (hereafter of *Rag2*^{R229Q} mice) were backcrossed to C57BL/6J strain for four generations. This resulted in chimeric mice with genetic background very close (85% as determined by SNPs analysis) to C57BL/6J strain. The colony was maintained in heterozygosity and littermates were kept in the same cage until weaning. *Rag1*$^{-/-}$ (*Rag1*$^{tm1Mom/J}$) mice were obtained from The Jackson Laboratory and C57BL/6 Ly5, OT-1 and OT-II mice from Charles River. *Rag2*^{R229Q}*Myd88*$^{-/-}$ double-mutant mice and littermate controls were generated from heterozygous–heterozygous crossing. All mice were housed in a specific pathogen-free facility. Both male and female mice aged between 8-12 weeks (as indicated) were used in the study. Age and sex matched controls were added in each experiment performed. All experiments were performed at least twice, with similar results. The animal procedures were performed according to protocols approved by the Istituto Clinico Humanitas and the Italian Institutional Animal Care and Use Committee.

8.2 Human Samples

Analysis of nine-unrelated patients with hypomorphic RAG defects whose clinical, immunological and molecular features were consistent with OS disease. Neonatal patient's samples were collected with the informed consent of their parents, by their respective clinicians, accordingly to the statements of the Ethical Committee of each referring medical centre. Peripheral blood mononuclear cells (PBMC) from peripheral blood of four RAG patients were purified on Ficoll gradient (Lympholyte cell separation media, Cedarlane).

8.2 Adoptive transfer experiments

For T cell transfer in immunodeficient hosts, total CD4$^+$ T cells derived from pooled MLNs of *Rag2*$^{+/+}$ and *Rag2*^{R229Q} mice were isolated with FACSAria cell sorter (purity>95%). 4x10^6 purified CD4$^+$ T cells were injected into recipient *Rag1*$^{-/-}$ mice

[165]. Weight loss was monitored daily. ELISA on colonic supernatants and FACS analysis were performed at the sacrifice.

For the colitis induction by T cell transfer, $CD4^+$ T cells were isolated by pooled spleens and MLNs of 10-wk-old *Rag2*$^{+/+}$ or *Rag2*^{R229Q} mice using CD4-specific magnetic beads via negative selection according to the manufacturer's instructions (Miltenyi Biotec). Enriched CD4 T cells were subsequently sorted into naive $CD4^+CD25^-CD45RB^{hi}$ and regulatory $CD4^+CD45RB^-CD25^{hi}$ populations (>98% purity) using a cell sorter (FACSAria; BD). For colitis induction, 4×10^5 WT $CD4^+CD25^-CD45RB^{hi}$ naive T cells were i.p. transferred into *Rag1*$^{-/-}$ mice alone or with $1.5x10^5$ $CD4^+CD25^{hi}$ T reg cells from *Rag2*$^{+/+}$ or *Rag2*^{R229Q} mice. Recipient mice were weighted twice a week and sacrificed at week four after the transfer, when IBD was diagnosed by severe weight loss, as described by [166].

For Treg transfer, $5x10^5$ $CD25^{hi}$ $GITR^+CD4^+$ Treg cells (purity >98%) were sorted from spleens of *Rag2*$^{+/+}$ mice and injected into *Rag2*^{R229Q} mice, as described by [167]. Mice were analysed after 4 weeks. FACS and gene expression analysis were performed on gut tissues. Histological analysis of the intestine was also performed.

For B cell adoptive transfer, $CD19^+$ B cells were enriched from pooled spleens, MLNs and PPs derived from WT CD45.1 donor mice with anti-CD19 magnetic beads (Miltenyi Biotec). Then, $B220^+IgM^+IgA^-$ B cells were isolated with FACSAria cell sorter (purity >98%) and immediately injected i.v. into *Rag2*^{R229Q} mice ($30x10^6$ B cells), as described by [168]. B cell reconstitution was monitored and recipient mice were analysed after 4 weeks. Concentration of IgA was measured by ELISA twice a week. Histological and gene expression analysis were performed on gut tissue at the sacrifice.

8.3 Antibiotic treatment and faecal transplantation

For antibiotic treatment, *Rag2*$^{+/+}$ and *Rag2*^{R229Q} mice underwent four week-antibiotic treatment by oral gavage: Ampicillin (2.5 mg), Metronidazole (2.5 mg) and Vancomicin (1.25 mg) were administered in a solution in 200 µl/mouse, as described by [169]. Importantly, the antibiotic regimen resulted in about 90% reduction of total intestinal bacterial DNA, as measured by quantitative PCR.

Faecal transplantation experiments were performed as described by [170]. For faecal transplantation experiments, recipient *Rag2*$^{+/+}$ and *Rag2*^{R229Q} mice received long-term antibiotic treatment (30 days) to deplete the resident microbiota. Then, faecal pellets were collected from donor *Rag2*$^{+/+}$ and *Rag2*^{R229Q} mice, suspended in sterile PBS and homogenized. The faecal suspension obtained was introduced by gavage with the flexible plastic tube into the stomachs of each donors. The faecal suspension was given twice, one week apart. After the transplantation, recipient *Rag2*$^{+/+}$ and *Rag2*^{R229Q} mice colonized with the same intestinal microbiota were maintained in dedicated cages until the sacrifice. Recipient mice were sacrificed 3wk after the second microbiota transfer.

8.4 IgA-coated bacteria

Faecal pellets were homogenized and stained with anti-mouse IgA (mA-6E1, eBioscience). The bacteria were suspended with 4% of formalin overnight at 4°C and re-suspended in DAPI/PBS for FACS analysis (CANTO II, BD) using forward scatter (FSC) and side scatter (SCC) parameters in logarithmic mode. FlowJo software (9.6.6, Tree Star) was used for data analysis.

8.5 ELISA assay

For faecal immunoglobulin evaluation, faecal pellets were collected, weighed and suspended in 1 ml of PBS containing 0,1% sodium azide and protein inhibitor. Faecal IgA/IgM levels were measured by a mouse IgA/IgM ELISA quantification set (Bethyl Laboratories, Inc.), according to the manufacture's instructors. Serum IgE was measured by specific ELISA (BD). Quantification of cytokines, such as IFNγ, TNFα, CCL17 and CCL22, was performed with mouse ELISA kit (R&D systems). Briefly, 1cm of colonic tissue was incubated at 37°C for 48h, then supernatants were collected and cytokines determination was performed using ELISA kit. Human CCL17 and CCL22 were detected with human ELISA kit (R&D systems).

8.6 LPS measurement

Sera were collected from *Rag2*$^{+/+}$ and *Rag2*^{R229Q} mice in endotoxin-free conditions and stocked at -20. LPS concentration was determined by Limulus amebocyte lysate assay (Lonza) according to the manufacturing's instructions. This method utilizes a preparation of Limulus Amebocyte lysate (LAL) and a synthetic color producing

substrate to detect endotoxin chromogenically. The lyophilized endotoxin (*E. Coli* 0111:B4) was used for preparing standard solutions, ranging from 1 to 0.1 EU/ml.

8.7 Quantification of adherent bacteria to mucosal and cutaneous epithelium

One cm of skin biopsies or 1 cm-terminal ileum were collected from age–and sex-matched mice using sterile condition and digested in lysis buffer (10 mM TRIS, 10 mM Tris, 100 mM NaCl, 10 mM EDTA, 0.5% SDS, and 0.4 mg/ml proteinase K). Total DNA was extracted with the isopropanol-ethanol method. The microbial load was determined with real time PCR (RT-PCR) (Syber Green) using 16s and 18s specific probes.

8.8 LP and skin preparation

Small intestines and colons were flushed to remove faecal contents, open longitudinally and cut into small pieces. To remove the epithelial layer, intestines were washed in HBSS buffer (0.5 M EDTA, 1 mM DTT, 15 mM Hepes, and 10% FCS) under agitation for 20 min at 37°C. Then, tissues were digested with Liberase TL (0.15 mg/ml, Roche, Sigma Aldrich, Taufkirchen, Germany) for 30 min at 37°C, washed and passed through 100-µm cell strainers. The cell suspension obtained was stratified with 44/67% Percoll Gradient (GE Healthcare) and centrifuged at 600g for 20 min at RT. Lymphocyte phase was collected and analysed by flow cytometry with or without pre-stimulation with PMA (20ng/ml) and Ionomycin (1µg/ml).

Skin tissue was digested with Liberase TL (0.45 mg/ml, Roche) for 1h at 37°C in agitation. Cells were washed and passed through 100-µm cell strainers. The resulting skin suspensions were further analysed by flow cytometry with or without pre-stimulation with PMA (5ng/ml) and Ionomycin (1µg/ml).

8.9 Lymph flow assessment using Evans blue dye

Three µL of 1% Evans blue dye solution in PBS was injected into the back of anesthetized *Rag2*^{R229Q} mice and controls using a Hamilton syringe. After 16h, all mice treated were sacrificed. Evans blue dye was extracted from the skin biopsies of the back by incubating them at 55°C for 5.5 hours in formamide (Fluka). The absorbance was measured with microplate reader at 620 nm. The dye concentration was calculated from

a standard curve of Evans blue dye in formamide and is represented as absolute amount of dye remained in the skin tissue.

8.10 OT-I and OT-2 adoptive transfer

Splenic $CD8^+$ OT-I cells or $CD4^+$ OT-II cells were sorted from donor mice (purity >98%). $CD8^+$ OT-I cells or $CD4^+$ OT-II cells ($3*10^6$) were adoptively transferred i.v. into $Rag2^{+/+}$ and $Rag2^{R229Q}$ mice (CD45.1). The day after, ears were immunized. Briefly, both sides of each ear were gently stripped 10 times with Scotch Tape (3M), then 25µl of acetone was applied and evaporated. Next, 20 µl of cholera toxin (CT) or CT+ 50 µl of Ovalbumin (100 mg/ml OVA, cod. A5503, Sigma Aldrich) was applied with a small paintbrush on the ears of recipient mice. $Rag2^{+/+}$ and $Rag2^{R229Q}$ mice were sacrificed after 7 days from topical immunization, as described by [171].

8.11 DSS chronic treatment

Chronic colitis was induced by adding dextran sulfate sodium (DSS, 2%) to drinking water ad libitum for 4 cycle. Control mice received water continuously thought all the experiment. At the end, mice were euthanized and skin tissues were collected for FACS and histological analysis.

8.12 Co-culture DC-T cells

Topical Immunization of ear skin of $Rag2^{+/+}$ and $Rag2^{R229Q}$ mice was performed as described above. Briefly, CT plus OVA or CT alone as control was applied directly on ear skin. After 4 days, DCs from spleen and cervical LNs were sorted with FACSAria cell sorter (purity >98%) from OVA immunized- $Rag2^{+/+}$ and $Rag2^{R229Q}$ mice and CT controls. OVA-loaded DCs were put in co-culture with $CD4^+$ OT-II cells harvested from OT-II mice in 96-well-round bottom plates. A 1:1 DC:T cell ratio was used for the assay. Co-cultures were maintained for 6 days and T cell proliferation was evaluated by the incorporation of (3H)-thymidine.

8.13 Topical and systemic LPS

$Rag2^{+/+}$ and $Rag2^{R229Q}$ mice, aged 8-10 weeks, were anesthetized and injected intra-dermally into the back with 100µg of LPS (right side) and PBS (left side) using Hamilton syringe. After 24h, LPS-treated mice were sacrificed and skin tissues were

processed for histological analysis and quantitative RT-PCR analysis. For systemic LPS administration, *Rag2*$^{+/+}$ and *Rag2*^{R229Q} mice were injected i.p. with 100μg of LPS. Systemic LPS-treated mice were sacrificed 24h later. Skin tissues were used for histological scores and transcriptional analysis.

8.14 OVA-intradermal injection

Rag2$^{+/+}$ and *Rag2*^{R229Q} mice, 8-10 weeks old, were injected intra-dermally into the ear's skin with 100 μg/ml OVA-Alexa Fluor™ (Thermo Fisher Scientific) with Hamilton syringe. After 6h, cervical LNs and ear tissues were collected and digested with Liberase TL (0.45 mg/ml, Roche, Sigma Aldrich, Taufkirchen, Germany) for 30 min at 37°C. The analysis of OVA-loaded CD11C^{+} DCs from ears and cervical LNs was performed by FACS. Mice injected intra-dermically with PBS$^{-/-}$ were used as negative control.

8.15 Flow cytometry

Cell suspensions obtained from intestines, spleens, MLNs, DLNs and skins were pre-incubated with FcγR-specific blocking antibodies (eBioscience) and stained with the following antibodies: TCR-β (clone H57.597, eBioscience), TCR-γδ (clone UC7-13D5, eBioscience), CD3 (clone 17A2, eBioscience), CD45 (clone 30-F11, eBioscience), CD4 (clone RM4-5, eBioscience), CD8a (clone 53-6.7, eBioscience), CD62L (clone Mel14, eBioscience), CD44 (clone IM7, BD), CD45R (B220; clone RA3-6B2, eBioscience), CD357 (GITR; clone DTA-1, eBioscience), CCR9 (clone eBio CW-1.2, eBioscience), α4β7 (clone DATK32, BioLegend), Foxp3 (clone MF23, eBioscience), IgA (clone mA-6E1, eBioscience), IgM (clone II/41, eBioscience), CD25 (clone PC61.5, eBioscience), CD103 (clone 2E7, eBioscience), CD45RB (clone C363-16A, BioLegend), CD11C (clone N418, eBioscience), MHCII (M5/114.15.2, eBioscience). Exclusion of dead cells was performed with Aqua Cell Stain kit (Invitrogen). For intracellular staining, cells were stimulated for 4h with PMA and Ionomycin. Golgi stop (1000x, BD) was added during the last 3h of stimulation. Cell fixation and permeabilization was performed using the intracellular fixation and permeabilization buffer kit (eBioscience). Intracellular staining was performed using the following antibodies: IL-17A (clone eBio17B7, eBioscience) and IFNγ (clone XMG1.2, eBioscience). For human samples, cells were stained with the following antibodies: CD4 (clone RPA-T4, eBioscience),

CD8 (clone RPA-T8), CD45RA (clone HI100, BD), CD45RO (clone UCHL1, BioLegend), CCR9 (clone BL/CCR9, BioLegend), CLA (clone HECA-452, BioLegend). FACS data were acquired with FACS CANTO II and analysed with FlowJo software (9.6.6, Tree Star).

8.16 Quantitative real time RT-PCR

Total cellular RNA was extracted from 1 cm of mouse ileal/colonic tissues or back skin. Tissues from intestines, skin, kidney, liver and lung were homogenised in PureZOL reagent (Bio-Rad Laboratories) using TissueLyzer II (QIAGEN). Then, RNA was extracted using RNeasy Lipid Tissue kit (QIAGEN). A total of 1 μg of RNA was used to synthetize cDNA using the High-Capacity cDNA Reverse Transcription Kit (Applied Biosystems). The expression of mouse cytokines and chemokines was investigated by SYBR-green RT-PCR using the CFX384 system (Bio-Rad Laboratories). For sorted cells, total RNA was extracted by RNeasy Plus Micro kit (QIAGEN), retro-transcribed and pre-amplified using TaqMan PreAmp MasterMix (Applied Biosystems). Quantitative RT-PCR was run on ViiA7 system (Thermo Fisher Scientific) with TaqMan probes. The housekeeping gene β-actin (Actb) ribosomal RNA was used as control. List of primers used in the study (**Table 2**).

8.17 Histology and immunohistochemistry

Mouse tissue samples were formalin-fixed and paraffin-embedded. Sections (1,5 μm) were used for routine hematoxylin and eosin (H&E) staining to check for basic histopathological changes. Moreover, sections were de-waxed, rehydrated, endogenous peroxidase activity blocked by 0.1% H_2O_2, nonspecific background reduced with Rodent Block (Biocare Medical) before microwaves or thermostatic bath treatment and incubated with primary antibodies for 1h at RT. The following primary antibodies were used: rabbit anti-CD3 (1:100; ThermoFisher Scientific; EDTA buffer pH 8.0), rat anti-FoxP3 (1:100; eBioscience; EDTA buffer pH 8.0) and goat anti-CD31 (1: 1000; R&D system; DIVA Decloaker 1x Biocare Medical). Depending on the primary antibodies and tissue used, sections were incubated with Goat-on-Mouse HRP-Polymer (Biocare Medical), MACH 1™ Universal HRP Polymer Kit (Biocare Medical), Rat-on-Mouse HRP-Polymer (Biocare Medical) or Real EnVision Rabbit-HRP (Dako), and reactions were developed in Biocare's Betazoid DAB and nuclei counterstained with Hematoxilin

(Dako). Digital images were acquired by Olympus XC50 camera mounted on a BX51 microscope (Olympus) or by Olympus DP70 camera mounted on a Bx60 microscope (Olympus), with CellF Imaging software (Soft Imaging System GmbH).

Quantification of $CD3^+$ cells and area of liver, lung, and kidney sections was performed by Aperio ScanScope CS Slide Scanner (Aperio Technologies) and the absolute number of $CD3^+$ cells was expressed as the number of $CD3^+$ cells/mm^2.

8.18 Histological score

Arbitrary gut (SI and colon) and skin histological score was calculated in double blind study by a pathologist. Scoring from 0 to 3 (where 0 is normal condition and 3 is severe structural changes) was adopted for evaluating different manifestations in each tissue. For gut analysis, a combined score was used: grade of inflammation, the structural changes of the glands, and the goblet cell depletion. For skin analysis, abnormalities of keratinocytes, increased immune cells in the dermis, alterations of the epidermis and presence of cutaneous abscesses were evaluated. Specifically, for DSS treatment, the number of $CD3^+$-aggregates was also analysed as additional parameter in the score.

8.19 Morphometric analysis

Villous height and crypt depth were randomly measured for 16 well-oriented villi of distal ileum per mouse and data were analyzed using commercial image analysis software (ImageJ; National Institutes of Health). CD31 morphometric analysis was performed using Olympus Slide Scanner VS120-L100 to acquire digital images and Image-pro software to evaluate coverage, vessels number and size.

8.20 Microbiota analysis

For the evaluation of intestinal microbiota, weaned *Rag2*^{R229Q} and *Rag2*$^{+/+}$ littermates were co-housed in the same cages until analysis. The bacterial microbiota of 20 faecal samples from 10 *Rag2*$^{+/+}$ and 10 *Rag2*^{R229Q} mice was explored by sequencing the V5-V6 hypervariable regions of 16S rDNA gene by using the Illumina MiSeq platform. The obtained 250 × 2 paired-end reads were taxonomically profiled by applying the BioMaS pipeline [172]. Paired-end reads of each sample were merged into consensus sequences using Flash (Adobe) and then dereplicated by Usearch (drive5). The unmerged reads were trimmed of low-quality regions (Phred score cutoff of 25), and paired ends

containing reads shorter than 50 nucleotides were removed. Both the merged sequences and the unmerged reads were mapped against the RDP II database (release 10.32) by using Bowtie 2. The mapping data were filtered according to query coverage (≥70%) and similarity percentage (≥97%) and were stored in a file format suitable for the taxonomic assignment steps. Finally, the Tango tool processed the similarity analysis data to assign the sequences to a taxonomic clade in the NCBI taxonomy. Statistically significant differences of the bacterial population in $Rag^{+/+}$ and $Rag2^{R229Q}$ mice were determined at family, genus, and species levels by using the R/Bioconductor DESeq package.

8.2.1 Cutaneous microbiota analysis

For the evaluation of cutaneous microbiota, weaned $Rag2^{+/+}$ and $Rag2^{R229Q}$ littermates were maintained in separated cages until analysis. Approximately 1-cm of cutaneous tissue was collected from the back of 10 $Rag2^{+/+}$ and 10 $Rag2^{R229Q}$ mice. Cutaneous tissues were weight and digested in lysis buffer (10 mM Tris, 100 mM NaCl, 10 mM EDTA, 0.5% SDS, and 0.4 mg/ml proteinase K). Total DNA was extracted with the isopropanol-ethanol method. The presence of bacterial DNA in all samples was verified by real-time PCR using specific primers for microbial 16s rRNA gene. Subsequently, the bacterial community structure of the DNA samples isolated from skin was profiled through by sequencing the V3 variable region (Illumina MiSeq technology) as described in [173]. The resulting sequence reads were managed by means of the pipeline Quantitative Insights Into Microbial Ecology (QIIME) version 1.7.0 with the GreenGenes database (version 13.5). To identify the specific bacterial taxa distinguishing the skin microbiota of $Rag2^{+/+}$ from $Rag2^{R229Q}$ mice, we used the linear discriminant analysis effect size (LEfSe) method.

8.22 Statistical analysis

Results were analyzed using the nonparametric Mann-Whitney test, Student's unpaired t test, and two-way ANOVA with Bonferroni post-test analysis. Results are presented as mean ± SEM. Values of $P < 0.05$ were considered statistically significant.

Table 2: List of primers used in the study

SyberGreen Primers	
Actb for	CTAAGGCCAACCGTGAAAAG
Actb rev	ACCAGAGGCATACAGGGACA
IL-17A for	TCCAGAAGGCCCTCAGACTA
IL-17A rev	TGAGCTTCCCAGATCACAGA
IFNγ for	TCAAGTGGCATAGATGTGGAAGAA
IFNγ rev	TGGCTCTGCAGGATTTTCATG
IL-22 for	TGACGACCAGAACATCCAGA
IL-22 rev	AATCGCCTTGATCTCTCCAC
IL-10 for	GGTTGCCAAGCCTTATCGGA
IL-10 rev	ACCTGCTCCACTGCCTTGCT
IL-5 For	ATCCAGGAACTGCCTCGTC
IL-5 Rev	ATCCAGGAACTGCCTCGTC
IL-13 For	CCTCTGACCCTTAAGGAGCTTAT
IL-13 Rev	CGTTGCACAGGGGAGTCT
IL-33 For	TCCTTGCTTGGCAGT
IL-33 Rev	TGCTCAATGTGTCAA
IL-6 for	GTAGCTATGGTACTCCAGAAGAC
IL-6 rev	ACGATGATGCACTTGCAGAA
TNFα for	GACGTGGAACTGGCAGAAGAG
TNFα rev	TTGGTGGTTTGTGAGTGTGAG
Reg3γ for	TTCCTGTCCTCCATGATCAAAA
Reg3γ rev	CATCCACCTCTGTTGGGTTCA
IL-1β for	GCCCATCCTCTGTGACTCAT
IL-1β rev	AGGCCACAGGTATTTTGTCG
CCL2 for	CTGGATCGGAACCAAATGAG
CCL2 rev	AAGGCATCACAGTCCGAGTC
CCL20 for	AACTGGGTGAAAAGGGCTGT
CCL20 rev	GTCCAATTCCATCCCAAAAA
CXCL10 for	GCTGCCGTCATTTTCTGC
CXCL10 rev	TCTCACTGGCCCGTCATC
CXCL9 for	CTTTTCCTCTTGGGCATCAT
CXCL9 rev	GCATCGTGCATTCCTTATCA
CCL5 for	GTGCCCACGTCAAGGGTAT
CCL5 rev	CCCACTTCTTCTCTCCTGGGTTG
CCL25 for	GAGTGCCACCCTAGGTCATC
CCL25 rev	CCAGCTGGTGCTTACTCTGA
16s for	GTGSTGCAYGGYTGTCGTCA
16s rev	ACGTCRTCCMCACCTTCCTC
18s for	CTCAACACGGGAAACCTCCTCAC
18s rev	CGCTCCACCAACTAAGAAGG
IL-4 for	CATCGGCATTTTGAACGAG
IL-4 rev	CGAGCTCACTCTCTGTGGTG
IL-23p19 for	AGCCAGTTCTGCTTGCAAAGG
IL-23p19 rev	GGAGGTTGTGAAGTTGCTCCATG
TGFβ for	TGGAGCAACATGTGGAACTC

TGFβ rev	GTCAGCAGCCGGTTACCA
IL-12p35 for	CTATCTGAGCTCCGCCTGAAAG
IL-12p35 rev	GGCCAAGACCACCTGACTCTTA
Jam-a for	AGAACAAAGAAAGGGACTGCAC
Jam-a rev	ACCAGGAACGACGAGGTCT
Occludin for	ATTCCGGCCGCCAAGGTTCG
Occludin rev	GCTGGCTGAGAGAGCATCGGC
Claudin-1 for	ACTGCCCTGCCCCAGTGGAA
Claudin-1 rev	TCAGCCCCAGCAGGATGCCA
Cramp For	AAGGAGACTGTATGTGGCAAGGCA
Cramp Rev	TTTCTTGAACCGAAAGGGCTGTGC
mBD-3 For	GTCAGATTGGCAGTTGTGGA
mBD-3 Rev	GCTAGGGAGCACTTGTTTGC
VEGF-A For	CAGGGCTTCATCGTTACAG
VEGF-A Rev	CATCTTCAAGCCGTCCTGT
TLR-2 For	AGCATCCTCTGAGATTTGA
TLR-2 Rev	GGGGCTTCACTTCTCTGCTT
TLR-3 For	TCCCCCAAAGGAGTACATT
TLR-3 Rev	GATACAGGGATTGCACCCA
TLR-4 For	GGACTCTGATCATGGCACTG
TLR-4 Rev	CTGATCCATGCATTGGTAGGT
TLR-5 For	CTGGAGCCGAGTGAGGTC
TLR-5 Rev	CGGCAAGCATTGTTCTCC
TLR-9 For	GAGAATCCTCCATCTCCCAAC
TLR-9 Rev	CCAGAGTCTCAGCCAGCAC
TSLP For	CAGCTTCGTCTCCTGA
TSLP Rev	AAATGTTTTGTCGGGGAGTG
CK5 For	CATTCTCAGCCGTGGTACG
CK5 Rev	CAGAGCTGAGGAACATGCAG
CK6 For	GTCCAGGACCTTGTTCTGCT
CK6 Rev	ATCCAGCGGGTCAGGACT
CCL22 For	CTGATGCAGGTCCTATGGT
CCL22 Rev	GGAGTAGCTTCTTCACCCAG
CCL17 For	TGCTTCTGGGGACTTTTCTG
CCL17 Rev	GAATGGCCCCTTTGAAGTAA

TaqMan Probes	
Actb	Mm00607939_s1
Rorc	Mm01261022_m1
Tbx21	Mm00450960_m1

9. RESULTS

9.1 Study of the intestinal pathology in Rag2^{R229Q} mice

9.1.1 Intestinal inflammation affects Rag2^{R229Q} mice

Analysis of intestinal disease in *Rag2^{R229Q}* mice revealed marked signs of intestinal inflammation but different degree of spontaneous colitis, wasting diarrhoea, and rectal prolapse. Approximately 5% of mutant mouse colony manifested rectal prolapse by 24 weeks of age. Histologically, colonic inflammation in *Rag2^{R229Q}* mice was characterized by epithelial hyperplasia, crypt elongation, and a large inflammatory infiltrate along the LP, with occasional crypt abscesses (**Figure 19A**). Several morphological alterations affected also the small intestine, including increased mucosal thickness and histological score with lower villus/crypt ratio (**Figure 19B-C**). Occasionally, large lymphoid aggregates containing $CD3^+$ T cells were observed in the peri-intestinal fat of *Rag2^{R229Q}* mice (data not shown). Moreover, immunophenotypic analysis demonstrated that intestinal LP infiltrates consisted of T cells, particularly of $CD4^+$, with very few $CD8^+$ T cells (**Figure 19D**). Furthermore, absolute counts of infiltrating T cells were three-six fold higher in mutant mice compared to controls, in sharp contrast with the overall lymphoid depletion observed in the other lymphoid organs, including thymus, spleen and lymph nodes (data not shown). The proportion of pro-inflammatory Th1/Th17 cells was enriched in the intestine of *Rag2^{R229Q}* mice compared to controls. Moreover, the IL-17/IFNγ double-producing population, frequently found in the intestine of patients with Crohn disease, was abundant in the mutant gut [174] (**Figure 19E-F**). To deeply characterize the intestinal inflammatory environment in *Rag2^{R229Q}* mice, we analysed the expression of several cytokines. Expression level of IFNγ, IL-17, IL-6, IL-2, IL-1β, IL-22 and TNFα were significantly up-regulated in both ileum and colonic tissues of *Rag2^{R229Q}* mice. On the contrary, IL-10 and IL-12p35 were significantly down-regulated, whereas IL-4, TGFβ and IL-23p19 did not change significantly (**Figure 19G**). Collectively, these results indicated that pathogenic Th1\Th17 cells mediate intestinal inflammation in *Rag2^{R229Q}* mice.

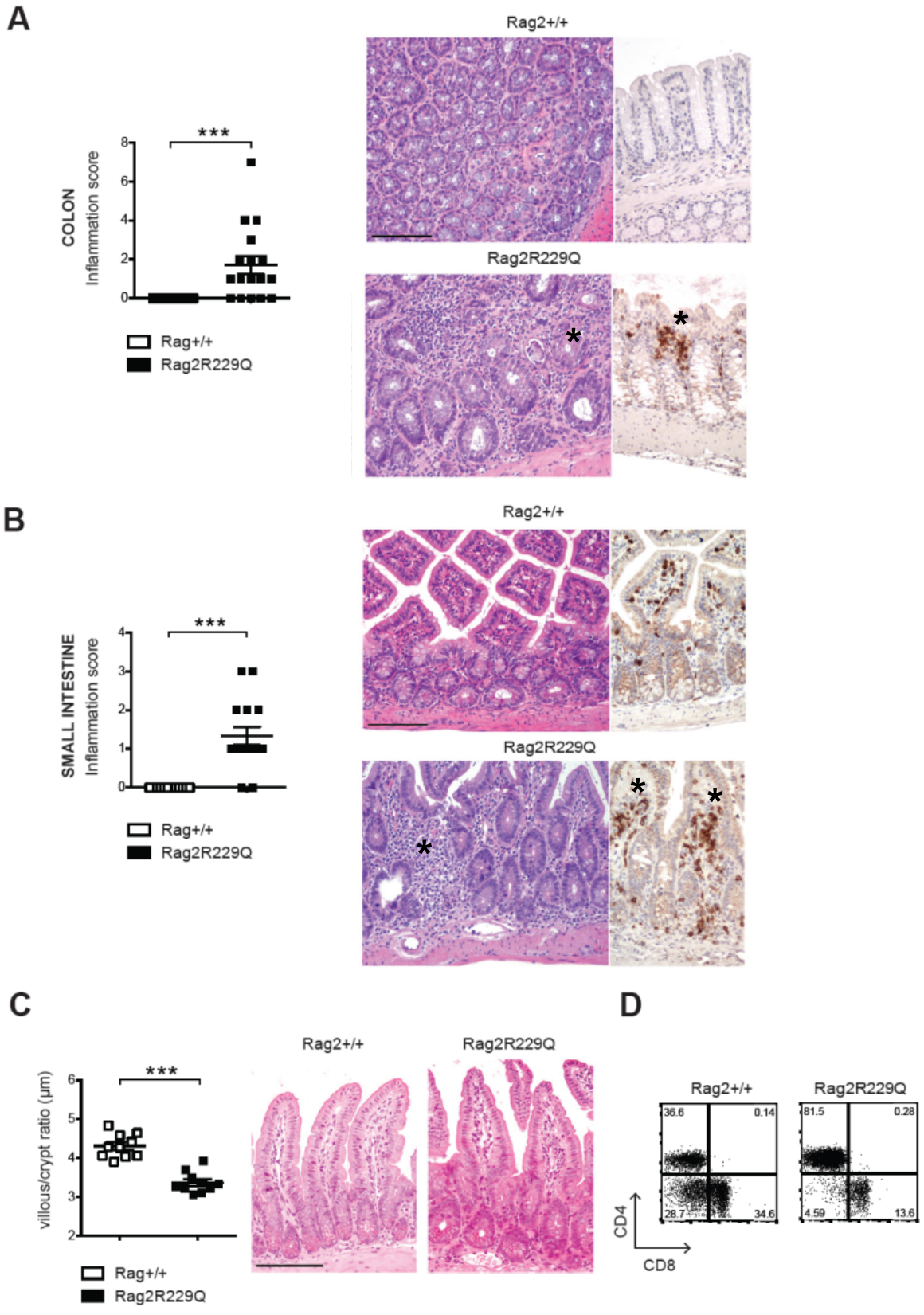
A
Rag2+/+
COLON
Inflammation score
***
8
6
4
2
0
Rag+/+
Rag2R229Q
Rag2R229Q
*
*
B
Rag2+/+
SMALL INTESTINE
Inflammation score
***
4
3
2
1
0
Rag+/+
Rag2R229Q
Rag2R229Q
*
*
*
C
villous/crypt ratio (µm)
***
6
5
4
3
2
Rag+/+
Rag2R229Q
Rag2+/+
Rag2R229Q
D
Rag2+/+
Rag2R229Q
36.6
0.14
28.7
34.6
81.5
0.28
4.59
13.6
CD4
CD8

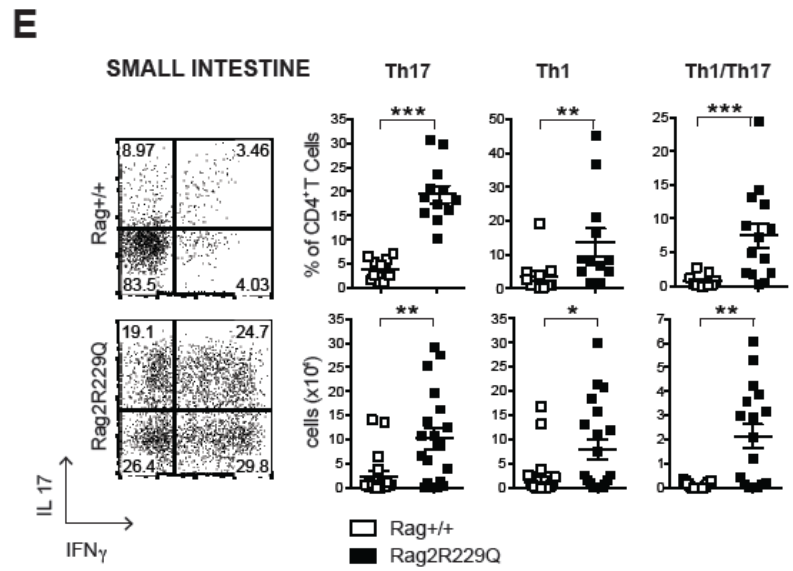
E
SMALL INTESTINE
Th17
Th1
Th1/Th17
Rag+/+
Rag2R229Q
8.97
3.46
83.5
4.03
19.1
24.7
26.4
29.8
IL 17
IFNγ
% of CD4+T Cells
cells (x10⁶)
Rag+/+
Rag2R229Q

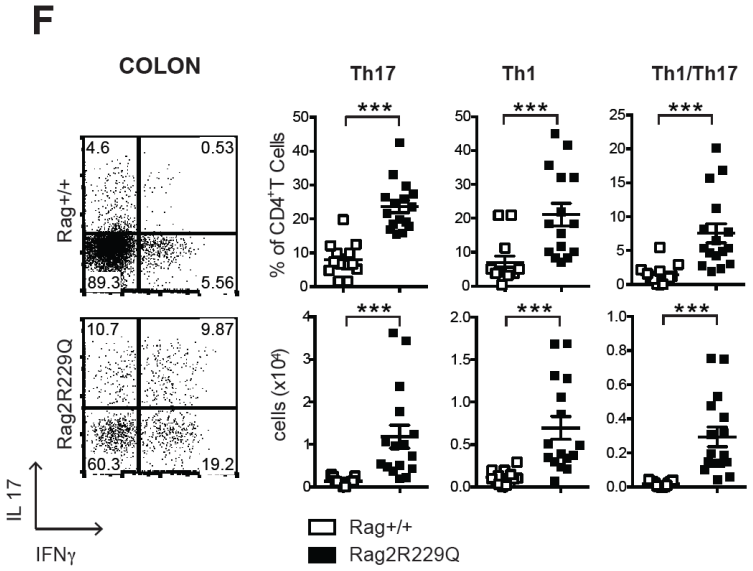
F
COLON
Th17
Th1
Th1/Th17
Rag+/+
Rag2R229Q
4.6
0.53
89.3
5.56
10.7
9.87
60.3
19.2
IL 17
IFNγ
% of CD4+T Cells
cells (x10⁶)
Rag+/+
Rag2R229Q

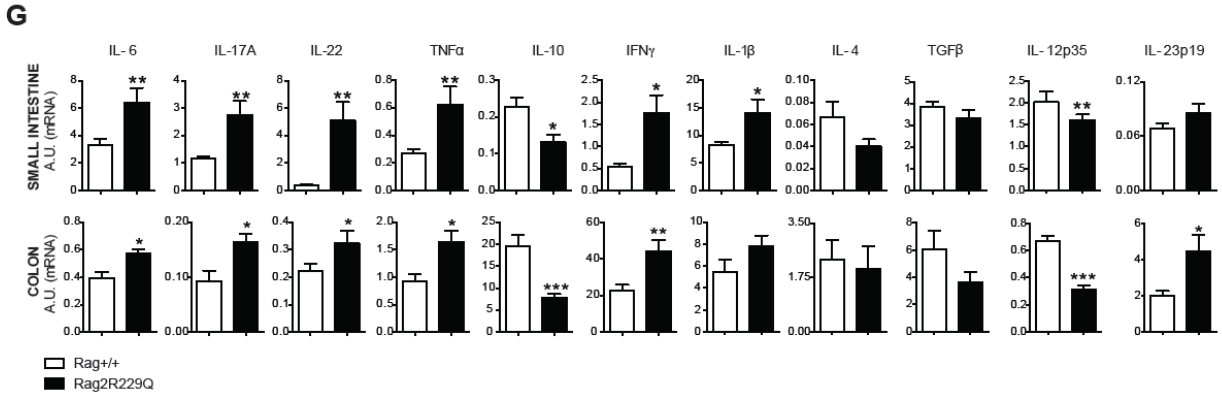
G
IL-6
IL-17A
IL-22
TNFα
IL-10
IFNγ
IL-1β
IL-4
TGFβ
IL-12p35
IL-23p19
SMALL INTESTINE
A.U. (mRNA)
COLON
A.U. (mRNA)
Rag+/+
Rag2R229Q

Figure 19: Characterization of intestinal inflammation in Rag2^{R229Q} mice. *Representative colonic (A) and SI (B) sections from Rag2^{R229Q} mice and controls stained with H&E and CD3 immunostaining. Graphs show the inflammatory scores. Asterisks indicate the area of infiltration. (C) Villus/crypt ratio and representative images of SI villi from Rag2^{R229Q} mice and controls. (D) Representative FACS dot plot of CD4/CD8 infiltrating intestinal LP. (E) Representative FACS dot plots, absolute counts and frequencies of Th17, Th1 and Th1/Th17 populations from SI and colonic LP. (G) Transcriptional expression of cytokines from SI and colonic tissues. RNA contents are shown as arbitrary units (A.U.). 8-12 week-old mice of indicated genotypes were analysed. Mann Whitney test; values are mean ± SEM. *, P < 0.05; **, P < 0.01; ***, P < 0.001.*

9.1.2 Rag2^{R229Q} CD4^{+} T cells have enhanced gut tropism and cause colitis

The migration to the intestinal mucosa requires the expression of specific gut homing receptors on T cells, the integrin α4β7 and the chemokine receptor CCR9 [175]. Consistently with the intestinal inflammation, we found increased frequency of CCR9 and a4b7-expressing CD4^{+} T cells in the MLNs of mutant mice compared to controls (**Figure 20A**). Interestingly, the proportion of CCR9 and a4b7-expressing splenic T cells was also augmented in *Rag2^{R229Q}* mice, indicating the peripheral dissemination of T cells activated within the intestine in mutant mice. To directly investigate whether CD4^{+} T cells could be sufficient to induce gut inflammation, we transferred total CD4^{+} T cells from *Rag2$^{+/+}$* and *Rag2^{R229Q}* MLNs into *Rag1$^{-/-}$* immunodeficient hosts. All mice transferred with *Rag2^{R229Q}* CD4^{+} T cells showed signs of colitis after 10 weeks. In particular, greater weight loss, colon shortening and high inflammatory score were detected in *Rag1$^{-/-}$* receiving mutant CD4^{+} T cells compared to mice receiving *wild-type* CD4^{+} T cells (**Figure 20B-C**). Of note, MLNs and spleens were enlarged in recipient mice receiving CD4^{+} T *Rag2^{R229Q}* cells (**Figure 20D**). Remarkably, in the MLNs of *Rag2^{R229Q}*-chimeric *Rag1$^{-/-}$* mice, we detected a prominent expansion of activated T cells (CD44^{hi}, CD45RB^{low}, CD25^{+}) with Th1/Th17 skewing, resembling the inflammatory state typical of *Rag2^{R229Q}* condition (**Figure 20E**). Interestingly, the analysis of the cytokine profile of chimeric *Rag1$^{-/-}$* mice revealed two to five fold increased level of IL-2, IFNγ, IL-17 and TNFα in the colonic supernatants of *Rag2^{R229Q}*-chimeric *Rag1$^{-/-}$* mice compared to *Rag2$^{+/+}$*-chimeric *Rag1$^{-/-}$* controls. On the contrary, the expression level of IL-4 and IL-10 were markedly reduced (**Figure 20F**).

Collectively, these results suggested that mutant $CD4^+$ T cells are sufficient to transfer the disease into immunodeficient host.

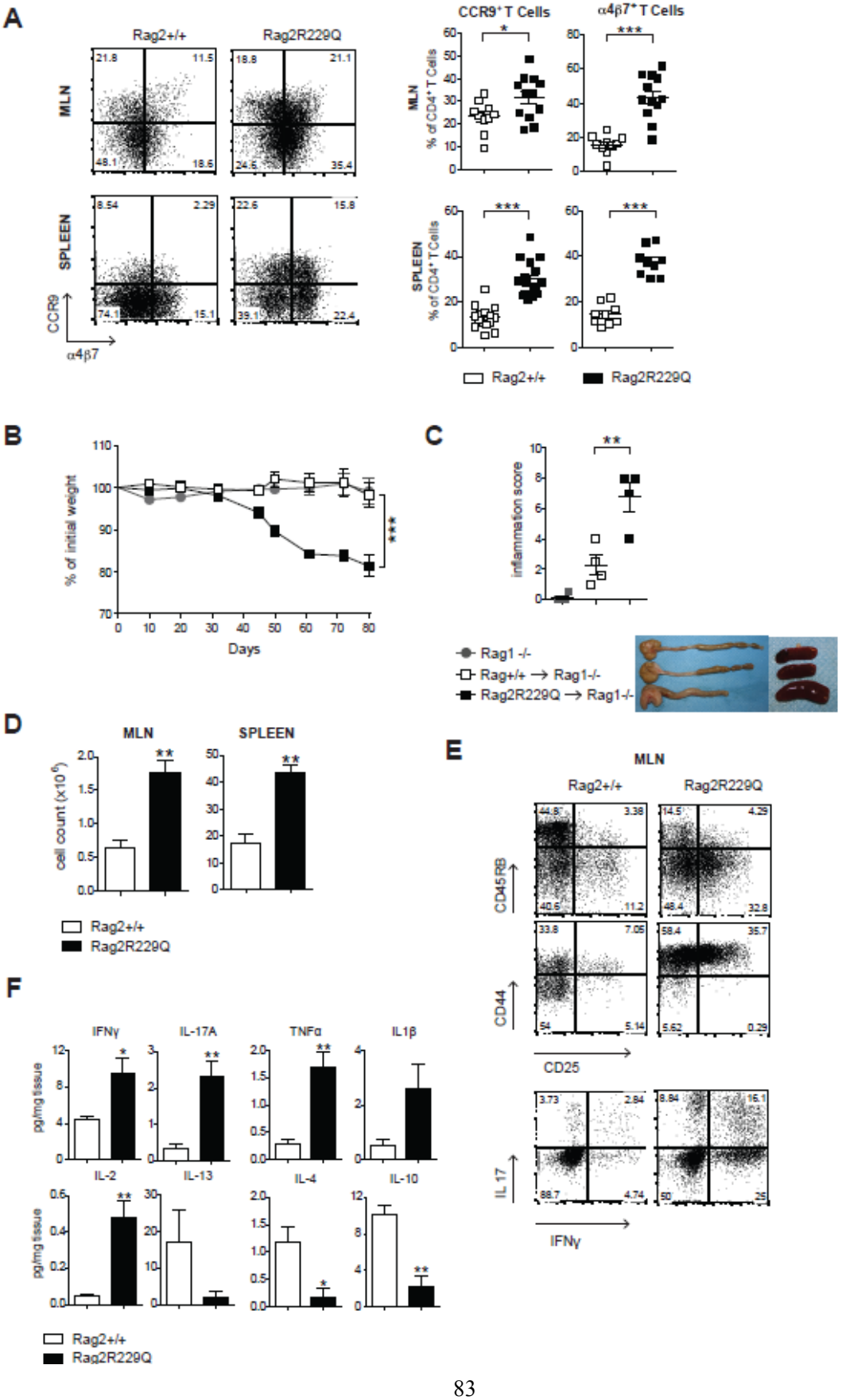

Figure 20: Rag2^{R229Q} CD4^{+} T cells transfer the disease into Rag1$^{-/-}$ mice. *A) FACS dot plots and frequencies of CCR9^{+} and α4β7-expressing CD4^{+} T cells derived from MLNs and spleen of Rag2^{R229Q} mice and wild-type mice. B) Body weight loss (%) of control Rag1$^{-/-}$ mice and Rag1$^{-/-}$ mice receiving Rag2$^{+/+}$and Rag2^{R229Q} total CD4^{+} T cells. C) Inflammatory score of colons at sacrifice. Representative images of macroscopic observation in colons and spleens. (D) Total cellularity of MLNs and spleens derived from Rag1$^{-/-}$ mice receiving Rag2$^{+/+}$and Rag2^{R229Q} total CD4^{+} T cells. E) Representative FACS dot plots of immune-phenotype of total CD4^{+} T cells isolated from MLNs. (F) Cytokine profile of cultured colonic tissues. RNA contents are shown as arbitrary units (A.U.). 8-12 week-old mice of indicated genotypes were analysed. Mann Whitney test; values are mean ± SEM. *, P < 0.05; **, P < 0.01; ***, P < 0.001.*

9.1.3 Treg impairment contributes to intestinal inflammation in Rag2^{R229Q} mice

In the gastrointestinal tract, regulatory T cells play a crucial role in maintaining immune homeostasis and promoting tolerance against intestinal antigens and commensal bacteria [176]. Interestingly, we detected higher absolute count and frequency of Foxp3^{+} GITR^{+} Treg cells in the mutant SI and colonic LP compared to controls. However, Treg cells were augmented only in frequency in the MLNs, underlying that Treg expansion represented a unique feature of the LP compartment (**Figure 21A**).

To understand whether mutant Tregs were able to suppress intestinal inflammation *in vivo*, we employed the experimental model of colitis induced by adoptive transfer of naïve CD45RB^{hi} cells in immunodeficient hosts. In particular, we transferred *wild-type* CD4^{+}CD45RB^{hi} into the *Rag1$^{-/-}$* mice, in presence or absence of CD4^{+}CD25^{hi} Tregs derived from *Rag2$^{+/+}$* and *Rag2^{R229Q}* mice. Recipient mice were sacrificed after 4 weeks. As expected, mice co-transferred with naïve T cells and *wild-type* Tregs showed reduced signs of colitis (**Figure 22A**). On the contrary, mutant Tregs failed to control efficiently intestinal inflammation in *Rag1$^{-/-}$* mice. These findings indicated that Treg function was compromised in *Rag2^{R229Q}* mice. To directly assess whether the gut inflammation could be a consequence of Treg impairment, we adoptively transferred *wild-type* Tregs into *Rag2^{R229Q}* mice. Specifically, recipient mice were injected i.v. with CD4^{+}CD25^{hi}GITR^{+} cells derived from *wild-type* 45.1 and were followed for 4 weeks (**Figure 22B**). Remarkably, at the sacrifice we observed amelioration of intestinal inflammation, characterized by reduced lymphocytic infiltration as well as decreased frequency of mucosal Th1/Th17 cells (**Figure 22C-E**). Consistently, lower expression

of IL-17 and IFNγ was detected in the intestinal tissue of Treg transferred-*Rag2*^{R229Q} mice (**Figure 22F**). These data indicated that transfer of *wild-type* Tregs could attenuate gut inflammation by reducing Th1/Th17 immune responses and confirmed that mutant Tregs failed to control colitis.

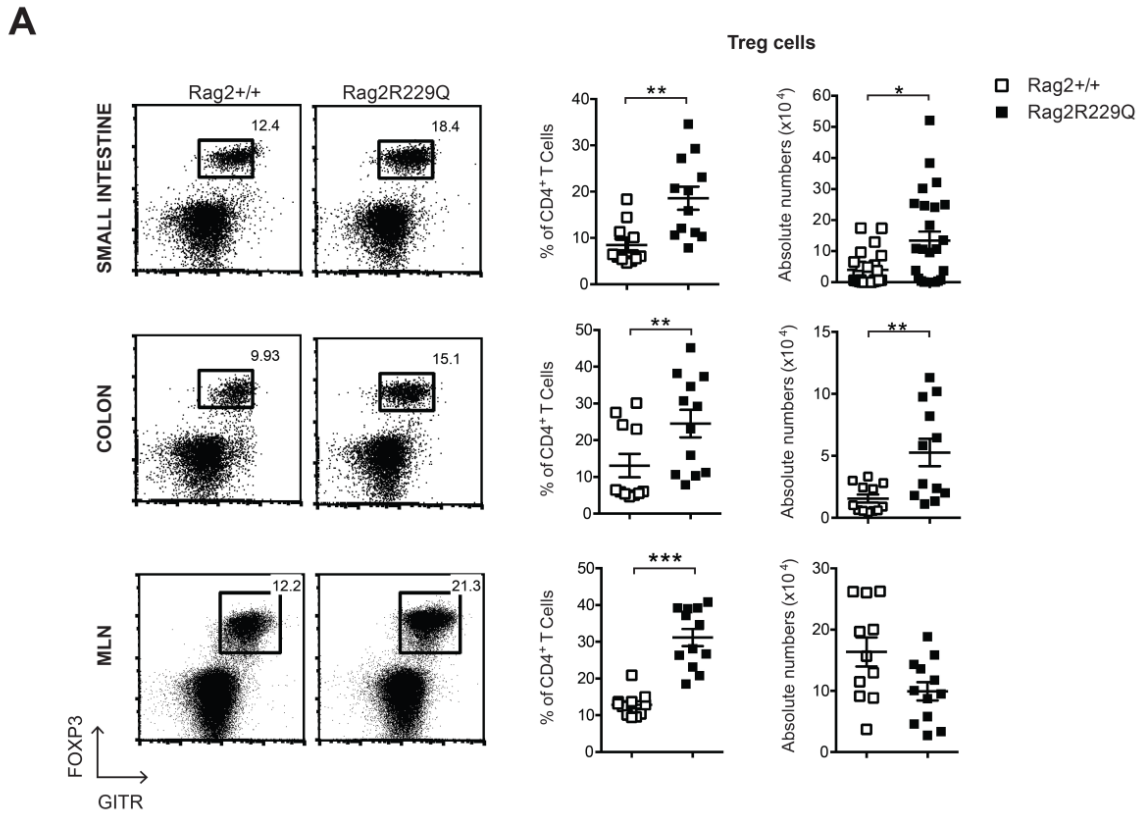

Figure 21: Treg expansion in the gut of Rag2^{R229Q} mice. *A) Representative FACS dot plots, frequencies and absolute counts of Foxp3^{+} GITR^{+} Treg cells in the SI, colon and MLNs. 8-12 week-old mice of indicated genotypes were analysed. Mann Whitney test; values are mean ± SEM. *, P < 0.05; **, P < 0.01; ***, P < 0.001.*

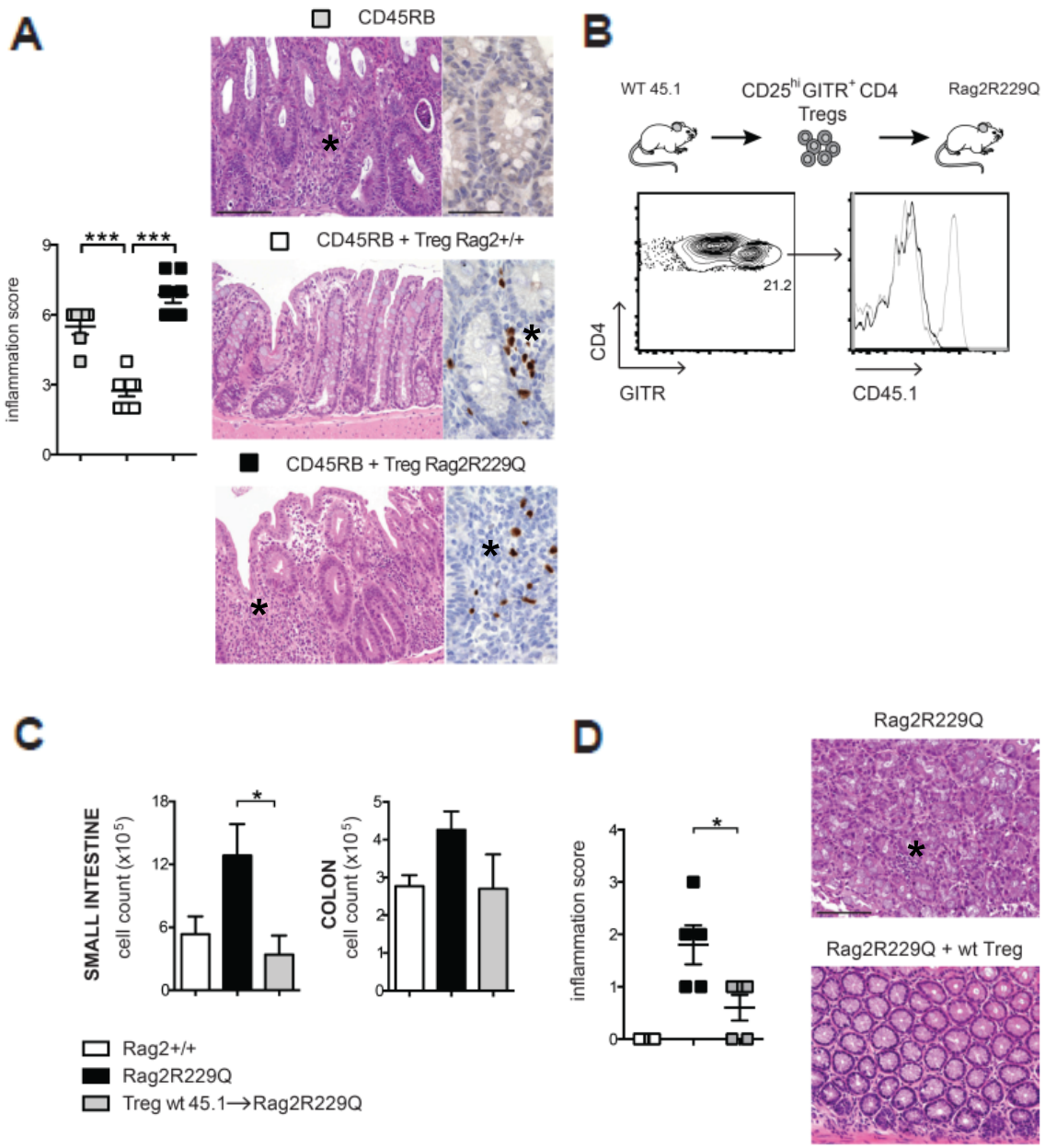
A
CD45RB
CD45RB + Treg Rag2+/+
CD45RB + Treg Rag2R229Q
inflammation score
***
***
B
WT 45.1
CD25hi GITR+ CD4 Tregs
Rag2R229Q
21.2
CD4
GITR
CD45.1
C
SMALL INTESTINE
cell count (x10^5)
COLON
cell count (x10^5)
Rag2+/+
Rag2R229Q
Treg wt 45.1→Rag2R229Q
D
inflammation score
Rag2R229Q
Rag2R229Q + wt Treg

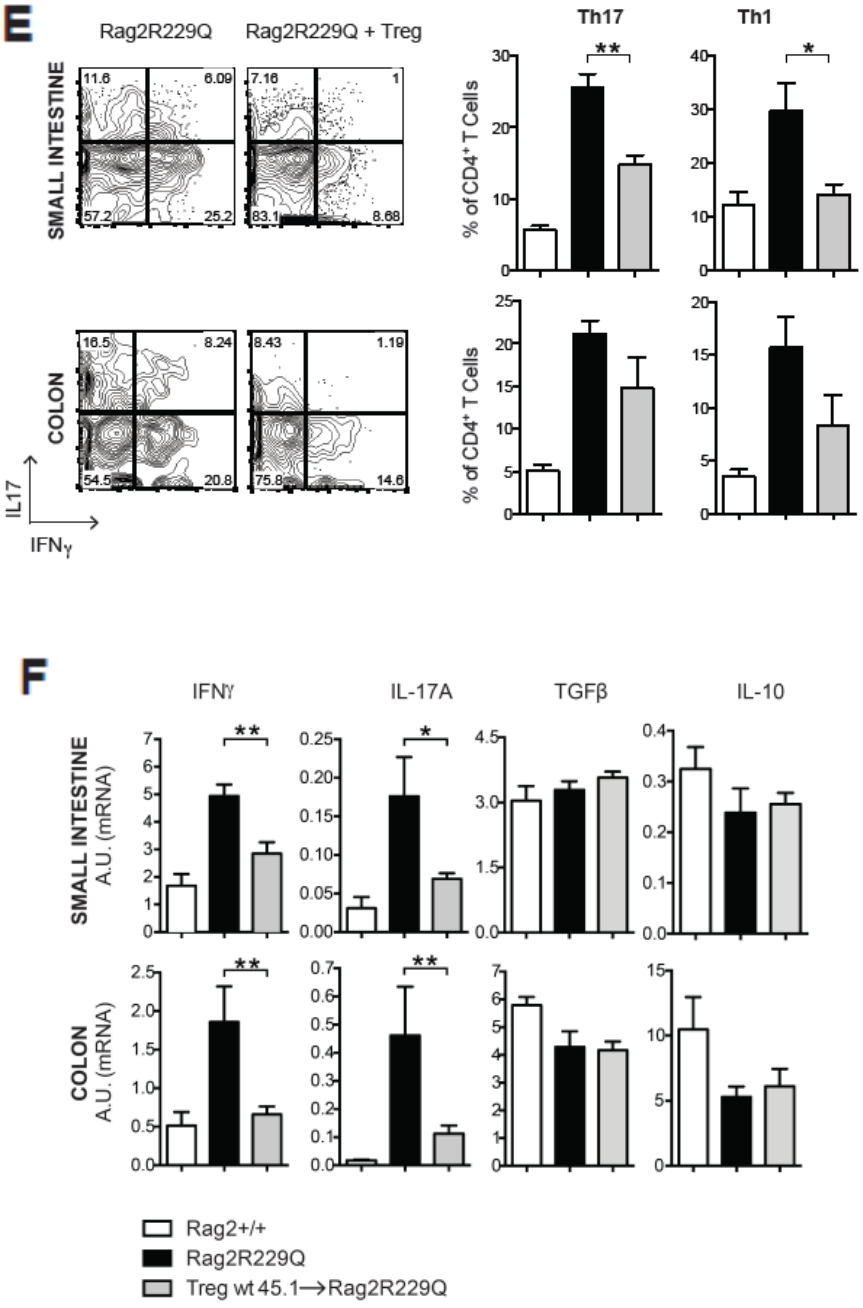

Figure 22: Treg impairment in Rag2^{R229Q} mice. *A) Colitis score and representative colonic sections from Rag1$^{-/-}$ transferred with CD45RB^{hi} alone or with Rag2$^{+/+}$ and Rag2^{R229Q} Tregs. Asterisks indicate the area of infiltration. B) Wild-type Tregs were adoptively transferred into Rag2^{R229Q} mice. C) Lymphocytes counts in the SI and colon. D) Representative colonic sections stained with H&E and colitis score in Treg cell transfer group and controls. Asterisk indicates the area of infiltration. E) Representative FACS dot plots and frequencies of LP Th17 and Th1 from SI and colon. F) Transcriptional expression of several cytokines. RNA contents are shown as*

*arbitrary units (A.U.). 8-12 week-old mice of indicated genotypes were analysed. Mann Whitney test; values are mean ± SEM. *, P < 0.05; **, P < 0.01; ***, P < 0.001.*

9.1.4 B cells are required to maintain intestinal homeostasis and avoid bacterial translocation in Rag2^{R229Q} mice

Mucosal IgA regulate the function and the composition of the intestinal microbiota to maintain mutualism between the host and the commensal bacteria [177]. In contrast to T cells, B cells were poorly present in the intestine of *Rag2*^{R229Q} mice, as shown by the lack of Peyer's Patches and the nearly absence of B220^{+} cells infiltrating the intestinal LP (**Figure 23A**). In agreement, we found reduced level of faecal IgA and IgM, suggesting a general B cell deficiency at the mucosal interfaces (**Figure 23B**). As expected, a marked reduction of IgA-coated bacteria was detected in the colon of mutant mice (**Figure 23C**). A recent study demonstrated the lack of IgA correlates with higher level of serum LPS [178]. In this regard, we found augmented adherent bacteria to the ileum mucosa, measured as a ratio between prokaryotic to eukaryotic DNA, and increased concentration of serum LPS (**Figure 23G-H**). These findings indicated that B cell deficiency associates to enhanced translocation of bacterial products from the intestinal lumen to the periphery. To better unravel the contribution of B cells in the intestinal disease pathogenesis, we transferred *wild-type*-B cells in mutant mice. Indeed, *wild-type*- CD19^{+}IgM^{+}IgD^{+} B cells from pooled spleens, lymph nodes and Peyer's Patches were isolated and injected into *Rag2*^{R229Q} mice (**Figure 23D**). IgA-producing plasma cells were generated rapidly in B cell-transferred group (**Figure 23E**). In response to elevated IgA levels, we detected a normalization of Reg3γ in the ileum tissue of B cell-transferred mutant mice, normally up-regulated in the intestinal tissue (**Figure 23F**). Interestingly, we found reduced mucosal adherent bacteria and lower LPS translocation in B cell transfer mutant group (**Figure 23G-H**). Moreover, reduced stimulation of intestinal mucosa attenuated the colonic inflammation in mutant mice (**Figure 23I**). Overall these results indicated that B cell compartment is essential but not sufficient to maintain intestinal homeostasis.

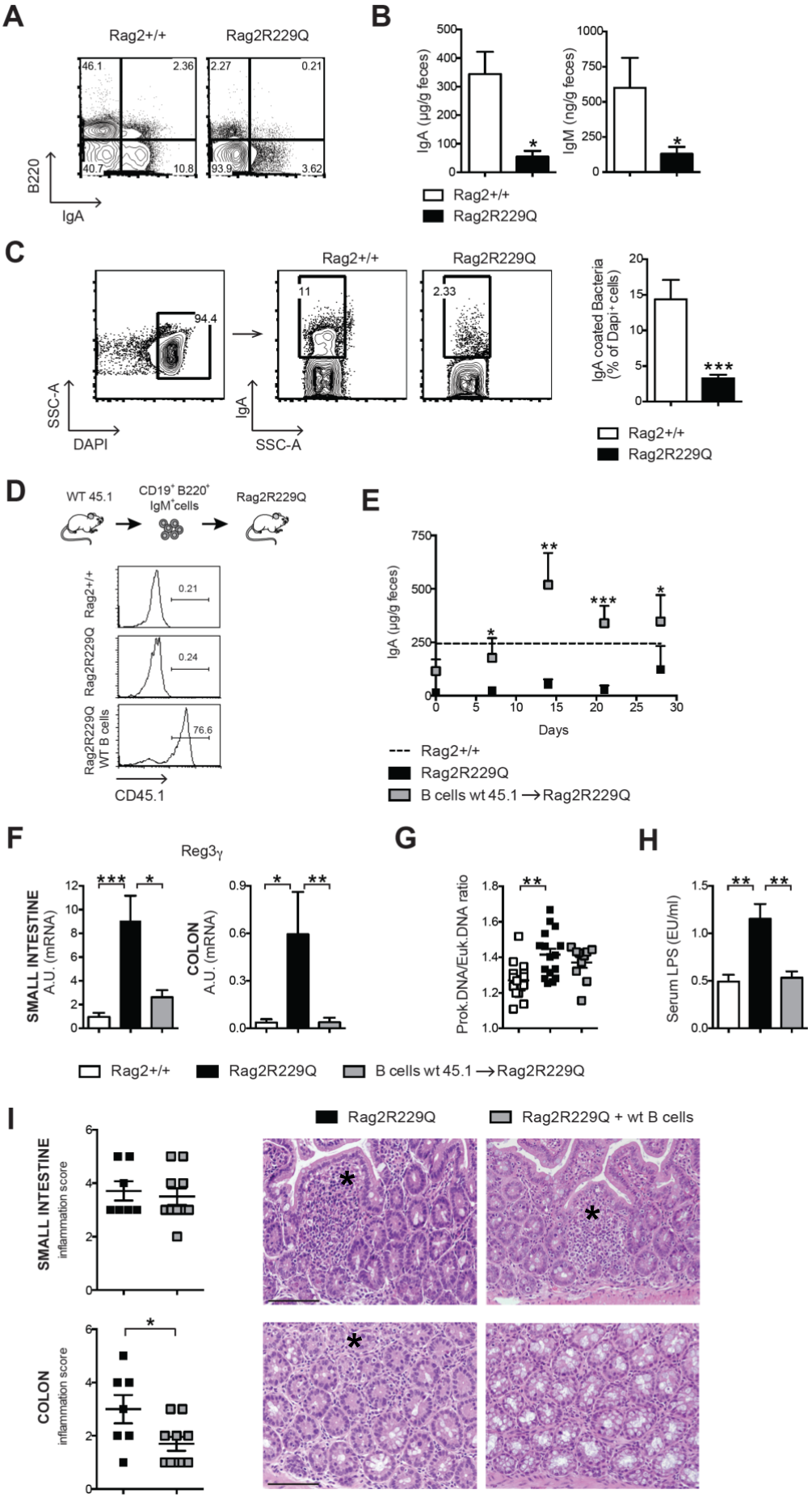
A
Rag2+/+
Rag2R229Q
46.1
2.36
40.7
10.8
2.27
0.21
93.9
3.62
B220
IgA
B
IgA (µg/g feces)
IgM (ng/g feces)
Rag2+/+
Rag2R229Q
C
Rag2+/+
Rag2R229Q
94.4
11
2.33
SSC-A
DAPI
IgA
SSC-A
IgA coated Bacteria (% of Dapi+ cells)
Rag2+/+
Rag2R229Q
D
WT 45.1
CD19+ B220+ IgM+cells
Rag2R229Q
Rag2+/+
Rag2R229Q
Rag2R229Q WT B cells
0.21
0.24
76.6
CD45.1
E
IgA (µg/g feces)
Days
Rag2+/+
Rag2R229Q
B cells wt 45.1 → Rag2R229Q
F
Reg3γ
SMALL INTESTINE A.U. (mRNA)
COLON A.U. (mRNA)
Rag2+/+
Rag2R229Q
B cells wt 45.1 → Rag2R229Q
G
Prok.DNA/Euk.DNA ratio
H
Serum LPS (EU/ml)
I
SMALL INTESTINE inflammation score
COLON inflammation score
Rag2R229Q
Rag2R229Q + wt B cells

Figure 23: Mucosal B cell deficiency in Rag2^{R229Q} mice. *A) Representative FACS dot plots of B cells-infiltrating intestinal LP of Rag2^{R229Q} mice and controls. B) ELISA of faecal IgA and IgM. C) Representative FACS dot plots and frequencies of IgA-coated bacteria derived from faeces of Rag2^{R229Q} and controls. D) Experimental procedure: wild-type-30*10^6 CD19$^+$B220$^+$IgM$^+$ B cells were transferred into Rag2^{R229Q} mice. Flow cytometry shows the percentage of B cells in the intestine of Rag2^{R229Q} mice after B cell transfer. E) Time course of faecal IgA levels after B cell transfer. F) Transcriptional expression of Reg3γ from SI and colonic tissues. G) Prokaryotic/eukaryotic ratio. H) Serum concentration of LPS. I) Representative SI and colon sections of B cell-transferred Rag2^{R229Q} and controls stained with H&E. Graphs represent the inflammatory score. Asterisks indicate the area of infiltration. 8-12 week-old mice of indicated genotypes were analysed. Mann Whitney test; values are mean ± SEM. *, P < 0.05; **, P < 0.01; ***, P < 0.001.*

9.1.5 Rag2^{R229Q} mice show altered microbial composition

Diversified IgAs contribute to maintenance of heterogeneous and balanced intestinal microbiota [104]. To explore whether *Rag2^{R229Q}* condition could be characterized by microbial alterations, we evaluated the microbiota composition in mutants and their cohoused *wild-type* littermates, by 16s sequencing of bacterial DNA extracted from caecal contents. By this approach, we investigated the relative abundance and the diversity of bacterial taxa in the microbiota profiles of *Rag2^{R229Q}* and *Rag2$^{+/+}$* mice.

Importantly, no substantial differences in the relative abundance of the dominant intestinal taxa were found (Actinobacteria, Bacteriodetes, Firmicutes and Proteobacteria) (data not shown). However, considerably less bacterial diversity at the family and genus levels was detected in *Rag2^{R229Q}* mice versus controls, as determined by the Shannon and the Chao1 index of α-diversity (**Figure 24A**).

Furthermore, hierarchical clustering based on the relative abundance of bacteria indicated that *Rag2^{R229Q}* and *Rag2$^{+/+}$* mice formed clusters according to the genotypes (**Figure 24B**). Moreover, we performed a partial least squares (PLS1) regression analysis to identify the bacterial taxa that better represented the difference between *Rag2^{R229Q}* mice and controls. The analysis took into consideration the overall composition of the intestinal microbiota, using genotypes as categorical responses and the relative abundance of bacterial genera as continuous predictors. PLS1 analysis confirmed the reduced bacterial richness that characterized *Rag2^{R229Q}* mice. Furthermore, the analysis revealed an important enrichment of several genera of the

phylum Proteobacteria, previously associated to IBD [179], in the mutant intestinal microbiota (**Figure 24C**). Overall these findings revealed that mutant microbiota exhibit less microbial diversity and high abundance of Proteobacteria

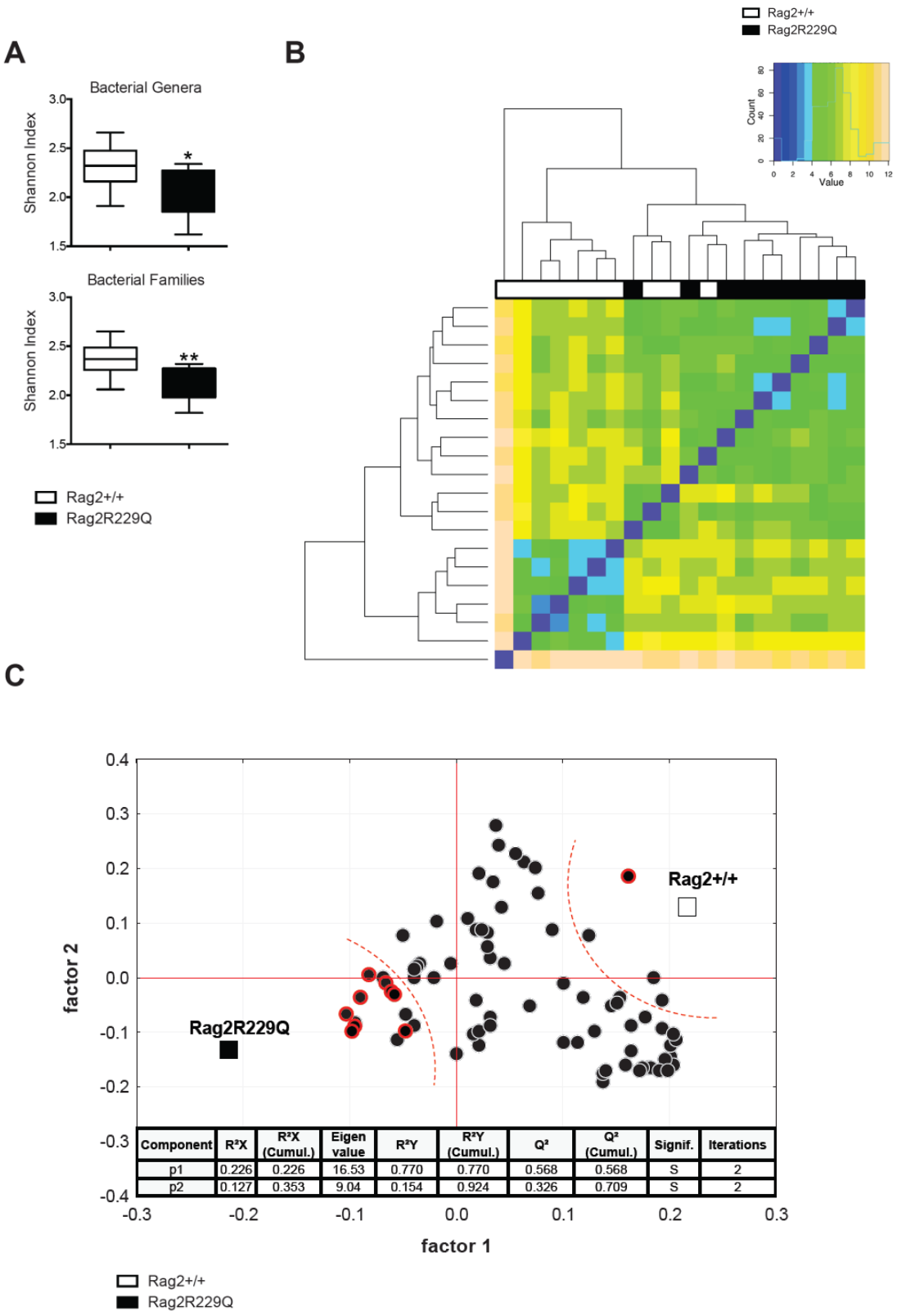

Figure 24: Altered microbiota composition in Rag2^{R229Q} mice. *A) Box and whisker plots of the Shannon diversity index at the bacterial genera and family level in Rag2$^{+/+}$ and Rag2^{R229Q} mice. B) Heatmap of the relative abundance of each bacterial family from sequencing of faecal samples of Rag2$^{+/+}$ mice and Rag2^{R229Q} mice. C) Correlation between mouse genotype and bacterial genera in faecal samples of Rag2$^{+/+}$ mice and Rag2^{R229Q} mice. X-and Y loading plots (factors 1 and 2) were obtained by partial least squares performed by using the genotype as categorical response and the relative abundance of bacterial genera as continuous predictors. Taxa belonging to the phylum Proteobacteria was showed with red circle. 8-12 week-old mice of indicated genotypes were analysed. (A) Mann Whitney test; *, P < 0.05; **, P < 0.01.*

9.1.6 Long-term antibiotic treatment dampens intestinal inflammation in Rag2^{R229Q} mice

To directly assess the role of commensal bacteria in the pathogenesis of gut inflammation, we depleted intestinal microbiota of *Rag2^{R229Q}* mice and controls, using a broad spectrum of antibiotics containing Ampicillin, Vancomycin and Metronidazole, given daily by oral gavage for four weeks. In antibiotic (ABX)-treated mutant mice, we found attenuated intestinal inflammation, characterized by a reduction of lymphocytic infiltrate as well as mucosal Th1/Th17 populations (**Figure 25A-C**). The proportion of these populations was low and unaffected in ABX *Rag2$^{+/+}$* mice. Interestingly, intestinal expression level of several inflammatory chemokines, including *cxcl9*, *cxcl10*, *ccl20*, *ccl2* and *ccl5* resulted normalized upon ABX treatment in *Rag2^{R229Q}* mice. Likewise, transcript level of *ccl25*, the chemokine supporting the recruitment of CCR9-expressing T cells to the small intestine [180], decreased to *wild-type* level in treated mutants (**Figure 25D**). All these results indicated that reduced bacterial load had a beneficial effect on mucosal inflammation.

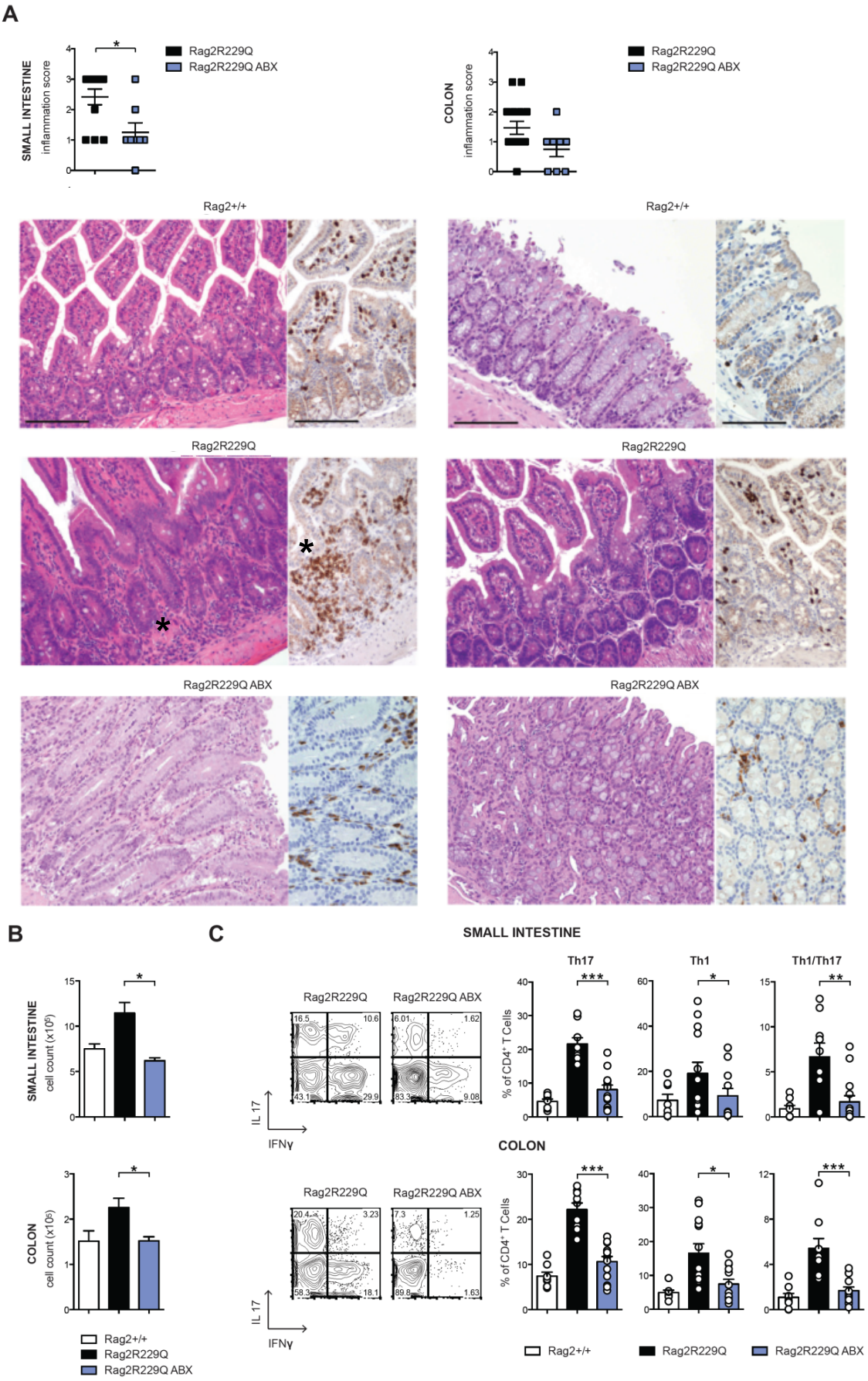
A
SMALL INTESTINE
inflammation score
Rag2R229Q
Rag2R229Q ABX
COLON
inflammation score
Rag2R229Q
Rag2R229Q ABX
Rag2+/+
Rag2+/+
Rag2R229Q
Rag2R229Q
Rag2R229Q ABX
Rag2R229Q ABX
B
SMALL INTESTINE
cell count (x10⁵)
COLON
cell count (x10⁵)
Rag2+/+
Rag2R229Q
Rag2R229Q ABX
C
SMALL INTESTINE
Th17
Th1
Th1/Th17
Rag2R229Q
Rag2R229Q ABX
16.5
10.6
43.1
29.9
6.01
1.62
83.3
9.08
IL 17
IFNγ
% of CD4⁺ T Cells
COLON
20.4
3.23
58.3
18.1
7.3
1.25
89.8
1.63
Rag2+/+
Rag2R229Q
Rag2R229Q ABX

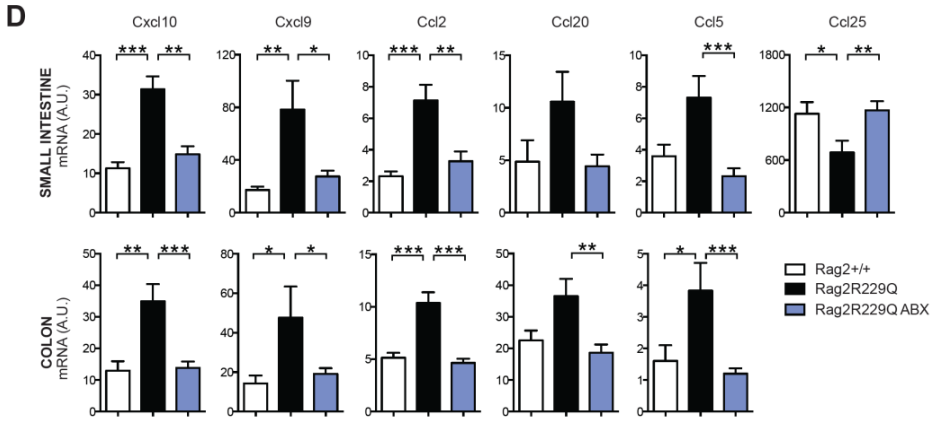

Figure 25: Long-term antibiotics attenuate intestinal inflammation in Rag2^{R229Q} mice. *(A) Representative SI and colonic section from ABX treated- Rag2^{R229Q} mice and controls stained with H&E and CD3 immunostaining. Graphs show the inflammatory scores after ABX treatment. Asterisks indicate the area of infiltration. (B) Cell counts of lymphocytes infiltrating SI and colonic LP. (C) Representative FACS dot plots, absolute counts and frequencies of Th1, Th17 and Th1/Th17 populations from SI and colon of ABX treated- Rag2^{R229Q} mice and controls. (D) Expression level of many cytokines in intestinal tissue. 8-12 week-old mice of indicated genotypes were analysed. Mann Whitney test; values are mean ± SEM. *, P < 0.05; **, P < 0.01; ***, P < 0.001.*

9.1.7 Absence of TLR microbial recognition do not reduce the intestinal inflammation in Rag2^{R229Q} mice

To specifically investigate the role of MyD88-dependent microbial recognition in the intestinal pathogenesis, we generated *Rag2^{R229Q}* mice carrying a complete deficiency in MyD88, the adaptor molecule common to most TLRs. Accumulating evidence demonstrated that Myd88 is essential for the induction of inflammatory cytokines, modulating both innate and adaptive immune responses [181]. Lymphocyte composition was not altered in *Myd88$^{-/-}$* mice compared to *Rag2$^{+/+}$* mice. Importantly, like mutant mice, *Rag2^{R229Q}* x *Myd88$^{-/-}$* mice showed intestinal disease as well as lymphocytic infiltration in the intestinal LP (**Figure 26A-B**). Remarkably, the lack of MyD88 affected Th1 but not Th17 T cell skewing, suggesting that Th17 generation might be independent by TLR-Myd88 mediated pathways (**Figure 26C**). Consistently, the expression of the transcription factor Tbet was lower on intestinal CD4^{+} T cells in *Rag2^{R229Q}* x *Myd88$^{-/-}$* compared to *Rag2^{R229Q}* mice (**Figure 26D**). These results indicated

that deficiency in the adaptor molecule MyD88 did not protect *Rag2*^{R229Q} mice from intestinal inflammation.

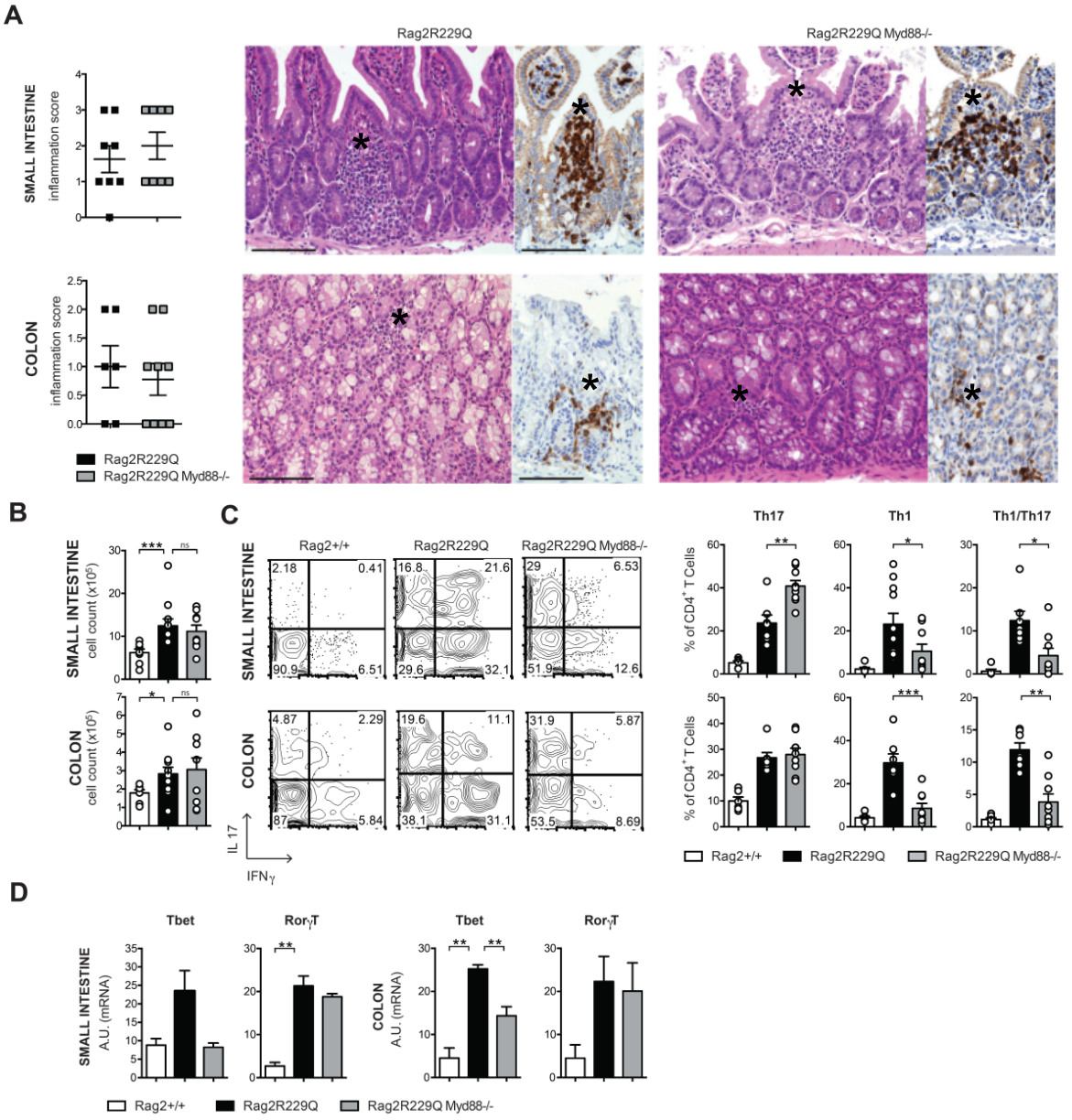

Figure 26: Myd88 deficiency affects only Th1 population in Rag2^{R229Q} mice*. A) Representative SI and colonic section from Rag2^{R229Q} and Rag2^{R229Q} x Myd88 $^{-/-}$ mice. Graphs represent the inflammatory scores. Asterisks indicate area of infiltration. B) Cell counts of lymphocytes from SI and colon. C) Representative FACS dot plots and frequencies of Th17, Th1 and Th1/Th17 cells from the intestine of Rag2^{R229Q} and Rag2^{R229Q} x Myd88 $^{-/-}$ mice. D) mRNA expression of Tbet and RorγT on sorted CD4^{+} cells from SI and colon. 8-12 week-old mice of indicated genotypes were analysed. Mann Whitney test; values are mean ± SEM. *, P < 0.05; **, P < 0.01; ***, P < 0.001.*

9.1.8 Long-term antibiotics treatment ameliorates systemic autoimmunity in Rag2^{R229Q} mice

To explore whether the effects of antibiotic treatment could extend beyond the gastrointestinal tract, we looked at the peripheral immune cell compartment. We observed reduced frequency of splenic Th1/Th17 and CCR9-expressing T cells in ABX-treated mutant mice, demonstrating a role for microbial signals in the maintenance of peripheral activated T cells (**Figure 27A-B**). The proportion of these populations was unaffected in ABX-treated *Rag2*$^{+/+}$mice. Interestingly, splenic GITR^{+} T cells were also reduced in ABX-treated mutant mice, indicating that most Treg cells were induced by commensal bacteria in *Rag2*^{R229Q} mice (**Figure 27C**). Moreover, ABX-treated mutant mice showed lower serum level of IFNγ and TNFα compared to controls (**Figure 27D**). Previous findings revealed extensive lymphocytic infiltration in target organs, including skin, kidney, liver and lung, which contribute to the systemic autoimmunity of *Rag2*^{R229Q} mice [65]. To assess whether long-term antibiotics attenuated the disease, we analysed tissue T cell infiltration. Remarkably, a significant reduction of CD3^{+} T cells infiltrating target organs was observed in ABX-treated mutant mice (**Figure 27E**). Consistently, we observed lower tissue expression of recruiting chemokines (*cxcl10* and *ccl2)* (**Figure 27F**). On the contrary, skin infiltration was not affected by ABX treatment, suggesting that additional independent pathogenic mechanisms contribute to determine cutaneous inflammation in mutant mice (data not shown). Importantly, reducing bacterial load normalized the serum IgE levels, the clinical hallmark of OS disease. A similar trend was observed for IgA and IgG, but not for IgM (**Figure 27G**). Collectively, these results indicated that reducing bacterial load attenuates systemic inflammation in *Rag2*^{R229Q} mice.

Next, to directly assess the pathogenicity of mutant intestinal microbiota independently of the host susceptibility, we performed experiments of faecal transplant by transferring mutant microbiota in *wild-type* recipients. Specifically, recipient mice were previously treated with long-term antibiotic treatment to deplete the resident microbiota. Then, faecal pellets were inoculated into recipient mice by oral gavage. Interestingly, re-colonization of *wild-type* mice with *Rag2*^{R229Q} faeces favoured the development of mucosal and splenic Th1/Th17 cells (**Figure 28A**). On the contrary, *Rag2*^{R229Q} mice colonized with *wild-type* microbiota attenuated significantly the Th1/Th17 profile both in the intestinal and systemic compartment. Interestingly, *Rag2*^{R229Q} mice colonized

with *Rag2*^{R229Q} microbiota further increased the intestinal and systemic inflammation (**Figure 28A**). Overall these data suggested that intestinal microbiota of *Rag2*^{R229Q} mice may be responsible for inflammatory exacerbation and shape both mucosal and systemic T cell responses towards Th1/Th17 skewing.

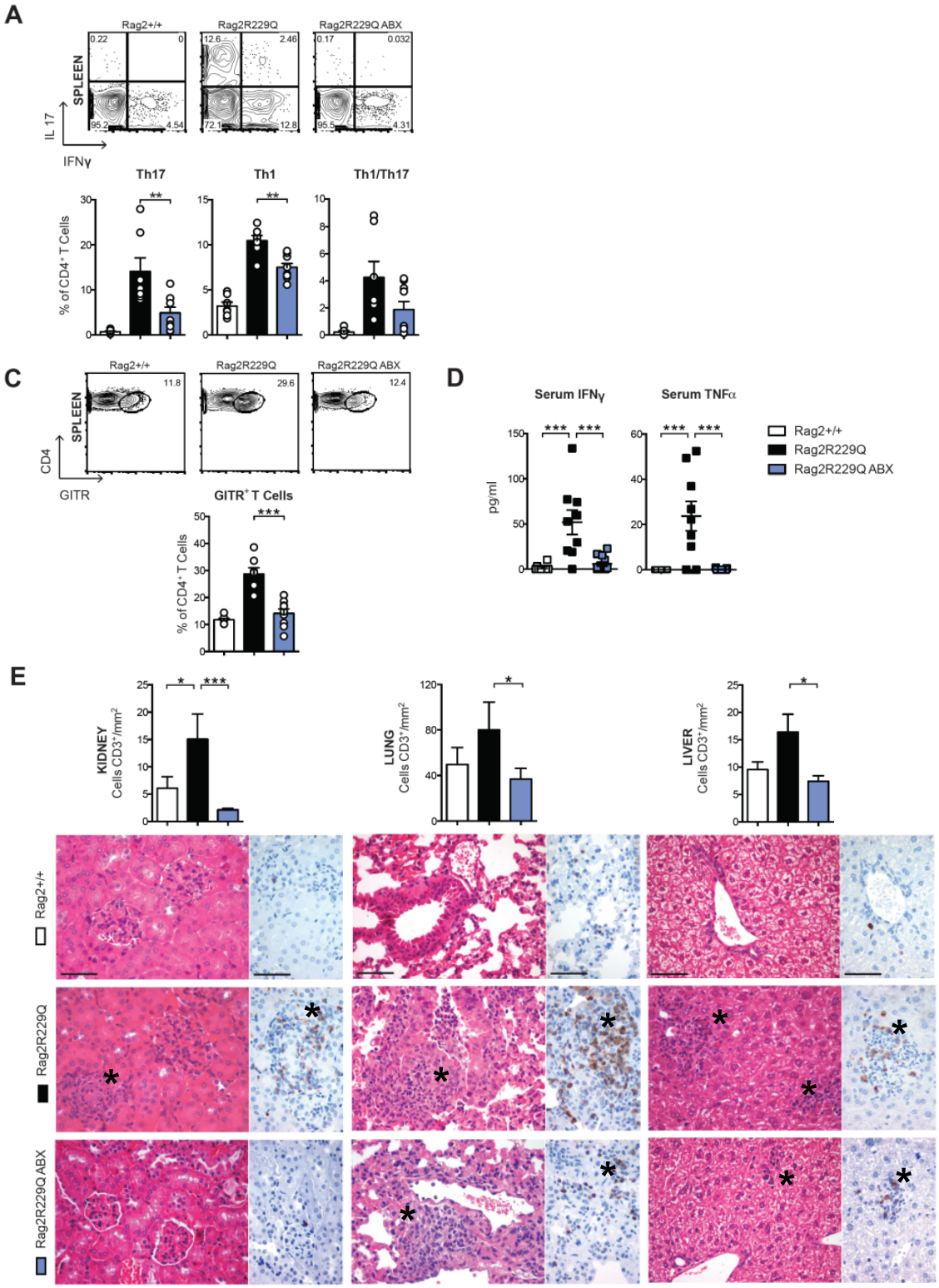

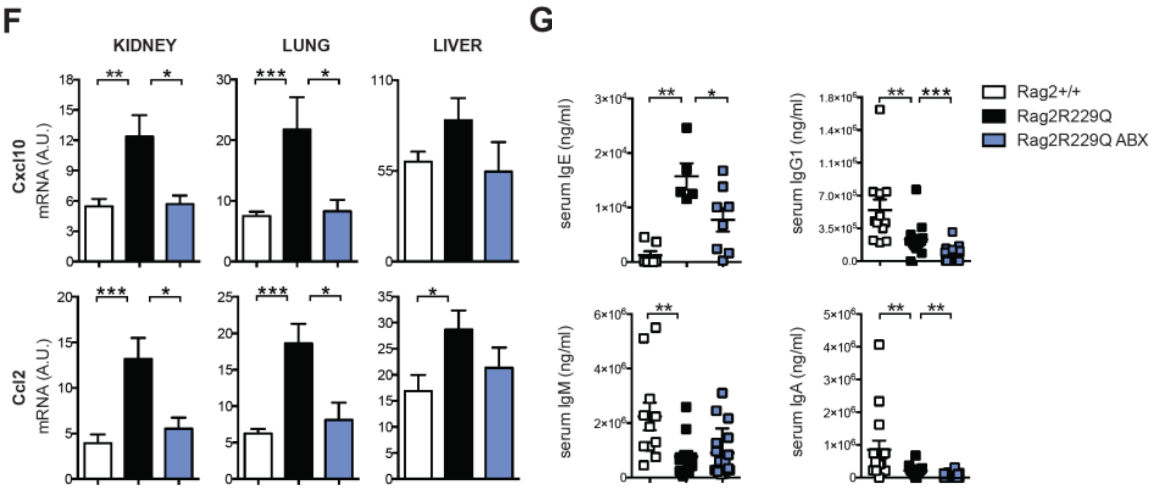

Figure 27: Reduced bacterial load dampens systemic inflammation in Rag2^{R229Q}mice. *A) Representative FACS dot plots and frequencies of Th1, Th17 and Th1/Th1,7 (B) CCR9^{+}-expressing T cells and GITR^{+} Treg cells (C) from spleen of ABX-treated Rag2^{R229Q} mice and controls. (D) Serum level of IFNγ and TNFα. (E) Representative kidney, liver and lung-sections from ABX-treated Rag2^{R229Q} mice, Rag2^{R229Q} mice and Rag2$^{+/+}$ mice stained with H&E and CD3 immunostaining. Histograms represent the number of CD3 positive cells per area. Asterisks indicate the area of infiltration. (F) Transcriptional level of several chemokines from intestinal tissues. (G) Serum level of immunoglobulins. 8-12 week-old mice of indicated genotypes were analysed. Mann Whitney test; values are mean ± SEM. *, P < 0.05; **, P < 0.01; ***, P < 0.001.*

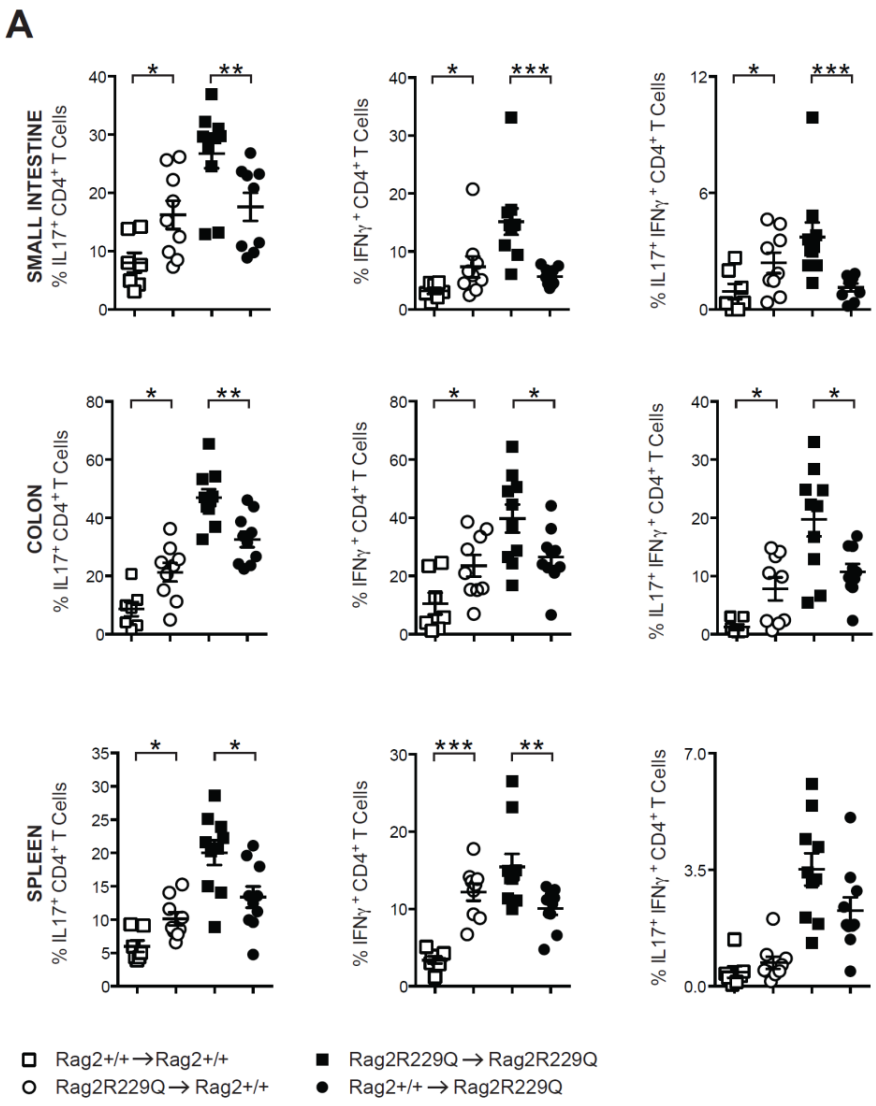

Figure 28: Faecal transplantation in Rag2^{R229Q} mice. *(A) Frequency of Th17, Th1 and Th1/Th17 cells in the small intestine, colon and spleen of Rag2^{R229Q} mice and Rag2$^{+/+}$ mice after faecal transplantation treatment. 8-12 week-old mice of indicated genotypes were analysed. Mann Whitney test; values are mean ± SEM. *, P < 0.05; **, P < 0.01; ***, P < 0.001.*

9.2 Study of the skin pathology in $Rag2^{R229Q}$ mice

9.2.1 $Rag2^{R229Q}$ mice exhibit severe skin inflammation

$Rag2^{R229Q}$ mice developed a severe inflammatory skin disease characterized by marked infiltration of oligoclonal-activated T cells [47, 65]. Approximately 10% of $Rag2^{R229Q}$ mice developed erythroderma-like phenotype by 6 months of age, while <1% developed other skin manifestations, including psoriasis, vitiligo and alopecia areata (**Figure 29A**). Histologically, the cutaneous inflammation is characterized by increased thickness of the epidermis, caused by hyperkeratosis and marked infiltration of immune cells in the dermis (**Figure 29B**). Occasionally, we observed the presence of inflammatory formations localized under the dermis and composed mainly by innate cells and few T cells. Interestingly, increased cellularity was detected in the skin of $Rag2^{R229Q}$ mice compared to $Rag2^{+/+}$ mice (**Figure 29C**). Immunophenotypic analysis of the skin infiltrate by flow cytometry confirmed an expansion of $CD45^+$ cells, particularly of $CD4^+$ and $CD8^+$ T cells (**Figure 29D-E**). In agreement, the expression of the chemokine receptor *cxcr3,* normally present on activated T cells, was augmented in mutant skin (**Figure 29F**). Interestingly, the epidermal alterations and the dermal lymphocytic infiltration were much more pronounced in mutant mice developing erythroderma-like phenotype (**Figure 29G**). Remarkably, the γδ T cell population was completely absent in the skin compartment of mutant mice, reflecting also its impaired thymic development (**Figure 29H** and data not shown).

The proportion of cutaneous IFNγ-producing T cells was significantly higher in $Rag2^{R229Q}$ mice compared to $Rag2^{+/+}$ mice. On the contrary, the frequency of Th17 did not change significantly, in agreement with the defect in γδ T cells, main producer of IL-17 in the skin (**Figure 29I**). Collectively, these results suggest that in $Rag2^{R229Q}$ mice skin inflammation is associated to the prominent accumulation of IFNγ-producing conventional T cells in the absence of γδ T cells.

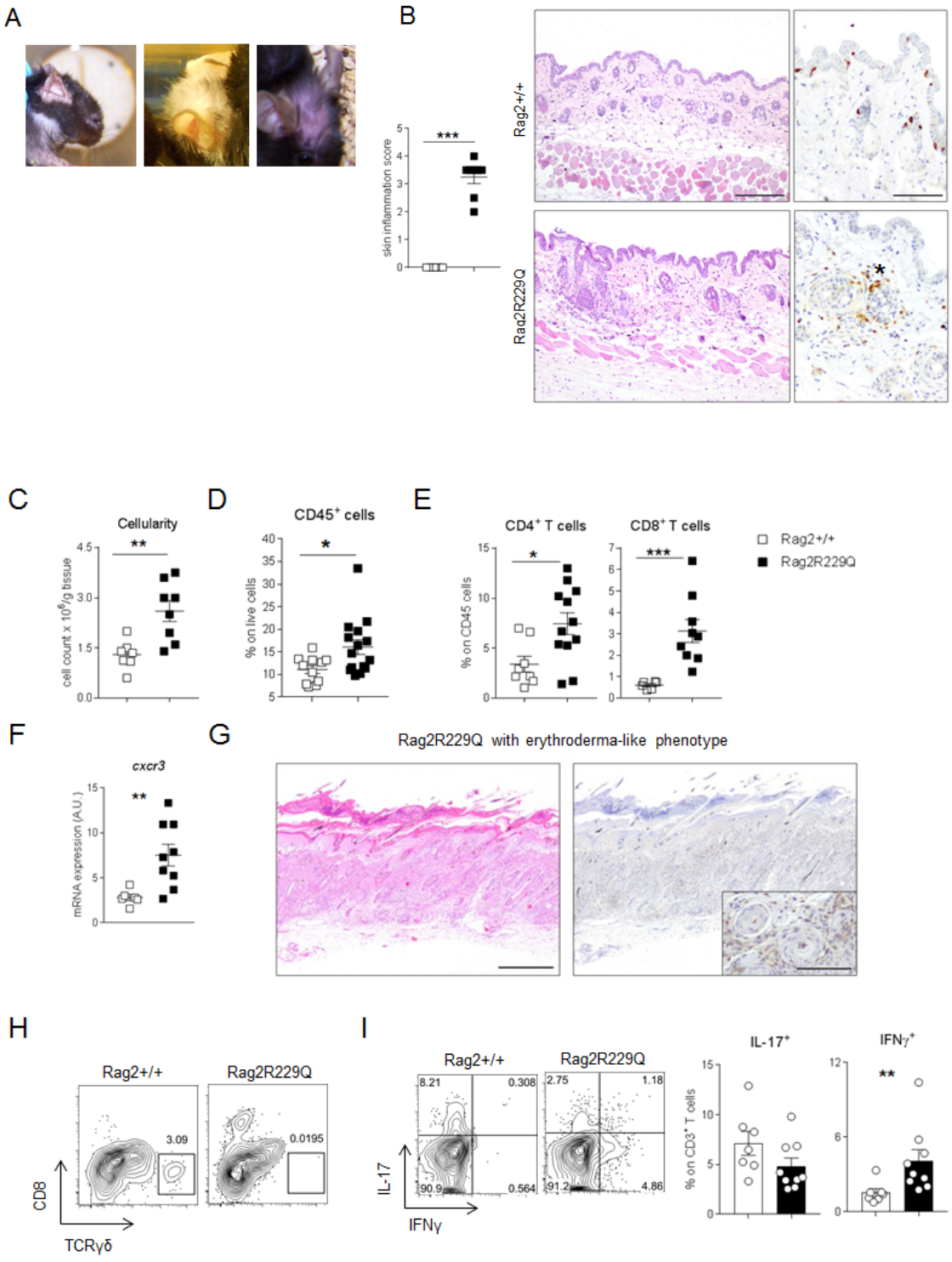
A
B
skin inflammation score
***
Rag2+/+
Rag2R229Q
*
C
Cellularity
**
cell count x 10^6/g tissue
D
CD45+ cells
*
% on live cells
E
CD4+ T cells
CD8+ T cells
*
***
% on CD45 cells
Rag2+/+
Rag2R229Q
F
cxcr3
**
mRNA expression (A.U.)
G
Rag2R229Q with erythroderma-like phenotype
H
Rag2+/+
Rag2R229Q
3.09
0.0195
CD8
TCRγδ
I
Rag2+/+
Rag2R229Q
8.21
0.308
90.9
0.564
2.75
1.18
91.2
4.86
IL-17
IFNγ
IL-17+
IFNγ+
**
% on CD3+ T cells

Figure 29: Characterization of cutaneous inflammation in Rag2^{R229Q} mice. *A) Cutaneous phenotype in OS disease: from the right, Rag2^{R229Q} mice affected by erythoderma, vitiligo and alopecia areata. B) Representative skin section of Rag2^{R229Q} mice with erythroderma-like phenotype stained with H&E (right) and CD3 immunostaining (left). Higher magnification revealed a marked inflammatory CD3^{+} infiltrate in the mutant dermis. Asterisk indicates the area of infiltration. C) Representative skin sections from Rag2$^{+/+}$ and Rag2^{R229Q} mice (8-12 weeks old) at steady state, stained with H&E and CD3 immunostaining. Histogram shows inflammation score in the skin. D) Representative FACS plots showing TCRγδ T cells within CD45^{+} population from skin tissue of Rag2$^{+/+}$ and Rag2^{R229Q} mice. (E) Total cellularity from skin of Rag2^{R229Q} mice and controls. (F) Cumulative frequencies of CD45^{+} cells, (G) CD4^{+} T cells and CD8^{+} T cells. (H) Transcriptional expression of cxcr3 on skin tissue. (I) Representative FACS plots and cumulative frequencies of cutaneous IL-17- and IFNγ- producing CD3^{+} T cells. 8-12 week-old mice of indicated genotypes were analysed. Mann Whitney test; values are mean ± SEM. *, P < 0.05; **, P < 0.01; ***, P < 0.001.*

9.2.2 Coexistence of skin and gut homing properties distinguishes the CD4^{+} T cells in Rag2^{R229Q} mice

Chemokine receptor CCR4 and its ligands, CCL17 and CCL22, are crucial for the recruitment of memory T cells into the skin in several cutaneous immune conditions [182]. In agreement with the consistent lymphocytic infiltration, the frequency of CCR4-expressing CD4^{+} T cells in the DLNs, spleen and MLNs of *Rag2^{R229Q}* mice was higher compared to *wild-type* mice (**Figure 30A**). This correlated with increased levels of serum CCL17 and CCL22 (**Figure 30B**). Remarkably, we observed that a significant proportion of these CCR4^{+} CD4^{+} T cells in mutant mice expressed also the gut-homing receptor CCR9, indicative of dual pattern of T cell migration. As expected, the expression of CCR9 on CD4^{+} T cells was higher in *Rag2^{R229Q}* mice compared to controls. Moreover, the proportion of CCR9^{-} CCR4^{-} expressing CD4^{+} T cells was reduced in the lymphoid organs of mutants (**Figure 30A**).

We also checked the CCR4^{+} and CCR9^{+} co-expression on CD8^{+} T cells, but we did not detect any significant changes (data not shown). This datum suggests that memory T cells in *Rag2^{R229Q}* mice can recirculate between skin and intestinal mucosa.

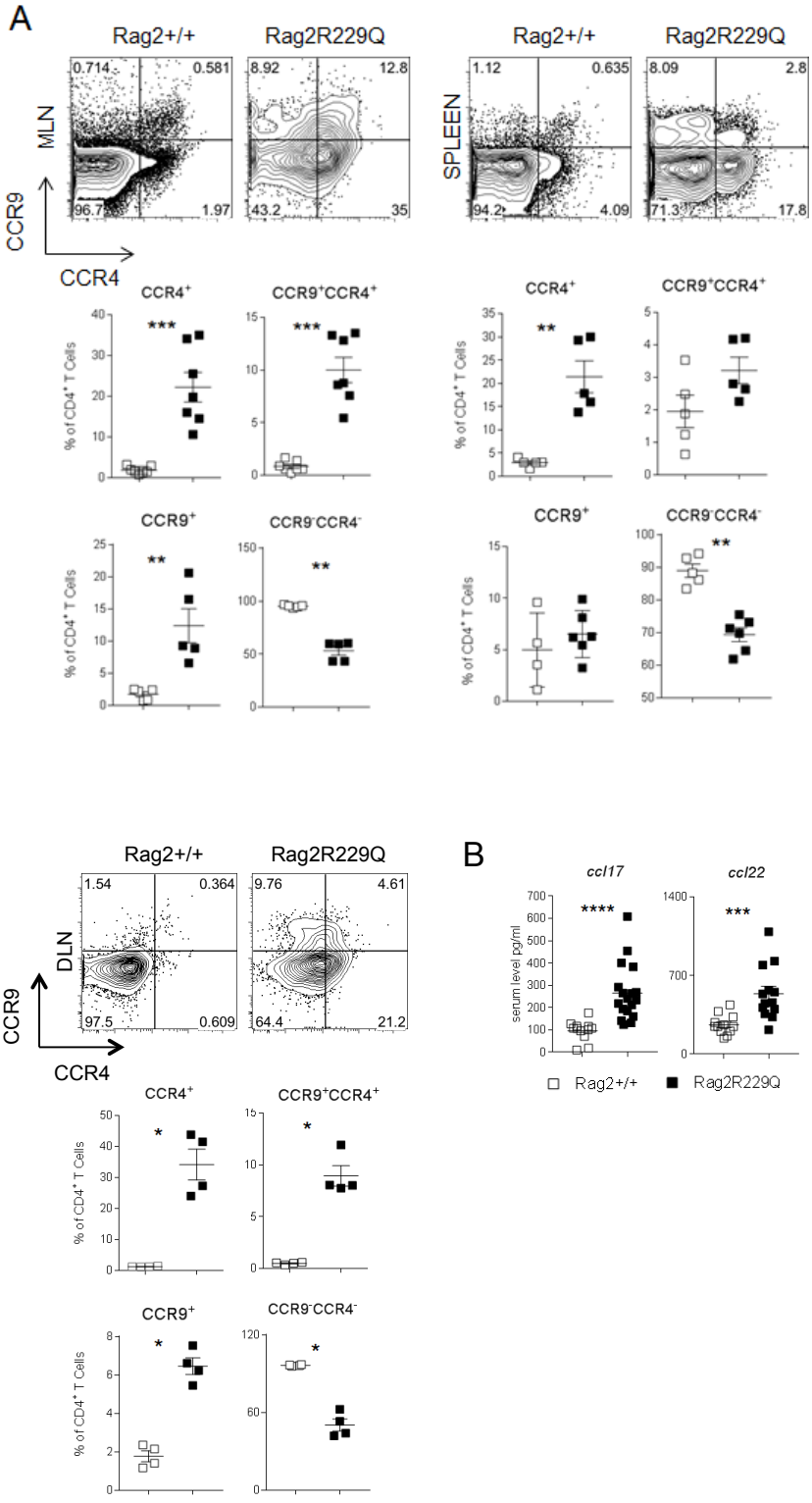
A
Rag2+/+
Rag2R229Q
Rag2+/+
Rag2R229Q
MLN
SPLEEN
0.714
0.581
96.7
1.97
8.92
12.8
43.2
35
1.12
0.635
94.2
4.09
8.09
2.8
71.3
17.8
CCR9
CCR4
CCR4+
CCR9+CCR4+
CCR9+
CCR9-CCR4-
% of CD4+ T Cells
***
**
B
ccl17
ccl22
serum level pg/ml
****
***
Rag2+/+
Rag2R229Q
DLN
1.54
0.364
97.5
0.609
9.76
4.61
64.4
21.2
*

Figure 30: Increased skin and gut homing receptors in Rag2^{R229Q} mice. *A) Representative dot plots and frequency of the CCR4^{+}, CCR4^{+}CCR9^{+}, CCR9^{+} and CCR4^{-}CCR9^{-} expressing CD4^{+} T cells from MLN, spleen and DLN of Rag2^{R229Q} mice and controls. B) Mouse serum level of CCL17 and CCL22. 8-12 week-old mice of indicated genotypes were analysed. Mann Whitney test; values are mean ± SEM. *, P < 0.05; **, P < 0.01; ***, P < 0.001.*

9.2.3 RAG patients showed increased frequency of CLA-expressing effector T cells

We had the opportunity to test the levels of CCR4-ligands in the sera of four OS patients bearing mutations in RAGs genes. Consistently with mouse findings, we detected increased serum level of CCL17 and CCL22 in RAG patients, compared to paediatric age-matched healthy donors (HD) (**Figure 31A**). In humans, cutaneous lymphocyte-associated antigen (CLA) expression targets skin-associated T cells to inflammatory cutaneous sites [183]. We checked also the expression of gut and skin homing receptors on CD4^{+} CD45RO^{+} or CD8^{+} CD45RO^{+} T cell subsets from PBMCs of RAG patients and HDs. Interestingly, we found increased expression of CLA on CD4^{+} CD45RO^{+} T cells and on CD8^{+} CD45RO^{+} T cells in RAG patients compared to controls, reflecting their preferential skin-migratory capacity. On the contrary, RAG patients showed lower frequencies of CCR9-expressing effector T cells. Moreover, we did not observe significant changes in the frequencies of CD4^{+} CD45RO^{+} and CD8^{+} CD45RO^{+} T cells expressing both gut and skin homing receptors (**Figure 31B-C**).

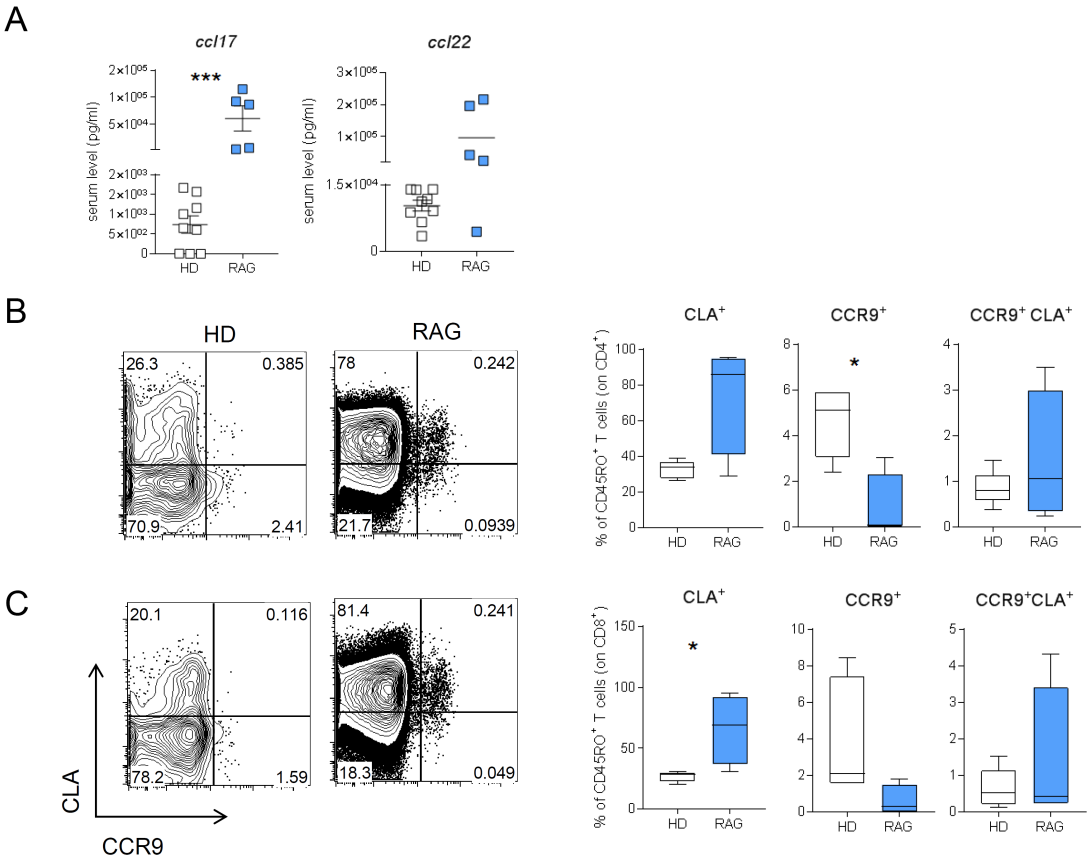

Figure 31: CLA-expressing effector T cells were increased in RAG patients. *A) Human serum levels of CCL17 and CCL22. B) Representative dot plots and frequencies of CLA and CCR9 on CD45RO$^+$ of CD4$^+$ or CD8$^+$ T cells. Mann Whitney test; values are mean ± SEM. *, P < 0.05; **, P < 0.01; ***, P < 0.001.*

9.2.3 Increased cutaneous DC trafficking characterized the Rag2^{R229Q} mice

Skin-derived DCs imprint skin homing tropism on T cells upon activation [184]. To investigate the role of DCs in the homing properties acquired by mutant T cells, we first assess the antigen-presentation capacity of cutaneous DCs from the *Rag2^{R229Q}* mice. Mouse ears contain lymphatic vessels that drain to the cervical LNs [185]. DCs are physically positioned to take up antigens from the skin and to carry them to the lymph nodes via lymphatic system. For tracking DC migration from the skin, APC-labelled OVA antigen was intra-dermally injected in the ears of mutant and control mice and its uptake by DCs was evaluated in the skin and cervical LN after 6h (**Figure 32A**). Interestingly, while similar frequencies of OVA-loaded DCs were detected in the

Rag2^{R229Q} and *Rag2*$^{+/+}$ skin tissue (**Figure 32B**), an higher proportion of DCs carrying the OVA antigen was recovered in the cervical LNs of mutant mice compared to controls **(Figure 32C)**, indicating an augmented trafficking from the skin. The homing programming of T cells by skin-derived DCs may also occur in lymphoid organs, other than cutaneous DLNs [186]. In *Rag2*^{R229Q} mice, lymph nodes are atrophic and devoid of germinal centres. Since the immature structures of the mutant LN would not allow the immune cell resting, we investigated whether mutant DCs could be able to traffic and to present antigens to T cells also in the periphery. To test this hypothesis, *Rag2*$^{+/+}$ and *Rag2*^{R229Q} mice were immunized on ear skin with OVA plus CT as adjuvant. After 4 days, CD11C^{+} cells were isolated from cervical LN and spleen and co-cultured with OT-II cells. At day 6 of culture, OVA-triggered T cell proliferation was evaluated by Thymidine incorporation (**Figure 32D**). We found that DCs isolated from cervical LNs of *Rag2*^{R229Q} mice induced less proliferation in OT-II cells compared to *wild-type* DCs (**Figure 32E**). In contrast, DCs recovered from the spleen of mutant mice were more potent stimulators of OT-II cell proliferation than control cells (**Figure 32F**). Since WT and mutant DCs were able to activate T cells to similar extent when exogenous OVA was added directly to the culture (data not shown), these results indicate that the DC populations isolated from these anatomical locations were differentially enriched in OVA-loaded cells between *Rag2*^{R229Q} and *wild-type* mice. Furthermore, these findings would suggest that whereas in *wild-type* mice skin immunization generates preferentially local (within the skin DLNs) DC-T cells interaction, in mutant mice skin-derived DCs are able to traffic and activate T cells in the periphery.

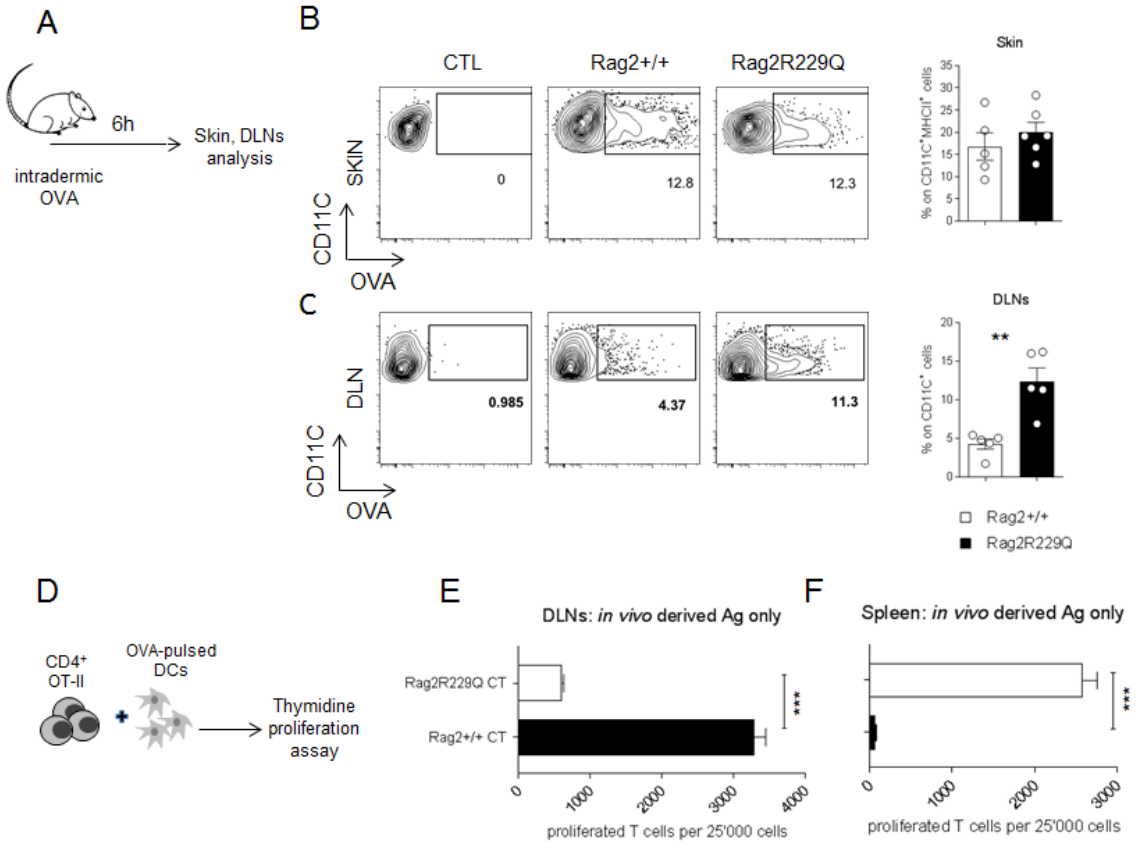

Figure 32: Increased DC trafficking in Rag2^{R229Q} mice. *A) APC-labelled OVA was injected intra-dermally into ears of Rag2^{R229Q} mice and controls. After 6h, OVA-loaded DCs were analysed in the skin and in the cervical LN by FACS. B) Representative dot plot and frequency of OVA-loaded CD11C^{+}MHCII^{+} cells in the skin. C) Representative dot plot and frequency of OVA-loaded CD11C^{+} cells in the cervical LNs. D) Rag2^{R229Q} mice and controls were immunized with CT + OVA on ear skin. After 4 days, DCs were isolated from cervical LN and spleen. DC and OT-II cells were plated for co-culture (1:1 DC:T cell ratio). After 6 days, the proliferation of OT-II cells was assessed by ^{H}3-thymidine incorporation after culture with DCs sorted from DLNs (E) and spleen (F). The average of triplicates is shown. 8-12 week-old mice of indicated genotypes were analysed. Mann Whitney test and unpaired t test; values are mean ± SEM. *, P < 0.05; **, P < 0.01; ***, P < 0.001.*

9.2.4 Increased vascularity characterizes the skin of Rag2^{R229Q} mice

The cutaneous lymphatic system plays a major role in controlling the local immune response [187]. To investigate whether chronic skin inflammation in OS might also be associated with increased vascular permeability, we injected Evans blue dye intra-dermally into the back of *Rag2^{R229Q}* mice (**Figure 33A**). Evans blue is specifically taken

up by the lymphatic vasculature upon intradermal injection [188]. After 16h, the dye was extracted from the mouse back and quantified by ELISA. This analysis showed that the *Rag2*^{R229Q} mice had significantly less amount of Evans Blue remaining localized in the skin compared to WT mice, indicative of enhanced lymphatic clearance (**Figure 33B**). Consistently, increased cutaneous expression of the vascular endothelial growth factor (VEGF-)A, representing the major driver of vascular remodelling and hyper-permeability, was detected in mutant mice (**Figure 33C**). Thus, increased lymphatic network and augmented lymphatic drainage characterized the skin environment of *Rag2*^{R229Q} mice.

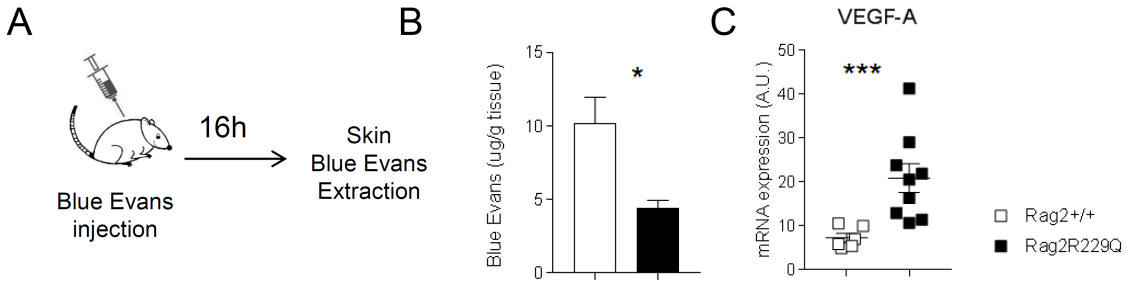

Figure 33: Increased lymphatic network in Rag2^{R229Q} mice. *A) Evans Blue dye was intra-dermally injected into the back of Rag2^{R229Q} mice and controls and was extracted after 16h. The total amount of dye remaining in the skin tissue was normalized on gr of tissue. B) Blue Evans dye remained in the skin tissue after 16h. C) Transcriptional level of VEGF-A in skin tissue. RNA contents are shown as arbitrary units (A.U.). 8-12 week-old mice of indicated genotypes were analysed. Mann Whitney test and unpaired t test; values are mean ± SEM. *, P < 0.05; **, P < 0.01; ***, P < 0.001.*

9.2.5 Epidermal barrier dysfunction characterizes the cutaneous compartment of Rag2^{R229Q} mice

The epidermal layer has a key role in the maintenance of the skin homeostasis, and alterations in its integrity could lead to the penetration of environmental antigens and induce immune reactions, contributing to chronic inflammation [189]. At steady state, the epidermis of *Rag2*^{R229Q} mice appears thickened compared to WT mice (**Figure 34A**). Consistently, the expression of keratin 5 (CK5) and keratin 6 (CK6) was significantly augmented in the mutant skin, underlying the increased production by

epidermal keratinocytes (**Figure 34B**). In agreement, we found higher expression of Loricrin, which facilitate the terminal differentiation of the epidermis (data not shown). Tight junction (TJ) abnormalities have been described in several skin inflammatory diseases, including atopic dermatitis [190]. However, the transcriptional analysis of the TJ-related protein (Claudin-4, ZO1 and Occludin) expression did not show significant alteration (data not shown). Acute and chronic injury leads to the induction of Cathelin-related antimicrobial peptides, Cramp and β-defensin 3 (mBD3), which are essential for the maintenance of barrier integrity [191]. Interestingly, we detected at least 0.5-fold increase of these peptides in the mutant skin, indicative of enhanced microbial stimulation of the cutaneous epithelium (**Figure 34C**). Consistently, bacteria adherent to the skin epithelium, measured as a ratio between prokaryotic to eukaryotic DNA, were significantly augmented in the mutant mice (**Figure 34D**). TLRs expression by keratinocytes are crucial for sensing skin invading pathogens and promoting cutaneous immune responses [192]. Expression of several TLRs, including TLR2, TLR3, TLR4, TLR5, TLR9 as well as the adaptor molecules Myd88 and TRIF, was markedly increased in the skin tissue of mutants (**Figure 34E** and data not shown). Together these findings indicate that *Rag2*^{R229Q} mice are characterized by altered barrier integrity and increased cutaneous bacterial load.

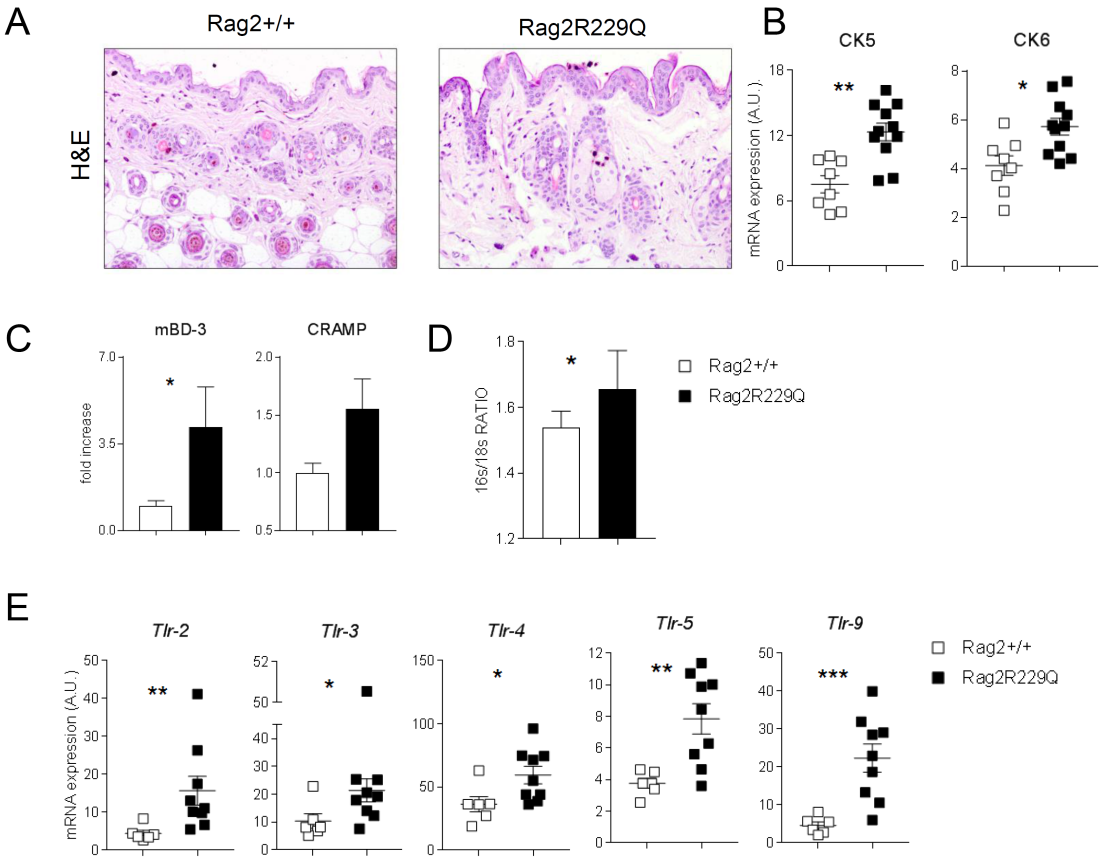

Figure 34: Alteration of the skin barrier integrity in Rag2^{R229Q} mice. *A) Representative skin sections from Rag2$^{+/+}$ and Rag2^{R229Q} mice stained with H&E. B) Gene expression analysis of CK5 and CK6 in the skin tissue of mice. RNA contents are shown as arbitrary units (A.U.). C) Tissue mRNA expression of antimicrobial peptides. Results are shown as fold increase compared to wild-type mice. D) Quantitative PCR analysis of cutaneous adherent bacteria in Rag2$^{+/+}$ and Rag2^{R229Q} mice expressed as prokaryotic/eukaryotic DNA ratio. E) Gene expression analysis of TLRs in the skin tissue. RNA contents are shown as arbitrary units (A.U.). 8-12 week-old mice of indicated genotypes were analysed. Mann Whitney test; values are mean ± SEM. *, P < 0.05; **, P < 0.01; ***, P < 0.001.*

9.2.6 Selective shift in Rag2^{R229Q} skin microbiota

Based on these results, we next analyzed the resident skin microbiota in *Rag2^{R229Q}* mice and their co-housed WT littermates by 16s rRNA gene profiling. Although we did not find significant differences in microbiota intra-sample (α) diversity, as determined by Shannon and Chao1 indexes (data not shown), we applied the LEfSe analysis to identify

bacterial taxa that were differentially abundant between the two groups. The analysis revealed that the relative abundance of two out of the four dominant taxa populating the skin organ, Actinobacteria and Firmicutes, were diminished in *Rag2*^{R229Q} mice compared to controls (p-value <0.05). Moreover, at the genus level of classification, *Propionibacterium* (p-value <0.05) (division Actinobacteria), *Streptococcus* and *Staphylococcus* (p-value <0.05) (division Firmicutes) were less represented in the *Rag2*^{R229Q} skin microbial composition, suggesting an important shift towards the loss of skin commensals (**Figure 35**). Indeed, the reduction of several cutaneous bacteria could impact severely on the skin ecology. For instance, *Staphylococcus epidermis* has beneficial functions, producing a variety of antimicrobial molecules, such as phenol soluble modulins, that interact with and cause leakage of lipid microbial membranes [193]. Furthermore, *Propionibacterium acnes* ferments carbohydrate to propionic acid, a SCFA with antimicrobial activity [194]. Overall these results underlined a selective shift in the microbial composition of skin microbiota of *Rag2*^{R229Q} mice, thus possibly contributing to its pathological state.

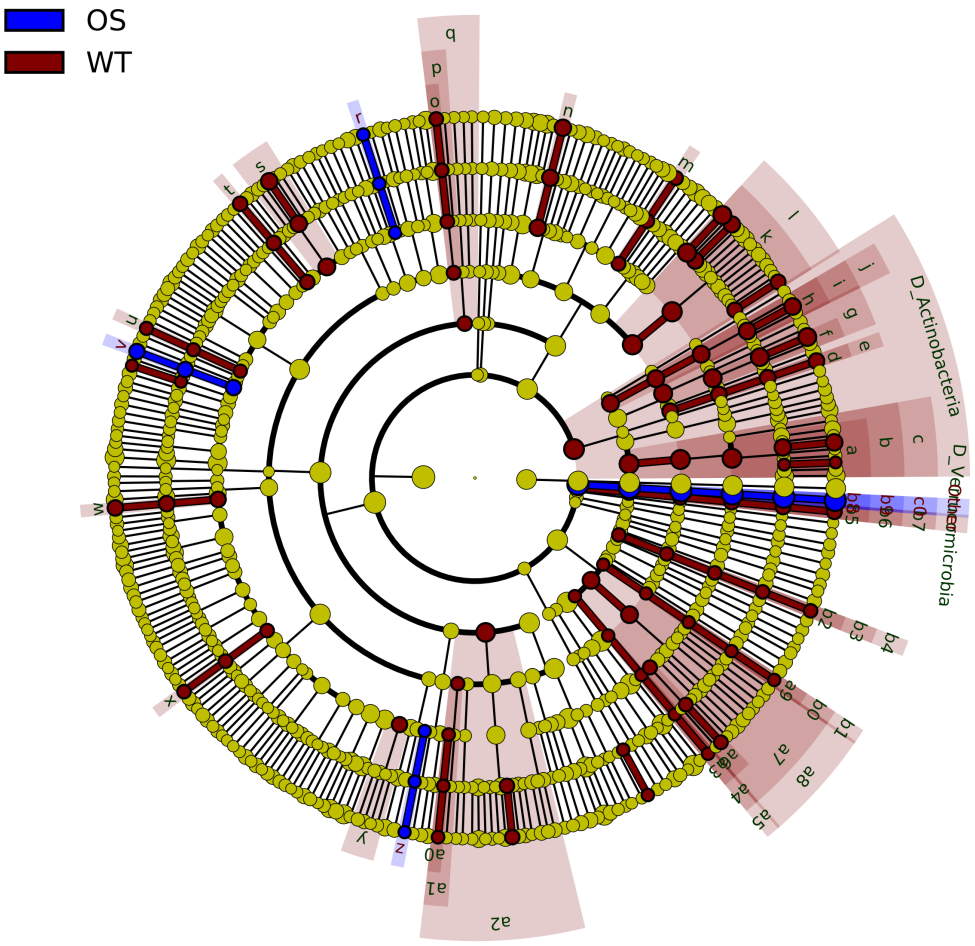

	Taxonomy	Increased in:
a	D_Actinobacteria_Bifidobacteriales_Bifidobacteriaceae_Bifidobacterium	WT
b	D_Actinobacteria_Bifidobacteriales_Bifidobacteriaceae	WT
c	D_Actinobacteria_Bifidobacteriales	WT
d	D_Actinobacteria_Micrococcales_Brevibacteriaceae_Brevibacterium	WT
e	D_Actinobacteria_Micrococcales_Brevibacteriaceae	WT
f	D_Actinobacteria_Micrococcales_Micrococcaceae_Kocuria	WT
g	D_Actinobacteria_Micrococcales_Micrococcaceae	WT
h	D_Actinobacteria_Propionibacteriales_Propionibacteriaceae_Propionibacterium	WT
i	D_Actinobacteria_Propionibacteriales_Propionibacteriaceae	WT
j	D_Actinobacteria_Propionibacteriales	WT
k	D_Bacteroidetes_Bacteroidales_Bacteroidaceae_Bacteroides	WT
l	D_Bacteroidetes_Bacteroidales_Bacteroidaceae	WT
m	D_Bacteroidetes_Bacteroidales_Bacteroidales_S24_7_group.Other	WT
n	D_Bacteroidetes_Bacteroidales_Prevotellaceae.Other	WT
o	D_Firmicutes_Bacillales_Staphylococcaceae_Staphylococcus	WT
p	D_Firmicutes_Bacillales_Staphylococcaceae	WT
q	D_Firmicutes_Bacillales	WT
r	D_Firmicutes_Clostridiales_Clostridiales_vadinBB60_group_uncultured_bacterium	OS
s	D_Firmicutes_Clostridiales_Lachnospiraceae_Blautia	WT
t	D_Firmicutes_Clostridiales_Lachnospiraceae_Eisenbergiella	WT
u	D_Firmicutes_Clostridiales_Lachnospiraceae_Lachnospiraceae_UCG_010	WT
v	D_Firmicutes_Clostridiales_Lachnospiraceae_Moryella	OS
w	D_Firmicutes_Clostridiales_Peptostreptococcaceae.Other	WT
x	D_Firmicutes_Clostridiales_Ruminococcaceae_Ruminococcaceae_NK4A214_group	WT
y	D_Firmicutes_Clostridiales_Ruminococcaceae_uncultured	WT
z	D_Firmicutes_Erysipelotrichales_Erysipelotrichaceae_Allobaculum	OS
a0	D_Firmicutes_Lactobacillales_Carnobacteriaceae_Atopostipes	WT
a1	D_Firmicutes_Lactobacillales_Carnobacteriaceae	WT
a2	D_Firmicutes_Lactobacillales	WT
a3	D_Proteobacteria_Desulfovibrionales_Desulfovibrionaceae_Bilophila	WT
a4	D_Proteobacteria_Desulfovibrionales_Desulfovibrionaceae	WT
a5	D_Proteobacteria_Desulfovibrionales	WT
a6	D_Proteobacteria_Enterobacteriales_Enterobacteriaceae_Citrobacter	WT
a7	D_Proteobacteria_Enterobacteriales_Enterobacteriaceae	WT
a8	D_Proteobacteria_Enterobacteriales	WT
a9	D_Proteobacteria_Neisseriales_Neisseriaceae_Neisseria	WT
b0	D_Proteobacteria_Neisseriales_Neisseriaceae	WT
b1	D_Proteobacteria_Neisseriales	WT
b2	D_Proteobacteria_Rhodospirillales_Rhodospirillaceae_Thalassospira	WT
b3	D_Proteobacteria_Rhodospirillales_Rhodospirillaceae	WT
b4	D_Proteobacteria_Rhodospirillales	WT
b5	D_Verrucomicrobia_Verrucomicrobiales_Verrucomicrobiaceae_Akkermansia	WT
b6	D_Verrucomicrobia_Verrucomicrobiales_Verrucomicrobiaceae	WT
b7	D_Verrucomicrobia_Verrucomicrobiales	WT
b8	D_Bacteria.Other.Other	OS
b9	D_Bacteria.Other.Other.Other	OS
c0	D_Bacteria.Other.Other.Other.Other	OS

Figure 35: Skin microbiota differs between Rag2^{R229Q} mice and controls. *A linear discriminant analysis effect size (Lefse) identifies the significant different abundance of bacteria taxa between Rag2^{R229Q} mice and controls. The taxa with significantly different abundances among the genotypes are represented by colored dots. From the center outward, they indicate the kingdom, phylum, class, order, family, and genus levels. The*

colored shadows represent trends of the significantly differed taxa. 8 week-old mice of indicated genotypes were analysed. Mann Whitney test; P < 0.05 was considered statistically significant.

9.2.7 Chronic activation of epithelial cells sustains skin inflammation in Rag2^{R229Q} mice

Constant microbial stimulation might induce keratinocytes activation. Activated keratinocytes produce inflammatory cytokines, adhesion, activatory and costimulatory molecules, which may allow them to act as primary antigen presenting cells (APC) [195]. In *Rag2^{R229Q}* mice, a significant fraction of epithelial cells expressed the MHCII molecules at high levels compared to controls, indicative of their activated status (**Figure 36A-B**). The frequency of proliferating Ki67^{+} epithelial cells did not differ significantly between mutants and controls (data not shown). However, a high number of proliferating Ki67^{+} cells resides in the epidermis and in the dermis of *Rag2^{R229Q}* mice with erythroderma-like phenotype (data not shown). To completely characterize the cutaneous inflammatory environment in the *Rag2^{R229Q}* mice, we measured the expression levels of several cytokines. Transcript mRNA of IFNγ, IL-13, TNFα, IL-23, IL-1β, IL-5, IL-33 and TSLP were significantly up-regulated in the *Rag2^{R229Q}* skin, whereas, as expected, the IL-17 expression did not change significantly (**Figure 36C**). Moreover, keratinocytes play an important role in orchestrating immune responses by producing chemokines following TLR engagement [196]. Consistently, transcript levels of *cxcl9*, *cxcl10, ccl20, ccl22* and *ccl17* chemokines were significantly up-regulated in the skin of *Rag2^{R229Q}* mice (**Figure 36D**). To test whether this inflammatory environment has a role in determining cutaneous T cell migration in *Rag2^{R229Q}* mice, we employed the trackable OVA-TCR transgenic system and adoptively transferred CD4 or CD8 splenocytes from OT-II or OT-I mice into *Rag2$^{+/+}$* and *Rag2^{R229Q}* recipients. Then, we topically immunized the ears once with OVA plus CT [144]. After 7 days, treated chimeric mice were sacrificed and cells were isolated from cervical LNs and skin biopsies (**Figure 37A**). Interestingly, OT-II cells were dramatically enriched within the skin and cervical LNs of OVA-treated *Rag2^{R229Q}* mice compared to controls (**Figure 37B-C**). The same enrichment was evident for OT-I cells (**Figure 37D-E**). This accumulation was Ag-dependent, because CT alone did not induce a relevant accumulation of OT-I or OT-II cells (**Figure 37B-D**). Overall, these findings indicate

that epithelial cells have the potential to release several chemokines that direct T cell infiltration at the cutaneous site.

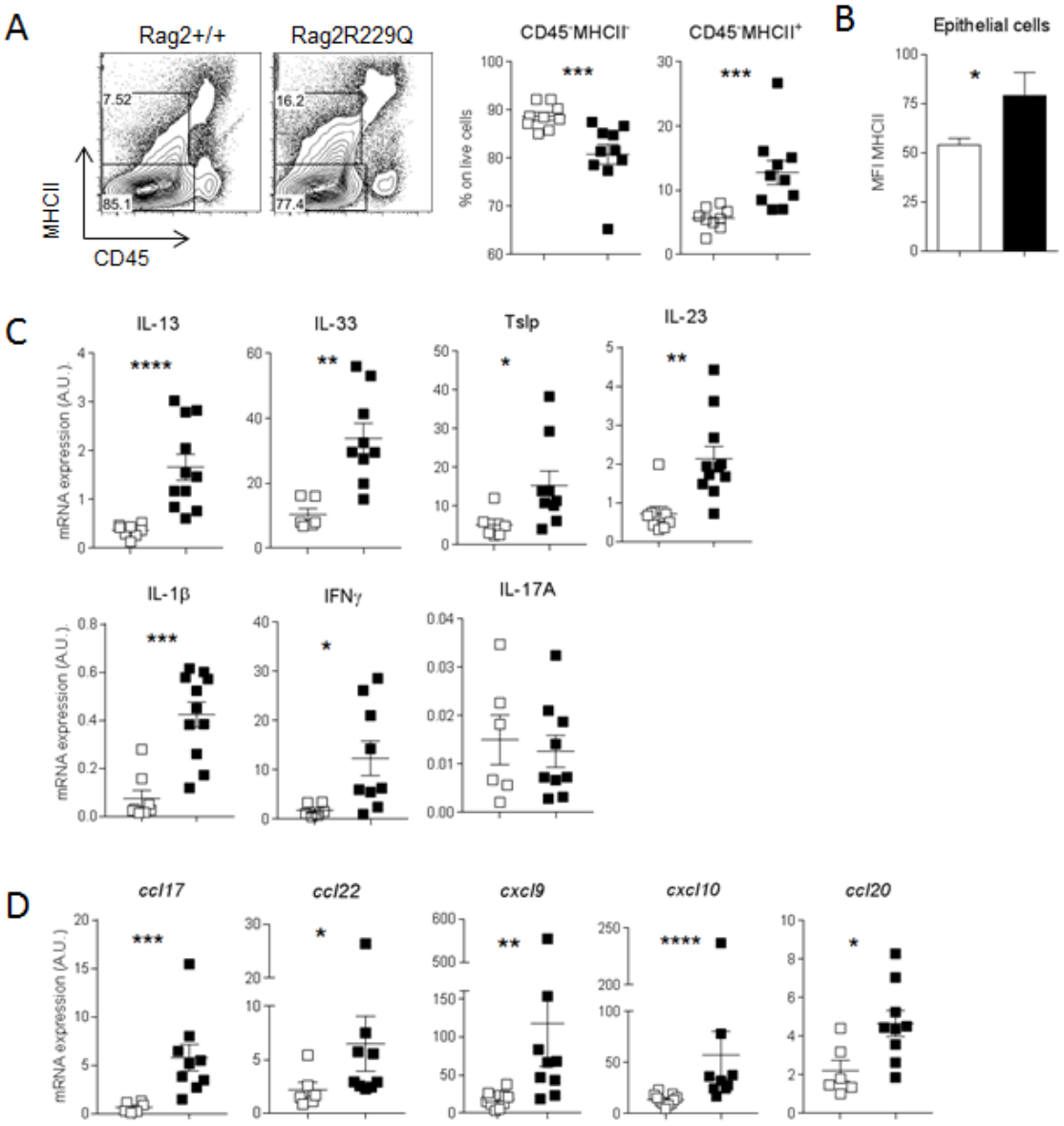

Figure 36: Activated epithelial cells in Rag2^{R229Q} mice*. A) Representative FACS plots and frequency of CD45$^-$MHCII$^+$ and CD45$^-$MHCII$^+$ cells in the skin of Rag2^{R229Q} mice and controls. B) Mean fluorescent intensity (MFI) of MHCII on CD45$^-$ cells. Transcriptional level of cytokines (C) and chemokines (D) in the skin tissue. 8-12 week-old mice of indicated genotypes were analysed. Mann Whitney test; values are mean ± SEM. *, P < 0.05; **, P < 0.01; ***, P < 0.001;**** P < 0.0001.*

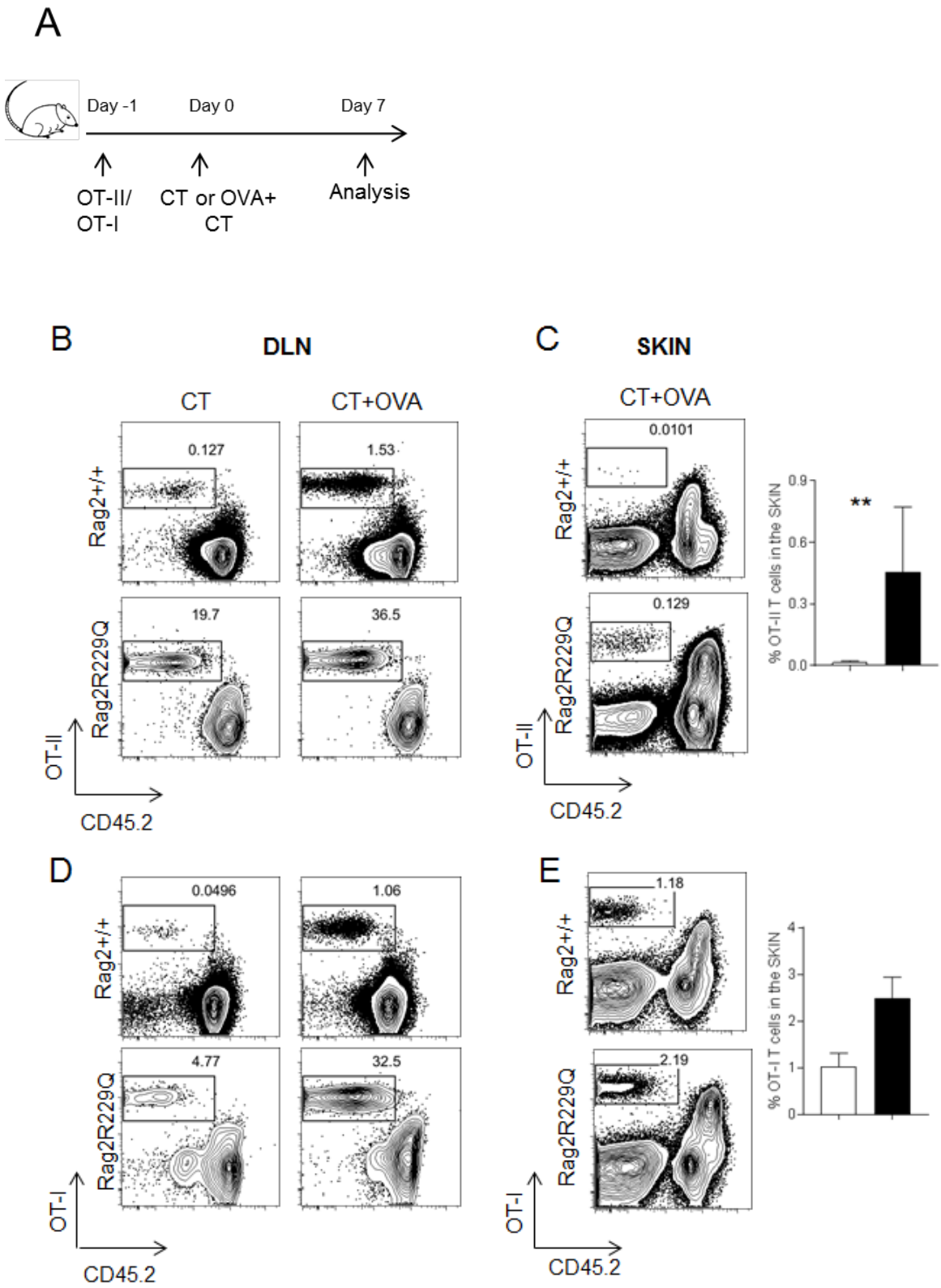
A
Day -1
Day 0
Day 7
OT-II/
OT-I
CT or OVA+
CT
Analysis
B
DLN
CT
CT+OVA
Rag2+/+
Rag2R229Q
0.127
1.53
19.7
36.5
OT-II
CD45.2
C
SKIN
CT+OVA
0.0101
0.129
% OT-II T cells in the SKIN
**
D
0.0496
1.06
4.77
32.5
OT-I
E
1.18
2.19
% OT-I T cells in the SKIN

***Figure 37: Enrichment of OVA-specific OT-II or OT-I cells in the Rag2^{R229Q} skin**. A) Splenic OT-II CD4^{+} T cells or OT-I CD8^{+} T cells were injected i.v. into mismatched host mice. Rag2^{R229Q} mice and controls were immunized in the ears with OVA plus CT or only CT. The enrichment of OT-II cells or OT-I cells in OVA-inflamed skins and cervical LNs were assessed at day 7. Representative dot plots of OT-II (B) or OT-I cells (D) from CT-treated mice and CT+OVA-treated mice from DLNs. Representative dot plots and frequency of OT-II cells or OT-I cells (C, E) within the skin at day 7. 8-12 week-old mice of indicated genotypes were analysed. Mann Whitney test; values are mean ± SEM. *, P < 0.05; **, P < 0.01; ***, P < 0.001.*

9.2.8 LPS-induced inflammation is profoundly enhanced in Rag2^{R229Q} mice

Since we found that *Tlr4* was the most highly expressed Toll-like receptor in the mutant skin, we tested the effect of acute stimulation by LPS-intradermal injection. In particular, mice received a single intradermal injection of 100 μg LPS on the right and PBS on the left. Mice were then sacrificed 24h later. (**Figure 38A**). Haemorrhage and dermal tissue necrosis was evident at the injection site 24h after LPS injection in all treated mice. Histological examination of cutaneous tissue revealed widespread epidermal thickening, increased abscesses formation and profound haemorrhage in *Rag2^{R229Q}* mice. However, mild signs of haemorrhage were evident also in *Rag2$^{+/+}$* mice (**Figure 38B**). To further explore the effect of LPS on skin tissue, we analysed the expression of pro-inflammatory cytokines, IFNγ and IL-1β. Both cytokines resulted strikingly elevated in mutant mice treated with intradermal LPS compared to controls. Moreover, the increased expression of the chemokine *Cxcl2* has the potential to induce a robust recruitment of innate cells to the mutant skin (**Figure 38C**), indicating that *Tlr4* stimulation induced strong inflammatory response in mutant mice.

As a consequence of the altered intestinal permeability, we have demonstrated high level of LPS in the circulation of *Rag2^{R229Q}* mice [197]. Therefore, to directly test whether endogenous level of serum LPS could be involved in the chronic stimulation of skin epithelium in *Rag2^{R229Q}* mice, we examined the cutaneous responses to systemic LPS. Mice received a single injection of 100 μg LPS i.p and were sacrificed 24h later (**Figure 39A**). *Rag2^{R229Q}* mice displayed a strong cutaneous inflammatory response to systemic LPS, characterized by dramatic upregulation of skin *Tlr4* mRNA and

expression of IFNγ (**Figure 39C**). Histologically, *Rag2*^{R229Q} mice showed a worsened inflammatory picture characterized by epidermal thickness with hyperkeratosis, occasionally abscesses and marked dermal inflammatory infiltrate. Signs of cutaneous inflammation were evident also in the skin of *Rag2*$^{+/+}$ LPS-treated mice, which reached the score of untreated *Rag2*^{R229Q} mice (**Figure 39B**). These data let us to hypothesize that peripherally translocated intestinal derived-LPS or other microbial products could be involved in the chronic stimulation of skin epithelium and activation of cutaneous immunity.

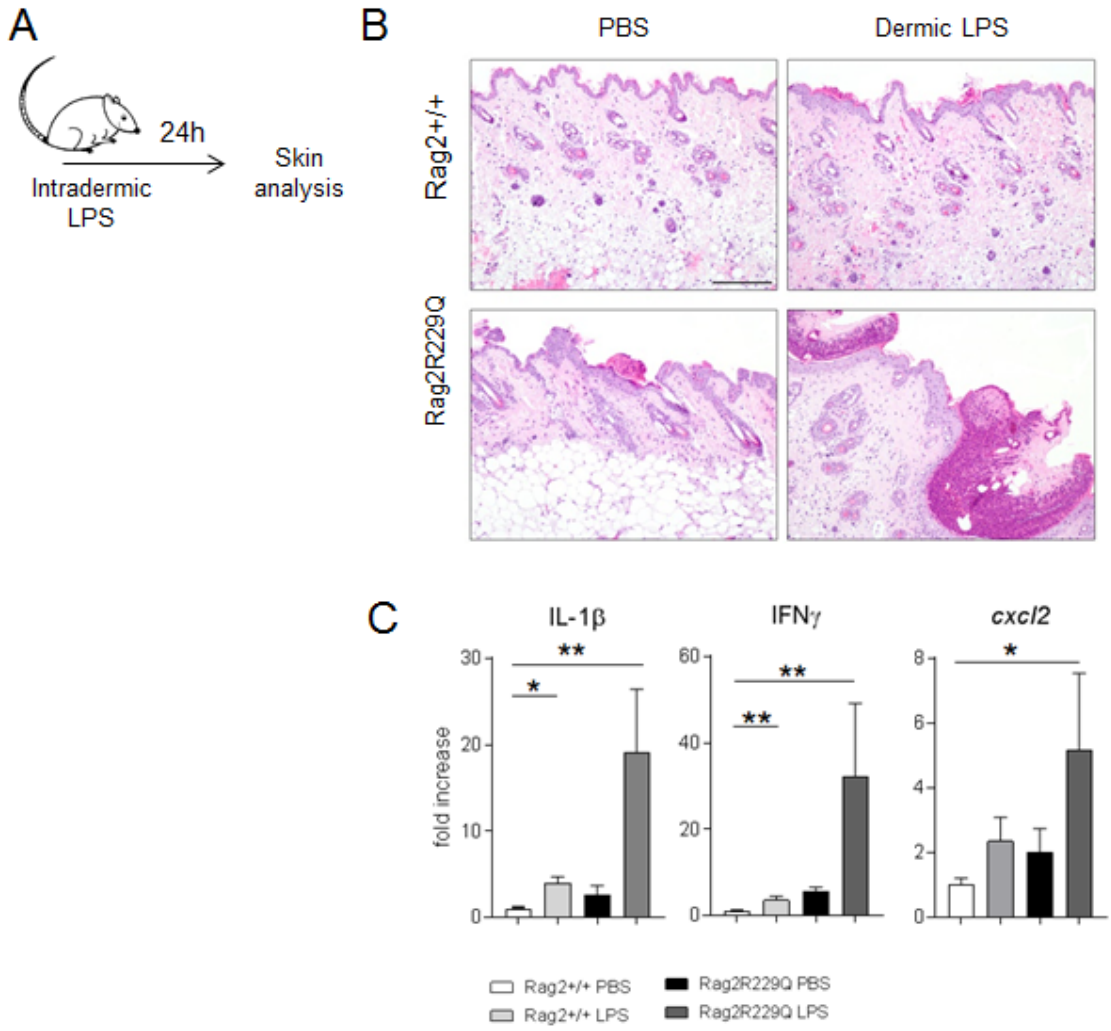

Figure 38: Intradermal LPS induces profound inflammation in Rag2^{R229Q} mice. *A) Dorsal skin of Rag2^{R229Q} mice and controls were injected s.c. with LPS (right side) or PBS control (left side). B) Representative skin sections from LPS-treated Rag2$^{+/+}$ and Rag2^{R229Q} mice and controls stained with H&E. C) Transcriptional analysis of cytokines in the total skin tissue. 8-12 week-old mice of indicated genotypes were analysed. Mann Whitney test; values are mean ± SEM. *, P < 0.05; **, P < 0.01.*

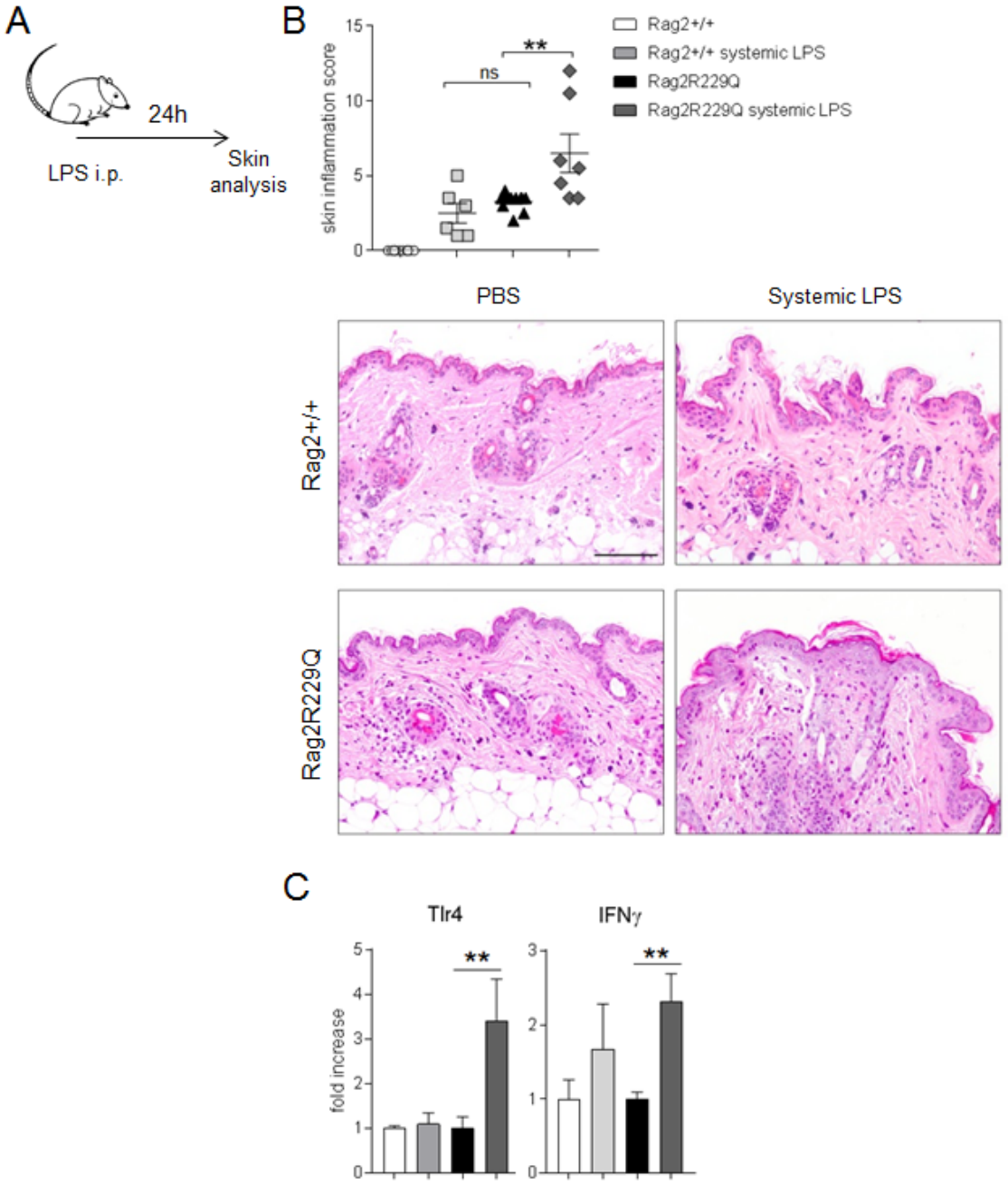

Figure 39: Systemic LPS induces strong inflammatory reaction in the skin of Rag2^{R229Q} mice*. A) Rag2$^{+/+}$ and Rag2^{R229Q} mice were treated with LPS systemically. B) Inflammatory score and representative skin sections from systemic LPS- treated Rag2$^{+/+}$ and Rag2^{R229Q} mice and controls. C) Cutaneous tissue expression of cytokines. 8-12 week-old mice of indicated genotypes were analysed. Mann Whitney test; values are mean ± SEM. *, P < 0.05; **, P < 0.01.*

9.2.9 Chronic DSS treatment increases T-cell mediated skin inflammation in Rag2^{R229Q} mice

To better investigate the link between intestinal inflammation, altered gut barrier permeability and skin degenerations in *Rag2*^{R229Q} mice, we sought to directly probe the role of gut inflammation in the homing of T cells to the cutaneous site. Therefore, we boosted intestinal inflammation in *Rag2*^{R229Q} mice by treating them with DSS. Histological analysis performed 4 weeks after the beginning of the chronic treatment revealed marked signs of skin inflammation in *Rag2*^{R229Q} mice, including epidermal thickness, hyperkeratosis and dermal CD3^{+} T cell infiltration (**Figure 40A)**.

In contrast, such skin alterations were not observed in DSS-treated *Rag2*$^{+/+}$ mice. Inflamed skin undergoes vascular remodelling, consisting of enlarged network of vessels with increased blood flow and influx of inflammatory cells [198]. To test whether vascular changes affect the skin compartment of DSS-treated-*Rag2*^{R229Q} mice, we analysed the blood vascular system by immunostaining for CD31. At steady state, we detected increased vessels coverage (% on area dermis) and number of blood vessels in *Rag2*^{R229Q} mice compared to controls, indicative of the vascular alteration. However, mutant blood vessels did not show changes in size measured by morphometric analysis. Interestingly, DSS-triggered inflammation led to blood vessel enlargement in the mutant skin (**Figure 40B-D**), which might potentially favour the influx of immune cells to the skin.

In parallel, we detected higher expression of T cell and innate cell-recruitment chemokines (**Figure 40E**). Consistently, we observed that the expression of MHCII marker was augmented in the CD45neg fraction of the skin cell suspension of *Rag2*^{R229Q} mice, indicative of epithelial cell hyper-activation upon DSS treatment. Moreover, analysis by FACS of cutaneous cell suspension confirmed that the proportion of CD4^{+} T cells and CD8^{+} T cells within the skin of DSS-treated *Rag2*^{R229Q} mice was augmented of 2-4 fold (**Figure 40F**). Overall, these findings suggest that chronic intestinal inflammation, typical of OS, induces extensive vascular skin alterations, resulting in marked influx of immune cells to the cutaneous site. In parallel, the intestinal barrier breakdown induced by DSS results in the release of LPS or other microbial peptides that may stimulate epithelial cells to release chemokines, contributing to the T cell migration to the cutaneous site.

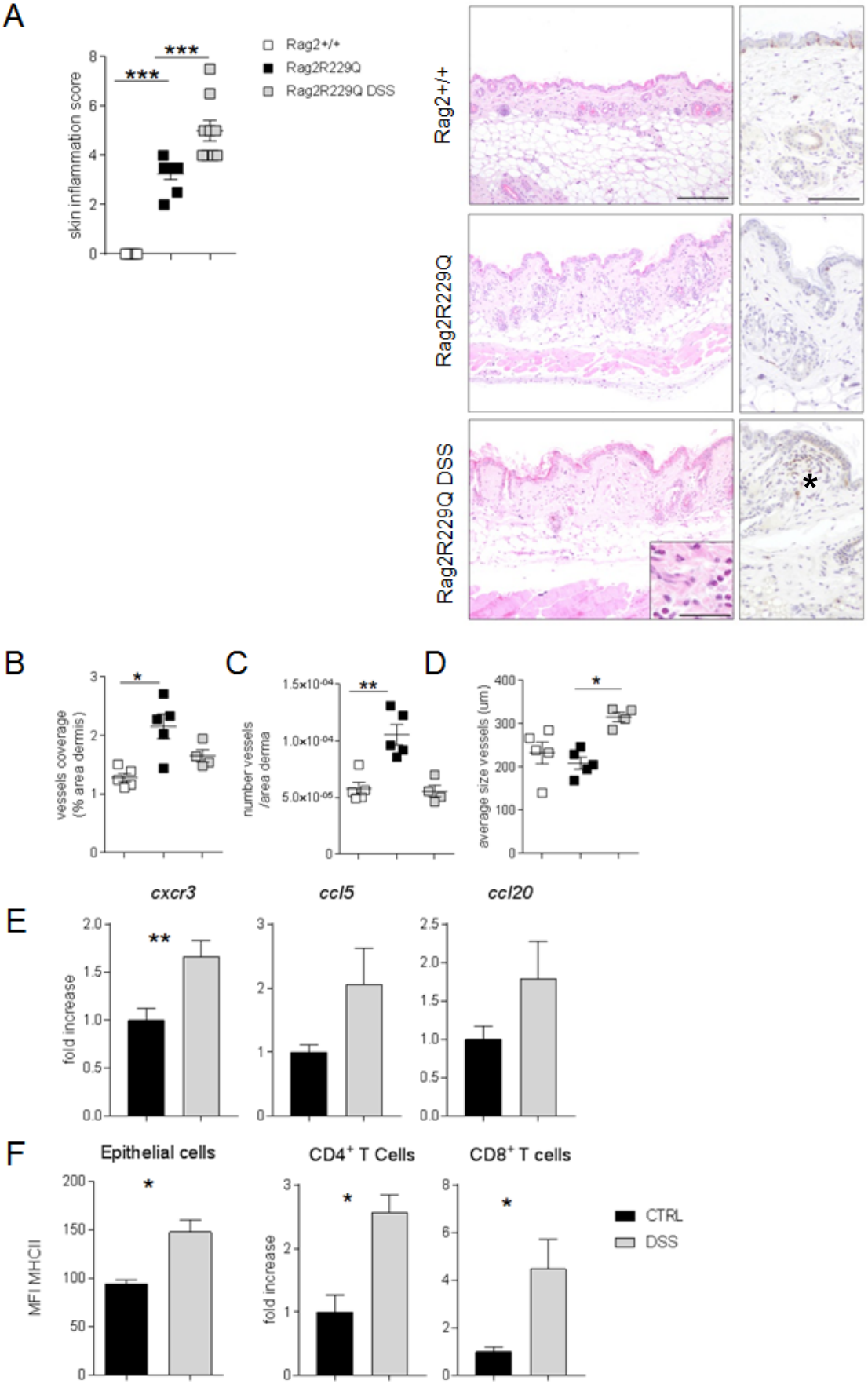
A
skin inflammation score
***
***
Rag2+/+
Rag2R229Q
Rag2R229Q DSS
Rag2+/+
Rag2R229Q
Rag2R229Q DSS
*
B
vessels coverage (% area dermis)
*
C
number vessels /area derma
**
D
average size vessels (um)
*
cxcr3
ccl5
ccl20
E
fold increase
**
F
Epithelial cells
CD4+ T Cells
CD8+ T cells
MFI MHCII
fold increase
CTRL
DSS

Figure 40: Intestinal inflammation affected skin compartment in Rag2^{R229Q} mice. *A) Representative skin section from Rag2$^{+/+}$, Rag2^{R229Q}, and DSS-treated Rag2^{R229Q} mice, stained with H&E and CD3 immunostaining. Histogram shows the inflammation score. Asterisks indicate the area of infiltration. Semi-quantitative analysis of vessels coverage (% on area dermis) (B), number of vessels (on area dermis) (C) and average size vessels (μm) of controls and DSS-treated Rag2^{R229Q} mice (D). (E) mRNA expression of several cytokines on skin tissue. (F)MFI of MHCII on CD45^{-} of Rag2^{R229Q} mice and DSS-treated Rag2^{R229Q} mice. Fold increase of CD4^{+} and CD8^{+} T cell population in the skin of DSS-treated Rag2^{R229Q} mice compared to controls. 8-12 week-old mice of indicated genotypes were analysed. Mann Whitney test; values are mean ± SEM. *, P < 0.05; **, P < 0.01; ***, P < 0.001.*

10. DISCUSSION

10.1 Study of the intestinal pathology in Rag2^{R229Q} mice

Hypomorphic mutations in the RAG genes lead to a profound immunodeficiency associated to multisystem autoimmune like-manifestations, mediated by oligoclonal self-reactive T cells [19, 65]. The severity of the clinical phenotype of RAG deficiency, correlates, at least in part, with the residual level of recombination activity of the mutant protein. However, environmental factors are also important, because patients with similar severe mutations may present with distinct phenotypes. In this regard, OS patients are highly susceptible to infection and develop fungal, bacterial and viral infection typical of SCID. Moreover, diet and lifestyle factors could also influence the disease. Furthermore, alteration of the intestinal microbiota has been recently associated with several inflammatory diseases, including IBD, rheumatoid arthritis and multiple sclerosis, but not yet explored in PIDs. Here, we demonstrated the crucial role of intestinal microbiota in driving the OS pathogenesis.

A primary goal of this thesis was to investigate the role of the intestinal immune responses and gut microbiota in the OS pathogenesis. We found that hypomorphic *Rag2^{R229Q}* mice manifest inflammatory-bowel illness, affecting both large and small intestine, characterized by marked T cell infiltration involving, intriguingly, also T regulatory cells. A broad variability in the inflammatory parameters emerged by the histopathological analysis of the mutant intestine, despite the presence of the same mutation. Similarly to humans, the stochastic nature of V(D)J rearrangements generating the T cell repertoire in combination with environmental factors may impinge on the inflammatory state in mice.

Moreover, a dominant mixed Th1/Th17 cell skewing, implicated in the experimental colitis in mice as well as in the pathogenesis of IBD, characterized the intestinal compartment of *Rag2^{R229Q}* mice [199, 200]. Consistently, we showed that mutant CD4$^+$ T cells, either isolated from apparently healthy or colitic mice, are sufficient to transfer the disease into immune-deficient hosts. However, recent data demonstrated that together with CD4$^+$ T cells, CD8$^+$ T cells participate to immune responses in IBD [201].

Thus, we could not exclude that $CD8^+$ T cells have also been implicated in driving intestinal inflammation.

In the gastrointestinal tract, T regulatory cells play a pivotal role in maintaining immune homeostasis and promoting tolerance against intestinal antigens and commensal bacteria [202]. In this thesis, several experiments addressed the role of Tregs in OS pathogenesis. In particular, *Rag2*^{R229Q} Tregs accumulate in the intestinal mucosa but fail to control intestinal inflammation, suggesting that mutant Tregs may not be functionally competent. By using an adoptive transfer model of colitis, we have demonstrated that *Rag2*^{R229Q} Treg cells co-transferred with *wild-type* $CD45RB^{hi}$ $CD4^+$ T cells are unable to control intestinal disease progression in an immunodeficient host. Moreover, the transfer of a limited number of *wild-type* Tregs ameliorates the intestinal inflammation in *Rag2*^{R229Q} mice, and is associated to the reduction of Th1/Th17 mucosal immune responses. Importantly, it has been shown that high TCR diversity is required for Tregs to maintain the tolerance to intestinal microbiota [176]. In this context, *Rag2*^{R229Q} mice might display selective defects in the acquisition of tolerance to commensal microbial stimuli because of the Treg oligoclonality, potentially skewing intestinal homeostasis to Th1/Th17 inflammation. Our findings suggested that Treg cells are not functionally competent, thus contributing to the autoimmunity of the OS disease.

Mucosal Tregs, together with secretory IgAs, critically protect the gut barrier integrity and control the microbiota diversification, thus maintaining the host-bacterial mutualism [104]. On the other hand, several bacterial species compromise intestinal barrier and induce immune hyperactivation, leading to the development of pro-inflammatory T cell responses [105, 203]. Here, we have shown that *Rag2*^{R229Q} mice are affected by a general B cell deficiency at the mucosal interfaces. Consistently, the analysis of the intestinal microbiota in *Rag2*^{R229Q} mice revealed a reduced bacterial diversity and enrichment of many genera belonging to Proteobacteria phylum, recently associated to IBD development in patients [204]. Additionally, we found high levels of serum LPS in *Rag2*^{R229Q} mice, indicating an important defect in the permeability of gut-blood barrier. Together these findings indicated that mucosal B cell deficiency in

Rag2^{R229Q} mice favours microbial access to the LP and circulation and impacts considerably on the microbial biodiversity.

Collectively, due to the relevance of RAG genes in the generation and the function of adaptive immune system impairment, different types of T and B cells are affected causing systemic disease. Our findings demonstrate that Treg functionality and B cell deficiency could both participate to the development and progression of intestinal disease in multiple synergistic ways. Importantly, the analysis of B and T cell compartment in adoptive cell transfer experiments could help to address how different populations interact among each other contributing to OS pathogenesis.

The clinical benefits deriving from antibiotic treatment implicate commensal bacteria in the pathogenesis. Long-term antibiotic treatment significantly improved the intestinal inflammation in *Rag2*^{R229Q} mice. In particular, we demonstrated that both mucosal and systemic pro-inflammatory Th1 and Th17 cells were significantly decreased in ABX-treated mice, indicating that Th- skewing in *Rag2*^{R229Q} mice is microbiota-dependent. Consistently, we showed that the transfer of altered microbiota isolated from *Rag2*^{R229Q} mice was sufficient to induce a skewed Th1/Th17 pro-inflammatory phenotype in *Rag2*$^{+/+}$mice, suggesting the pathogenic pro-inflammatory properties of the mutant microbiota, independently of the genetic susceptibility. Additional co-housing experiments would help to shed light more on the role of the microbiota in the pathogenesis. Furthermore, we observed that the majority of circulating CCR9^{+} T cells markedly reduced after ABX treatment. Since CCR9 marker is commonly expressed by T cells upon priming by GALT-dendritic cells [205], we speculate that its presence on the majority of T cells may reflect their intestinal origin.

The signalling via MyD88 plays an important role in intestinal homeostasis. In contrast to previous studies describing its protective effects on IBD induced by immune deficiencies [206, 207], we observed that inhibition of Myd88 did not protect *Rag2*^{R229Q} mice from intestinal inflammation. Moreover, several works demonstrated that Myd88-dependent pathway is required for the induction of both Th1 and Th17 immune responses [208, 209]. Our data clearly demonstrated that signalling through Myd88 is

crucial only for Th1 differentiation, but not essential for the Th17 generation and other sensors might be involved in the Th17 generation. As instance, *Atarashi* and collaborators proposed a Myd88/TRIF independent and ATP dependent mechanism of Th17 development in the intestine [95].

Many studies underlined the ability of intestinal microbiota to extend their effects beyond the gastrointestinal tract via immune system modulation. Importantly, reducing intestinal microbial load visibly reduced the systemic autoimmunity in *Rag2*^{R229Q} mice. In particular, a decreased number of infiltrating T cells was detected in the kidney, liver and lung after ABX treatment in *Rag2*^{R229Q} mice. In contrast, skin inflammation did not apparently benefit from ABX treatment. Different explanations could be considered: 1) to be effective at the cutaneous compartment, which likely experiences diverse drug absorption kinetics compared to systemic organs, the oral treatment with ABX might require different dosage and/or administration time; 2) the resident skin microbiota might have a synergistic, yet prominent, role in controlling and modulating local T cell responses in *Rag2*^{R229Q} mice.
Moreover, our findings revealed that reducing bacterial load with antibiotics was beneficial for normalizing serum IgE levels, the clinical hallmark of the disease. Our previous findings indicate that B cell abnormalities and plasma cells differentiation are dependent on the presence of hyperactivated $CD4^+$ T cells [44]. In ABX-treated *Rag2*^{R229Q} mice, the dramatic drop in IgG1, IgA and particularly in IgE production, compared to controls, could be related to the reduced serum concentration of cytokines, responsible for promoting class switch recombination. Microbial exposure during early life and a critical level of bacterial diversity are crucial to establish a proper immunoregulatory network, inhibiting IgE production [210]. In this regard, high IgE serum levels in mutant mice may reflect the low bacterial diversity that is likely defective in promoting immune regulation.

Based on our findings, microbial-induced proliferation could explain the significant number of T cells in the intestinal LP of mutants, in sharp contrast with the overall lymphoid depletion found in other peripheral organs. In addition to this mechanism, we could not exclude that a small proportion of T cells is generated in extra-thymic sites, in

particular locally in the gut. In athymic mice, it has been shown that during embryonic stage, γδ T cells develop within the gut and do not require the thymic education for their differentiation [211]. In this regard, gut cryptopatches, small aggregates of lymphocytes at close contact of the epithelium are the extrathymic source of lymphopoiesis [212]. Future studies will investigate the mutant intestine as potential site for T cell generation.

In summary, hypomorphic Rag defects compromise gut barrier integrity and alter bacterial composition, inducing translocation of the systemic bacterial products in the periphery, which sustains immune dysregulation/autoimmunity typical of OS. In addition, loss of tolerance to commensal bacteria probably leads to Th1/Th17 inflammation, which sustains dysbiosis in a well-recognized regulatory loop. Decreasing bacterial load in *Rag2*^{R229Q} mice with long-term antibiotic treatment ameliorated both local and systemic autoimmunity, by reducing the frequency of circulating CCR9-expressing T cells and Th1/Th17 populations. In addition, serum hyper-IgE was normalized upon antibiotic treatment. Overall these findings revealed that commensal bacteria might have a crucial role in OS pathogenesis.
The evidence that this inflammatory immune phenotype is transmissible to an intact immune system via microbiota-dependent manner let us to speculate that pharmacological gut contamination may constitute a valid strategy to reduce side effects of hematopoietic stem cell transplantation in these patients [213]. On the other hand, interventions aimed at promoting diversification of the intestinal microbiota may improve immunological outcome in OS transplant setting.

10.2 Study of the skin pathology in Rag2^{R229Q} mice

This thesis investigated also the role of cutaneous immune responses in the pathogenesis of OS. A large portion of mice develops cutaneous abnormalities resembling several aspects of human erythroderma. Indeed, although only a minority of mutant mice manifests overt skin phenotype at steady state, the majority of them show however important cutaneous alterations, including increased epidermal thickness with hyperkeratosis and inflammatory infiltrates in the dermis. In particular, we found that cutaneous tissue of *Rag2*^{R229Q} mice exhibited increased cellularity with a prominent expansion of CD45$^+$ cells. Importantly, a deeper analysis revealed lack of γδ T cells in the skin, confirmed also by its lack in the thymus. Compelling evidence indicates the critical role-played by the γδ T cells in tissue homeostasis and repair. In mice lacking γδ T cells (TCRδ$^{-/-}$), wound repair is disrupted and epithelial homeostasis is not maintained. Particularly, keratinocytes undergo increased apoptosis and the αβ T cell population is not maintained in the epidermis, suggesting the importance of the correct TCR for epithelial homeostasis maintenance [214]. Also in the gut compartment, TCRδ$^{-/-}$ mice showed reduced proliferation of epithelial cells in both large and small intestine. Why the γδ T cell development is blocked in the mutant thymus and which immunological implications could lead at the mucosal interfaces remains to be completely addressed.

On the other hand, the expanded CD4$^+$/CD8$^+$ T cell populations in the dermis might be crucial for driving local inflammation. Indeed, CD8$^+$ T cell are predominantly localized to the epidermis, in contrast to the predominantly dermal CD4$^+$ T cells. During infection or inflammation, effector CD8$^+$ T cells enter the dermis from the blood and can then be recruited into the epidermis [215]. The molecular signals that regulate the abundant localization of CD8$^+$ T cells in the dermis of *Rag2*^{R229Q} mice, instead of the normal presence in the epidermis, remain to be identified.

Moreover, we showed that the resident *Rag2*^{R229Q} T cells, producing high amounts of IFNγ, might constitute the main skin-inflammation drivers. Moreover, the synergic activity of other cytokines, including IL-13, TNFα, IL-23, IL-1β, IL-5 and IL-33, increase further the inflammatory environment in mutant mice.

Recent literature suggests that cutaneous exposure to food antigens can reprogram gut homing effector T cells in lymph nodes to express skin homing receptors, eliciting skin inflammation [186]. CCR4 constitutes a necessary component of skin specific lymphocyte trafficking [144]. In the peripheral lymphoid organs of *Rag2*^{R229Q} mice, we found an increase frequency of CCR4-expressing CD4^{+} T cells, suggesting enhanced T cell migration to the skin compartment, likely due to the cutaneous antigen stimulation. Interestingly, a significant proportion of CCR4-expressing CD4^{+} T cells expressed also the gut homing receptor CCR9. This co-expression underlined the dual homing potential of T cells to the gut and to the skin.

This datum opens the possibility that pathogenic gut-originated T cells, once disseminated in the periphery, migrate to the skin compartment, by upregulating the skin tropic receptor after exposure to skin-derived antigens.

However, studies in human samples did not reproduce the overall mouse findings: the majority of effector T cells express the skin homing receptor CLA in RAG patients compared to T cells isolated from the blood of HDs. Importantly, the CCR9^{+} CLA^{+} -and the CCR9^{+}-expressing T cell populations are almost absent in RAG patients. The reason why the expression of CCR9 is lower in RAG patients compared to HDs remains to be explained on the basis of clinical findings. Skin rashes and lesions are the hallmark of patients with Omenn while IBD-like manifestations occur at low frequency. This could be related to the relative immaturity of intestinal flora in newborns. Indeed, it is known that intestinal dysbiosis play a major role in the development of intestinal inflammation. Importantly, OS is a severe disease and patients are usually treated with antibiotics and immunosuppressive drugs until they undergo HSCT. This represents a great limitation for our studies trying to validate mouse findings in humans. Therefore, extend our analysis to adult patients affected by chronic intestinal inflammatory diseases associated to cutaneous co-morbidities could be useful to investigate our hypothesis.

Dendritic cells have a key role in presenting cutaneous antigens and imprinting T cells with skin homing profiles [171]. Interestingly, we have demonstrated that skin-derived DC trafficking to draining lymph nodes is increased and strongly correlates with abundant lymphatic network in *Rag2*^{R229Q} mice. Furthermore, we observed that skin-derived DCs were also able to traffic and activate T cells in the spleen after OVA-

topical immunization, suggesting that skin barrier defects may eventually increase the propensity of antigen-presenting cells to take up antigens and present them to T cells in periphery. Thus, overall our results sustain the notion that skin homing reprogramming of gut-originated inflammatory T cells is a key pathogenic mechanism contributing to skin degeneration in *Rag2*^{R229Q} mice.

The recruitment of T cells to the skin is also regulated by several chemokines released by keratinocytes [216]. Firstly, we showed that mutant keratinocytes display an abnormal activation, which is in agreement with a chronic stimulation sustained by environmental and bacterial factors. Moreover, we observed a prominent up-regulation in tissue expression of T cell targeting-chemokines that may reflect the marked lymphocytic infiltration in the dermis. Consistently, the transfer of OT-1 or OT-II cells in *Rag2*$^{+/+}$ or *Rag2*^{R229Q} mice after OVA topical immunization clearly revealed the preferential accumulation of T cells into the inflamed skin of *Rag2*^{R229Q} mice.

The epithelial barriers of our bodies are continually exposed to environmental stimuli and must respond properly to maintain the barrier integrity [217]. In our study, we found that epidermis thickness was greatly increased in *Rag2*^{R229Q} mice, correlating with the augmented expression of keratin markers. Consistently, we observed increased expression of antimicrobial peptides and of several TLRs in the skin tissue of mutant mice, indicative of important alterations in the integrity of epithelial skin barrier, which may lead to compromised protection against environmental and pathogenic insults. Loss of structural and functional barrier integrity, and consequent penetration of pathogens induce skin inflammation. Recent studies have correlated the presence of certain bacteria with specific disease state. In particular, in psoriatic lesions, Firmicutes are more abundant while Actinobacteria and Proteobacteria are relatively less represented within the skin commensal community compared to healthy skins [160]. Moreover, increased prevalence of *Staphylococci*, including both *S.aureus* and *S. epidermis,* was found in patients with atopic dermatitis [218]. Based on these studies, selective shift in the skin microbiome has been associated with several skin disorders. Here, have demonstrated that *Rag2*^{R229Q} mice manifested a selective shift in resident skin microbiota with decreased abundance of commensal bacteria belonging to Actinobacteria and Firmicutes phyla. Specifically, the loss of some bacteria genera

(*Streptococcus*, *Staphylococcus* and *Propionibacterium*) might contribute to render the *Rag2*^{R229Q} skin more susceptible to colonization by pathogenic bacteria. Furthermore, in mutant mice these alterations were compensated by an important expansion of unknown and uncultivable bacteria.

Interestingly, among the TLRs investigated, we observed that TLR4 was the most highly expressed in the mutant skin. Keratinocytes are known to express functional TLR4 and secrete pro-inflammatory cytokines in response to TLR4 interaction [219]. Therefore, we sought to deeper evaluate the effect of TLR4 stimulation on the cutaneous compartment of mutant mice. We found that upon LPS intradermal injection, the skin of *Rag2*^{R229Q} mice experienced a strong inflammatory response, characterized by important epidermal structural changes and acute Th1 mediated responses. Interestingly, such responses were also evident, although to a lesser extent, in the *wild-type* mice, in which the inflammatory parameters reached those observed in the mutants at steady state, thus supporting the pivotal mechanistic contribution of this microbial molecule in the pathogenic mechanisms underlying skin disease in *Rag2*^{R229Q} mice.

We reported high levels of LPS in the serum of *Rag2*^{R229Q} mice, consequence of the compromised intestinal barrier permeability [197]. Importantly, we demonstrated that this circulating microbial product could have a causative role in determining the chronic activation of the cutaneous epithelial barrier in the mutant mice. Sensing of systemic LPS by skin epithelial cells is indeed proved by the rapid and significant increase in TLR4 tissue expression of mutant mice, following i.p administration. Consistent with our conclusions are also reports showing both the presence of, and high reactivity to, LPS endotoxins in the blood of patients with skin conditions [220].

Emerging evidence support the existence of communication axes between gut and skin organs. It has been documented that atopic dermatitis and rosacea are both associated with changes in gut barrier and intestinal microbiota [221, 222]. Furthermore, association between imbalances of the intestinal microbiota and development of skin inflammation have been described in mice and patients [223, 224]. However, the cellular and molecular mechanisms whereby gut inflammation could be linked to skin disorders are largely unexplored. In coeliac disease, the generation of circulating antibodies, produced by the intestinal immune reaction to gluten, could be able to

trigger inflammation and dermatitis [225], confirming the possibility that immune cells could traffic in and out the skin compartment. Moreover, cutaneous exposure to food antigens was shown to reprogram gut homing effector T cells in lymph nodes to express skin homing receptors, eliciting skin inflammation [186]. In OS, systemically translocated commensal antigens in the presence of breaches of the gut barrier could potentially reprogram T cells to express skin homing potential. Intestinal-derived LPS could be considered as a potential trigger in driving this process. However, it remains to elucidate whether other microbial compounds could be involved.

Despite several evidence linking IBD-like disease and skin inflammation in OS pathogenesis, the possible mechanisms of gut T cell reprogramming after cutaneous antigen exposure remain to be elucidated by future studies. Moreover, the analysis of the TCR repertoire of T cells isolated from cutaneous and intestinal sites will be useful for supporting our hypothesis.

Multiple disease may arise or be exacerbate due to a leaky gut, including autoimmune diaseses, inflammatory bowel disease, celiac disease, autoimmune hepatitis, type 1 diabetes (T1D), multiple sclerosis, and systemic lupus erythematosus (SLE) [226].

In OS mutants, T cells co-express gut and skin homing receptors and showing potential trafficking between the mucosal compartments. In particular, we showed that boosted intestinal inflammation worsens skin degeneration in *Rag2*^{R229Q} mice. On the other hand, we could not exclude that the skin is the first point of contact where the inflammation starts in OS. Indeed, the skin is in direct contact with the environment and it is constantly exposed to microorganims. In particular, changes in the resident communities could perturb the overall ecosystem to induce disease conditions, even in the absence of pathogen colonization. Exposure to allergens or irritants can also trigger inflammatory reactions at the cutaneous sites. Testing this other possibility may help to shed light on the pathogenic mechanisms underlying OS skin autoimmunity.

Here, we have demonstrated the existence and the contribution of a gut-skin axis in the OS pathogenesis. We have first shown that compromised gut barrier integrity and loss of tolerance to commensal bacteria leads to systemic Th1/Th17 cell dissemination in *Rag2*^{R229Q} mice [197]. Then, we found that chronic DSS treatment, administered to

boost intestinal inflammation in *Rag2*^{R229Q} mice, worsened the cutaneous disease in treated mice, inducing hyper-activation of keratinocytes, abnormal release of leucocyte-attracting chemokines and enhanced T cell recruitment to the cutaneous site. Thus, these results indicate that gut inflammation and dysbiosis significantly impacts on the pathogenesis of skin degeneration in *Rag2*^{R229Q} mice.

10.3 Conclusive remarks and future directions

OS is a peculiar immunodeficiency caused by hypomorphic mutations in RAG genes, allowing residual T and B-cell development. OS patients develop IBD-like disease associated to a spectrum of cutaneous manifestations, whose underlying immunological mechanisms remained incompletely understood. Taking advantage of the mouse model of the disease, the *Rag2*^{R229Q} mice, we have provided novel insights into disease pathogenesis, showing that gut commensals and/or commensal bacteria-derived signals might play a substantial role in determining the distinctive immune dysregulation and autoimmune manifestations in RAG-associated immune deficiency. Moreover, our results, indicating that microbiota can constitute a pharmacological target for these crucial pathogenetic aspects of the disease, may represent the groundwork for novel approaches in OS patient's management.

Defects in the function of intestinal mucosal barrier as well as inappropriate immune responses to gut microbiota are recognized disease mechanisms of IBD [227]. Based on these similarities, understanding of OS disease can complement the comprehension of IBD pathogenesis and might also provide novel treatment options for affected patients.

The skin represents one of the most common extra-intestinal system affected in patients with IBD, including CD or UC [228]. The most common cutaneous lesions associated with IBD are erythema nodosum, pyoderma gangrenosum, and aphthous stomatitis [229]. Other skin manifestations such as psoriasis and vilitigo have been also associated [230]. In the gastrointestinal tract, the equilibrium between mucosal epithelium, commensal microbes and host immune responses is essential for maintaining intestinal homeostasis and mucosal T cells represent the key players [231]. Aberrant T cell response to microbial antigens can perturb the equilibrium and could be the mechanism that causes inflammation and the release of inflammatory cytokines, resulting in the development of IBD [232]. In this context, the extra-intestinal manifestations seen in IBD may be the results of immune dysregulation, and, particularly, of a T cell-mediated destructive process. For instance, Adams and Eksteen proposed an explanation for IBD patients with hepatic complications. In particular, mucosal T cells aberrantly travel from the intestine to the liver, becoming exposed to hepatic antigens and, ultimately leading to hepatic inflammation [233]. In our study, we have demonstrated that such a mechanism could be also at the basis of the communication axes between gut and

distant organs, such as the skin, and explain the pathogenesis of a rare form of immunodeficiency, presenting with IBD-like intestinal inflammation and skin co-morbidity. Investigating whether same cellular and molecular dynamics extend to IBD patients presenting skin extra-intestinal manifestations could advance the comprehension of IBD immunopathology. Furthermore, the management of skin manifestations and IBD may benefit from the targeting of the gut-skin axis. It is possible that the therapeutic modulation of the intestinal microbiota (via AMPs, antibiotics and antiseptics) modifies the secretory, metabolic and hormonal activity of the skin, impacting directly on cutaneous inflammation. The ability to modify the function of one organ by the manipulation of the other would constitute a novel therapeutic strategy.

11. BIBLIOGRAPHY

1. Geha, R.S., et al., *Primary immunodeficiency diseases: an update from the International Union of Immunological Societies Primary Immunodeficiency Diseases Classification Committee.* J Allergy Clin Immunol, 2007. **120**(4): p. 776-94.
2. Notarangelo, L.D., *Primary immunodeficiencies.* J Allergy Clin Immunol, 2010. **125**(2 Suppl 2): p. S182-94.
3. Holland, S.M., *Chronic granulomatous disease.* Clin Rev Allergy Immunol, 2010. **38**(1): p. 3-10.
4. Unsworth, D.J., *Complement deficiency and disease.* J Clin Pathol, 2008. **61**(9): p. 1013-7.
5. Fischer, A., et al., *Severe combined immunodeficiency. A model disease for molecular immunology and therapy.* Immunol Rev, 2005. **203**: p. 98-109.
6. Conley, M.E., et al., *Primary B cell immunodeficiencies: comparisons and contrasts.* Annu Rev Immunol, 2009. **27**: p. 199-227.
7. Vetrie, D., et al., *The gene involved in X-linked agammaglobulinaemia is a member of the src family of protein-tyrosine kinases.* Nature, 1993. **361**(6409): p. 226-33.
8. Buckley, R.H., *Pulmonary complications of primary immunodeficiencies.* Paediatr Respir Rev, 2004. **5 Suppl A**: p. S225-33.
9. Cunningham-Rundles, C., *Physiology of IgA and IgA deficiency.* J Clin Immunol, 2001. **21**(5): p. 303-9.
10. Malacarne, F., et al., *Reduced thymic output, increased spontaneous apoptosis and oligoclonal B cells in polyethylene glycol-adenosine deaminase-treated patients.* Eur J Immunol, 2005. **35**(11): p. 3376-86.
11. Noguchi, M., et al., *Interleukin-2 receptor gamma chain: a functional component of the interleukin-7 receptor.* Science, 1993. **262**(5141): p. 1877-80.
12. Macchi, P., et al., *Mutations of Jak-3 gene in patients with autosomal severe combined immune deficiency (SCID).* Nature, 1995. **377**(6544): p. 65-8.

13. Puel, A., et al., *Defective IL7R expression in T(-)B(+)NK(+) severe combined immunodeficiency.* Nat Genet, 1998. **20**(4): p. 394-7.
14. Nekrep, N., et al., *When the lymphocyte loses its clothes.* Immunity, 2003. **18**(4): p. 453-7.
15. Frank, J., et al., *Exposing the human nude phenotype.* Nature, 1999. **398**(6727): p. 473-4.
16. Villa, A., et al., *V(D)J recombination defects in lymphocytes due to RAG mutations: severe immunodeficiency with a spectrum of clinical presentations.* Blood, 2001. **97**(1): p. 81-8.
17. de Saint-Basile, G., et al., *Restricted heterogeneity of T lymphocytes in combined immunodeficiency with hypereosinophilia (Omenn's syndrome).* J Clin Invest, 1991. **87**(4): p. 1352-9.
18. Rieux-Laucat, F., et al., *Highly restricted human T cell repertoire in peripheral blood and tissue-infiltrating lymphocytes in Omenn's syndrome.* J Clin Invest, 1998. **102**(2): p. 312-21.
19. Villa, A., et al., *Partial V(D)J recombination activity leads to Omenn syndrome.* Cell, 1998. **93**(5): p. 885-96.
20. Villa, A., et al., *Genetically determined lymphopenia and autoimmune manifestations.* Curr Opin Immunol, 2008. **20**(3): p. 318-24.
21. Dvorak, C.C. and M.J. Cowan, *Radiosensitive severe combined immunodeficiency disease.* Immunol Allergy Clin North Am, 2010. **30**(1): p. 125-42.
22. O'Driscoll, M., et al., *DNA ligase IV mutations identified in patients exhibiting developmental delay and immunodeficiency.* Mol Cell, 2001. **8**(6): p. 1175-85.
23. van der Burg, M., et al., *A DNA-PKcs mutation in a radiosensitive T-B- SCID patient inhibits Artemis activation and nonhomologous end-joining.* J Clin Invest, 2009. **119**(1): p. 91-8.
24. Bacchetta, R. and L.D. Notarangelo, *Immunodeficiency with autoimmunity: beyond the paradox.* Front Immunol, 2013. **4**: p. 77.
25. Villa, A., L.D. Notarangelo, and C.M. Roifman, *Omenn syndrome: inflammation in leaky severe combined immunodeficiency.* J Allergy Clin Immunol, 2008. **122**(6): p. 1082-6.

26. Sobacchi, C., et al., *RAG-dependent primary immunodeficiencies.* Hum Mutat, 2006. **27**(12): p. 1174-84.
27. Ege, M., et al., *Omenn syndrome due to ARTEMIS mutations.* Blood, 2005. **105**(11): p. 4179-86.
28. Roifman, C.M., Y. Gu, and A. Cohen, *Mutations in the RNA component of RNase mitochondrial RNA processing might cause Omenn syndrome.* J Allergy Clin Immunol, 2006. **117**(4): p. 897-903.
29. Giliani, S., et al., *Omenn syndrome in an infant with IL7RA gene mutation.* J Pediatr, 2006. **148**(2): p. 272-4.
30. Roifman, C.M., et al., *Adenosine deaminase deficiency can present with features of Omenn syndrome.* J Allergy Clin Immunol, 2008. **121**(4): p. 1056-8.
31. Pirovano, S., et al., *Impaired thymic output and restricted T-cell repertoire in two infants with immunodeficiency and early-onset generalized dermatitis.* Immunol Lett, 2003. **86**(1): p. 93-7.
32. Shibata, F., et al., *Skin infiltration of CD56(bright) CD16(-) natural killer cells in a case of X-SCID with Omenn syndrome-like manifestations.* Eur J Haematol, 2007. **79**(1): p. 81-5.
33. Gennery, A.R., et al., *Mutations in CHD7 in patients with CHARGE syndrome cause T-B + natural killer cell + severe combined immune deficiency and may cause Omenn-like syndrome.* Clin Exp Immunol, 2008. **153**(1): p. 75-80.
34. Grunebaum, E., A. Bates, and C.M. Roifman, *Omenn syndrome is associated with mutations in DNA ligase IV*. J Allergy Clin Immunol, 2008. **122**(6): p. 1219-20.
35. Omenn, G.S., *Familial Reticuloendotheliosis with Eosinophilia.* N Engl J Med, 1965. **273**: p. 427-32.
36. Schuetz, C., et al., *Lesson from hypomorphic recombination-activating gene (RAG) mutations: Why asymptomatic siblings should also be tested.* J Allergy Clin Immunol, 2014. **133**(4): p. 1211-5.
37. Schuetz, C., et al., *An immunodeficiency disease with RAG mutations and granulomas.* N Engl J Med, 2008. **358**(19): p. 2030-8.

38. van der Burg, M. and A.R. Gennery, *Educational paper. The expanding clinical and immunological spectrum of severe combined immunodeficiency.* Eur J Pediatr, 2011. **170**(5): p. 561-71.
39. Harville, T.O., et al., *Oligoclonal expansion of CD45RO+ T lymphocytes in Omenn syndrome.* J Clin Immunol, 1997. **17**(4): p. 322-32.
40. Cavadini, P., et al., *AIRE deficiency in thymus of 2 patients with Omenn syndrome.* J Clin Invest, 2005. **115**(3): p. 728-32.
41. Poliani, P.L., et al., *Early defects in human T-cell development severely affect distribution and maturation of thymic stromal cells: possible implications for the pathophysiology of Omenn syndrome.* Blood, 2009. **114**(1): p. 105-8.
42. Cassani, B., et al., *Defect of regulatory T cells in patients with Omenn syndrome.* J Allergy Clin Immunol, 2010. **125**(1): p. 209-16.
43. Poliani, P.L., W. Vermi, and F. Facchetti, *Thymus microenvironment in human primary immunodeficiency diseases.* Curr Opin Allergy Clin Immunol, 2009. **9**(6): p. 489-95.
44. Cassani, B., et al., *Homeostatic expansion of autoreactive immunoglobulin-secreting cells in the Rag2 mouse model of Omenn syndrome.* J Exp Med, 2010. **207**(7): p. 1525-40.
45. Walter, J.E., et al., *Expansion of immunoglobulin-secreting cells and defects in B cell tolerance in Rag-dependent immunodeficiency.* J Exp Med, 2010. **207**(7): p. 1541-54.
46. Walter, J.E., et al., *Broad-spectrum antibodies against self-antigens and cytokines in RAG deficiency.* J Clin Invest, 2015. **125**(11): p. 4135-48.
47. Maina, V., et al., *Hypomorphic mutation in the RAG2 gene affects dendritic cell distribution and migration.* J Leukoc Biol, 2013. **94**(6): p. 1221-30.
48. Matangkasombut, P., et al., *Lack of iNKT cells in patients with combined immune deficiency due to hypomorphic RAG mutations.* Blood, 2008. **111**(1): p. 271-4.
49. Scheimberg, I., et al., *Omenn's syndrome: differential diagnosis in infants with erythroderma and immunodeficiency.* Pediatr Dev Pathol, 2001. **4**(3): p. 237-45.
50. Gomez, L., et al., *Treatment of Omenn syndrome by bone marrow transplantation.* J Pediatr, 1995. **127**(1): p. 76-81.

51. Mazzolari, E., et al., *Hematopoietic stem cell transplantation in Omenn syndrome: a single-center experience.* Bone Marrow Transplant, 2005. **36**(2): p. 107-14.
52. Hacein-Bey-Abina, S., et al., *A modified gamma-retrovirus vector for X-linked severe combined immunodeficiency.* N Engl J Med, 2014. **371**(15): p. 1407-17.
53. Aiuti, A., et al., *Gene therapy for immunodeficiency due to adenosine deaminase deficiency.* N Engl J Med, 2009. **360**(5): p. 447-58.
54. Candotti, F., et al., *Gene therapy for adenosine deaminase-deficient severe combined immune deficiency: clinical comparison of retroviral vectors and treatment plans.* Blood, 2012. **120**(18): p. 3635-46.
55. Lagresle-Peyrou, C., et al., *Long-term immune reconstitution in RAG-1-deficient mice treated by retroviral gene therapy: a balance between efficiency and toxicity.* Blood, 2006. **107**(1): p. 63-72.
56. Pike-Overzet, K., et al., *Correction of murine Rag1 deficiency by self-inactivating lentiviral vector-mediated gene transfer.* Leukemia, 2011. **25**(9): p. 1471-83.
57. van Til, N.P., et al., *Correction of murine Rag2 severe combined immunodeficiency by lentiviral gene therapy using a codon-optimized RAG2 therapeutic transgene.* Mol Ther, 2012. **20**(10): p. 1968-80.
58. Persons, D.A., *Gene therapy: Targeting beta-thalassaemia.* Nature, 2010. **467**(7313): p. 277-8.
59. Durandy, A., et al., *Prenatal testing for inherited immune deficiencies by fetal blood sampling.* Prenat Diagn, 1982. **2**(2): p. 109-13.
60. D'Alton, M.E. and A.H. DeCherney, *Prenatal diagnosis.* N Engl J Med, 1993. **328**(2): p. 114-20.
61. Villa, A., et al., *Prenatal diagnosis of RAG-deficient Omenn syndrome.* Prenat Diagn, 2000. **20**(1): p. 56-9.
62. Fang, M., et al., *Next Generation Sequencing Data Analysis in Primary Immunodeficiency Disorders - Future Directions.* J Clin Immunol, 2016. **36 Suppl 1**: p. 68-75.
63. Meyts, I., et al., *Exome and genome sequencing for inborn errors of immunity.* J Allergy Clin Immunol, 2016. **138**(4): p. 957-969.

64. Khiong, K., et al., *Homeostatically proliferating CD4 T cells are involved in the pathogenesis of an Omenn syndrome murine model.* J Clin Invest, 2007. **117**(5): p. 1270-81.
65. Marrella, V., et al., *A hypomorphic R229Q Rag2 mouse mutant recapitulates human Omenn syndrome.* J Clin Invest, 2007. **117**(5): p. 1260-9.
66. Giblin, W., et al., *Leaky severe combined immunodeficiency and aberrant DNA rearrangements due to a hypomorphic RAG1 mutation.* Blood, 2009. **113**(13): p. 2965-75.
67. Marrella, V., et al., *Anti-CD3epsilon mAb improves thymic architecture and prevents autoimmune manifestations in a mouse model of Omenn syndrome: therapeutic implications.* Blood, 2012. **120**(5): p. 1005-14.
68. Worthey, E.A., et al., *Making a definitive diagnosis: successful clinical application of whole exome sequencing in a child with intractable inflammatory bowel disease.* Genet Med, 2011. **13**(3): p. 255-62.
69. Glocker, E.O., et al., *Inflammatory bowel disease and mutations affecting the interleukin-10 receptor.* N Engl J Med, 2009. **361**(21): p. 2033-45.
70. Agarwal, S. and L. Mayer, *Diagnosis and treatment of gastrointestinal disorders in patients with primary immunodeficiency.* Clin Gastroenterol Hepatol, 2013. **11**(9): p. 1050-63.
71. Rohr, J., et al., *Chronic inflammatory bowel disease as key manifestation of atypical ARTEMIS deficiency.* J Clin Immunol, 2010. **30**(2): p. 314-20.
72. Agarwal, S., et al., *Characterization of immunologic defects in patients with common variable immunodeficiency (CVID) with intestinal disease.* Inflamm Bowel Dis, 2011. **17**(1): p. 251-9.
73. Levy, J., et al., *Clinical spectrum of X-linked hyper-IgM syndrome.* J Pediatr, 1997. **131**(1 Pt 1): p. 47-54.
74. Mowat, A.M. and W.W. Agace, *Regional specialization within the intestinal immune system.* Nat Rev Immunol, 2014. **14**(10): p. 667-85.
75. Okumura, R. and K. Takeda, *Roles of intestinal epithelial cells in the maintenance of gut homeostasis.* Exp Mol Med, 2017. **49**(5): p. e338.

76. Vaishnava, S., et al., *The antibacterial lectin RegIIIgamma promotes the spatial segregation of microbiota and host in the intestine.* Science, 2011. **334**(6053): p. 255-8.
77. Brogden, K.A., *Antimicrobial peptides: pore formers or metabolic inhibitors in bacteria?* Nat Rev Microbiol, 2005. **3**(3): p. 238-50.
78. Johansen, F.E. and C.S. Kaetzel, *Regulation of the polymeric immunoglobulin receptor and IgA transport: new advances in environmental factors that stimulate pIgR expression and its role in mucosal immunity.* Mucosal Immunol, 2011. **4**(6): p. 598-602.
79. Mabbott, N.A., et al., *Microfold (M) cells: important immunosurveillance posts in the intestinal epithelium.* Mucosal Immunol, 2013. **6**(4): p. 666-77.
80. Mora, J.R., et al., *Selective imprinting of gut-homing T cells by Peyer's patch dendritic cells.* Nature, 2003. **424**(6944): p. 88-93.
81. Mora, J.R., et al., *Generation of gut-homing IgA-secreting B cells by intestinal dendritic cells.* Science, 2006. **314**(5802): p. 1157-60.
82. Iwata, M., et al., *Retinoic acid imprints gut-homing specificity on T cells.* Immunity, 2004. **21**(4): p. 527-38.
83. Villablanca, E.J., et al., *beta7 integrins are required to give rise to intestinal mononuclear phagocytes with tolerogenic potential.* Gut, 2014. **63**(9): p. 1431-40.
84. Wagner, N., et al., *Critical role for beta7 integrins in formation of the gut-associated lymphoid tissue.* Nature, 1996. **382**(6589): p. 366-70.
85. Zabel, B.A., et al., *Human G protein-coupled receptor GPR-9-6/CC chemokine receptor 9 is selectively expressed on intestinal homing T lymphocytes, mucosal lymphocytes, and thymocytes and is required for thymus-expressed chemokine-mediated chemotaxis.* J Exp Med, 1999. **190**(9): p. 1241-56.
86. Stock, A., G. Napolitani, and V. Cerundolo, *Intestinal DC in migrational imprinting of immune cells.* Immunol Cell Biol, 2013. **91**(3): p. 240-9.
87. Kagnoff, M.F., *Current concepts in mucosal immunity. III. Ontogeny and function of gamma delta T cells in the intestine.* Am J Physiol, 1998. **274**(3 Pt 1): p. G455-8.

88. Ismail, A.S., C.L. Behrendt, and L.V. Hooper, *Reciprocal interactions between commensal bacteria and gamma delta intraepithelial lymphocytes during mucosal injury.* J Immunol, 2009. **182**(5): p. 3047-54.
89. Mazmanian, S.K., et al., *An immunomodulatory molecule of symbiotic bacteria directs maturation of the host immune system.* Cell, 2005. **122**(1): p. 107-18.
90. Round, J.L. and S.K. Mazmanian, *The gut microbiota shapes intestinal immune responses during health and disease.* Nat Rev Immunol, 2009. **9**(5): p. 313-23.
91. Ivanov, II, et al., *Specific microbiota direct the differentiation of IL-17-producing T-helper cells in the mucosa of the small intestine.* Cell Host Microbe, 2008. **4**(4): p. 337-49.
92. Ivanov, II, et al., *Induction of intestinal Th17 cells by segmented filamentous bacteria.* Cell, 2009. **139**(3): p. 485-98.
93. Wu, H.J., et al., *Gut-residing segmented filamentous bacteria drive autoimmune arthritis via T helper 17 cells.* Immunity, 2010. **32**(6): p. 815-27.
94. Lee, Y.K., et al., *Proinflammatory T-cell responses to gut microbiota promote experimental autoimmune encephalomyelitis.* Proc Natl Acad Sci U S A, 2011. **108 Suppl 1**: p. 4615-22.
95. Atarashi, K., et al., *ATP drives lamina propria T(H)17 cell differentiation.* Nature, 2008. **455**(7214): p. 808-12.
96. Chung, H., et al., *Gut immune maturation depends on colonization with a host-specific microbiota.* Cell, 2012. **149**(7): p. 1578-93.
97. Josefowicz, S.Z., L.F. Lu, and A.Y. Rudensky, *Regulatory T cells: mechanisms of differentiation and function.* Annu Rev Immunol, 2012. **30**: p. 531-64.
98. Atarashi, K., Y. Umesaki, and K. Honda, *Microbiotal influence on T cell subset development.* Semin Immunol, 2011. **23**(2): p. 146-53.
99. Atarashi, K., et al., *Induction of colonic regulatory T cells by indigenous Clostridium species.* Science, 2011. **331**(6015): p. 337-41.
100. Geuking, M.B., et al., *Intestinal bacterial colonization induces mutualistic regulatory T cell responses.* Immunity, 2011. **34**(5): p. 794-806.
101. Mazmanian, S.K., J.L. Round, and D.L. Kasper, *A microbial symbiosis factor prevents intestinal inflammatory disease.* Nature, 2008. **453**(7195): p. 620-5.

102. Smith, P.M., et al., *The microbial metabolites, short-chain fatty acids, regulate colonic Treg cell homeostasis.* Science, 2013. **341**(6145): p. 569-73.
103. Chang, P.V., et al., *The microbial metabolite butyrate regulates intestinal macrophage function via histone deacetylase inhibition.* Proc Natl Acad Sci U S A, 2014. **111**(6): p. 2247-52.
104. Kawamoto, S., et al., *Foxp3(+) T cells regulate immunoglobulin a selection and facilitate diversification of bacterial species responsible for immune homeostasis.* Immunity, 2014. **41**(1): p. 152-65.
105. Kamada, N., et al., *Role of the gut microbiota in immunity and inflammatory disease.* Nat Rev Immunol, 2013. **13**(5): p. 321-35.
106. Macpherson, A.J., et al., *The immune geography of IgA induction and function.* Mucosal Immunol, 2008. **1**(1): p. 11-22.
107. Fagarasan, S., et al., *Adaptive immune regulation in the gut: T cell-dependent and T cell-independent IgA synthesis.* Annu Rev Immunol, 2010. **28**: p. 243-73.
108. Pabst, O., *New concepts in the generation and functions of IgA.* Nat Rev Immunol, 2012. **12**(12): p. 821-32.
109. Tezuka, H., et al., *Prominent role for plasmacytoid dendritic cells in mucosal T cell-independent IgA induction.* Immunity, 2011. **34**(2): p. 247-57.
110. Frank, D.N., et al., *Molecular-phylogenetic characterization of microbial community imbalances in human inflammatory bowel diseases.* Proc Natl Acad Sci U S A, 2007. **104**(34): p. 13780-5.
111. Issa, M., A.N. Ananthakrishnan, and D.G. Binion, *Clostridium difficile and inflammatory bowel disease.* Inflamm Bowel Dis, 2008. **14**(10): p. 1432-42.
112. Winter, S.E., et al., *Host-derived nitrate boosts growth of E. coli in the inflamed gut.* Science, 2013. **339**(6120): p. 708-11.
113. Devkota, S., et al., *Dietary-fat-induced taurocholic acid promotes pathobiont expansion and colitis in Il10-/- mice.* Nature, 2012. **487**(7405): p. 104-8.
114. Garrett, W.S., et al., *Communicable ulcerative colitis induced by T-bet deficiency in the innate immune system.* Cell, 2007. **131**(1): p. 33-45.
115. Garrett, W.S., et al., *Enterobacteriaceae act in concert with the gut microbiota to induce spontaneous and maternally transmitted colitis.* Cell Host Microbe, 2010. **8**(3): p. 292-300.

116. Powell, N., et al., *The transcription factor T-bet regulates intestinal inflammation mediated by interleukin-7 receptor+ innate lymphoid cells.* Immunity, 2012. **37**(4): p. 674-84.
117. Scher, J.U., et al., *Expansion of intestinal Prevotella copri correlates with enhanced susceptibility to arthritis.* Elife, 2013. **2**: p. e01202.
118. Ochoa-Reparaz, J., et al., *Role of gut commensal microflora in the development of experimental autoimmune encephalomyelitis.* J Immunol, 2009. **183**(10): p. 6041-50.
119. Ochoa-Reparaz, J., et al., *A polysaccharide from the human commensal Bacteroides fragilis protects against CNS demyelinating disease.* Mucosal Immunol, 2010. **3**(5): p. 487-95.
120. Kriegel, M.A., et al., *Naturally transmitted segmented filamentous bacteria segregate with diabetes protection in nonobese diabetic mice.* Proc Natl Acad Sci U S A, 2011. **108**(28): p. 11548-53.
121. Lehman, H., *Skin manifestations of primary immune deficiency.* Clin Rev Allergy Immunol, 2014. **46**(2): p. 112-9.
122. Winkelstein, J.A., et al., *Chronic granulomatous disease. Report on a national registry of 368 patients.* Medicine (Baltimore), 2000. **79**(3): p. 155-69.
123. Puck, J.M., *Primary immunodeficiency diseases.* JAMA, 1997. **278**(22): p. 1835-41.
124. Loyola Presa, J.G., et al., *Cutaneous manifestations in patients with Wiskott-Aldrich syndrome submitted to haematopoietic stem cell transplantation.* Arch Dis Child, 2013. **98**(4): p. 304-7.
125. Dohil, M., et al., *Cutaneous manifestations of chronic granulomatous disease. A report of four cases and review of the literature.* J Am Acad Dermatol, 1997. **36**(6 Pt 1): p. 899-907.
126. Arunachalam, M., et al., *Common variable immunodeficiency in vitiligo.* G Ital Dermatol Venereol, 2010. **145**(6): p. 783-8.
127. Spickett, G., et al., *Alopecia totalis and vitiligo in common variable immunodeficiency.* Postgrad Med J, 1991. **67**(785): p. 291-4.
128. Koskinen, S., *Long-term follow-up of health in blood donors with primary selective IgA deficiency.* J Clin Immunol, 1996. **16**(3): p. 165-70.

129. Ahonen, P., et al., *Clinical variation of autoimmune polyendocrinopathy-candidiasis-ectodermal dystrophy (APECED) in a series of 68 patients.* N Engl J Med, 1990. **322**(26): p. 1829-36.
130. Oh, J., et al., *The altered landscape of the human skin microbiome in patients with primary immunodeficiencies.* Genome Res, 2013. **23**(12): p. 2103-14.
131. Solanas, G. and S.A. Benitah, *Regenerating the skin: a task for the heterogeneous stem cell pool and surrounding niche.* Nat Rev Mol Cell Biol, 2013. **14**(11): p. 737-48.
132. Maricich, S.M., et al., *Merkel cells are essential for light-touch responses.* Science, 2009. **324**(5934): p. 1580-2.
133. Pasparakis, M., I. Haase, and F.O. Nestle, *Mechanisms regulating skin immunity and inflammation.* Nat Rev Immunol, 2014. **14**(5): p. 289-301.
134. Grice, E.A. and J.A. Segre, *The skin microbiome.* Nat Rev Microbiol, 2011. **9**(4): p. 244-53.
135. Di Meglio, P., G.K. Perera, and F.O. Nestle, *The multitasking organ: recent insights into skin immune function.* Immunity, 2011. **35**(6): p. 857-69.
136. Liang, S.C., et al., *Interleukin (IL)-22 and IL-17 are coexpressed by Th17 cells and cooperatively enhance expression of antimicrobial peptides.* J Exp Med, 2006. **203**(10): p. 2271-9.
137. Dieu-Nosjean, M.C., et al., *Macrophage inflammatory protein 3alpha is expressed at inflamed epithelial surfaces and is the most potent chemokine known in attracting Langerhans cell precursors.* J Exp Med, 2000. **192**(5): p. 705-18.
138. Albanesi, C., et al., *Keratinocytes in inflammatory skin diseases.* Curr Drug Targets Inflamm Allergy, 2005. **4**(3): p. 329-34.
139. Nickoloff, B.J. and L.A. Turka, *Immunological functions of non-professional antigen-presenting cells: new insights from studies of T-cell interactions with keratinocytes.* Immunol Today, 1994. **15**(10): p. 464-9.
140. Nestle, F.O., et al., *Skin immune sentinels in health and disease.* Nat Rev Immunol, 2009. **9**(10): p. 679-91.

141. Nagy, I., et al., *Propionibacterium acnes and lipopolysaccharide induce the expression of antimicrobial peptides and proinflammatory cytokines/chemokines in human sebocytes.* Microbes Infect, 2006. **8**(8): p. 2195-205.
142. Guilliams, M., et al., *Skin-draining lymph nodes contain dermis-derived CD103(-) dendritic cells that constitutively produce retinoic acid and induce Foxp3(+) regulatory T cells.* Blood, 2010. **115**(10): p. 1958-68.
143. Igyarto, B.Z., et al., *Skin-resident murine dendritic cell subsets promote distinct and opposing antigen-specific T helper cell responses.* Immunity, 2011. **35**(2): p. 260-72.
144. Campbell, J.J., D.J. O'Connell, and M.A. Wurbel, *Cutting Edge: Chemokine receptor CCR4 is necessary for antigen-driven cutaneous accumulation of CD4 T cells under physiological conditions.* J Immunol, 2007. **178**(6): p. 3358-62.
145. Sigmundsdottir, H., et al., *DCs metabolize sunlight-induced vitamin D3 to 'program' T cell attraction to the epidermal chemokine CCL27.* Nat Immunol, 2007. **8**(3): p. 285-93.
146. Sigmundsdottir, H. and E.C. Butcher, *Environmental cues, dendritic cells and the programming of tissue-selective lymphocyte trafficking.* Nat Immunol, 2008. **9**(9): p. 981-7.
147. Mackay, L.K., et al., *The developmental pathway for CD103(+)CD8+ tissue-resident memory T cells of skin.* Nat Immunol, 2013. **14**(12): p. 1294-301.
148. Gebhardt, T., et al., *Memory T cells in nonlymphoid tissue that provide enhanced local immunity during infection with herpes simplex virus.* Nat Immunol, 2009. **10**(5): p. 524-30.
149. Bromley, S.K., et al., *Recirculating memory T cells are a unique subset of CD4+ T cells with a distinct phenotype and migratory pattern.* J Immunol, 2013. **190**(3): p. 970-6.
150. Bromley, S.K., S.Y. Thomas, and A.D. Luster, *Chemokine receptor CCR7 guides T cell exit from peripheral tissues and entry into afferent lymphatics.* Nat Immunol, 2005. **6**(9): p. 895-901.
151. Di Cesare, A., P. Di Meglio, and F.O. Nestle, *The IL-23/Th17 axis in the immunopathogenesis of psoriasis.* J Invest Dermatol, 2009. **129**(6): p. 1339-50.

152. Di Cesare, A., P. Di Meglio, and F.O. Nestle, *A role for Th17 cells in the immunopathogenesis of atopic dermatitis?* J Invest Dermatol, 2008. **128**(11): p. 2569-71.
153. Havran, W.L., Y.H. Chien, and J.P. Allison, *Recognition of self antigens by skin-derived T cells with invariant gamma delta antigen receptors.* Science, 1991. **252**(5011): p. 1430-2.
154. Cai, Y., et al., *Pivotal role of dermal IL-17-producing gammadelta T cells in skin inflammation.* Immunity, 2011. **35**(4): p. 596-610.
155. Naik, S., et al., *Compartmentalized control of skin immunity by resident commensals.* Science, 2012. **337**(6098): p. 1115-9.
156. Heath, W.R. and F.R. Carbone, *The skin-resident and migratory immune system in steady state and memory: innate lymphocytes, dendritic cells and T cells.* Nat Immunol, 2013. **14**(10): p. 978-85.
157. Nakamura, Y., et al., *Staphylococcus delta-toxin induces allergic skin disease by activating mast cells.* Nature, 2013. **503**(7476): p. 397-401.
158. Rudikoff, D. and M. Lebwohl, *Atopic dermatitis.* Lancet, 1998. **351**(9117): p. 1715-21.
159. Iwase, T., et al., *Staphylococcus epidermidis Esp inhibits Staphylococcus aureus biofilm formation and nasal colonization.* Nature, 2010. **465**(7296): p. 346-9.
160. Gao, Z., et al., *Substantial alterations of the cutaneous bacterial biota in psoriatic lesions.* PLoS One, 2008. **3**(7): p. e2719.
161. Fitz-Gibbon, S., et al., *Propionibacterium acnes strain populations in the human skin microbiome associated with acne.* J Invest Dermatol, 2013. **133**(9): p. 2152-60.
162. Palmer, C.N., et al., *Common loss-of-function variants of the epidermal barrier protein filaggrin are a major predisposing factor for atopic dermatitis.* Nat Genet, 2006. **38**(4): p. 441-6.
163. Kobayashi, T., et al., *Dysbiosis and Staphylococcus aureus Colonization Drives Inflammation in Atopic Dermatitis.* Immunity, 2015. **42**(4): p. 756-66.
164. Belkaid, Y. and S. Tamoutounour, *The influence of skin microorganisms on cutaneous immunity.* Nat Rev Immunol, 2016. **16**(6): p. 353-66.

165. Wirtz, S., et al., *Interleukin-35 mediates mucosal immune responses that protect against T-cell-dependent colitis.* Gastroenterology, 2011. **141**(5): p. 1875-86.
166. Mottet, C., H.H. Uhlig, and F. Powrie, *Cutting edge: cure of colitis by CD4+CD25+ regulatory T cells.* J Immunol, 2003. **170**(8): p. 3939-43.
167. Park, S.G., et al., *T regulatory cells maintain intestinal homeostasis by suppressing gammadelta T cells.* Immunity, 2010. **33**(5): p. 791-803.
168. Fagarasan, S., et al., *In situ class switching and differentiation to IgA-producing cells in the gut lamina propria.* Nature, 2001. **413**(6856): p. 639-43.
169. Hill, D.A., et al., *Metagenomic analyses reveal antibiotic-induced temporal and spatial changes in intestinal microbiota with associated alterations in immune cell homeostasis.* Mucosal Immunol, 2010. **3**(2): p. 148-58.
170. Ericsson, A.C., et al., *Variable Colonization after Reciprocal Fecal Microbiota Transfer between Mice with Low and High Richness Microbiota.* Front Microbiol, 2017. **8**: p. 196.
171. Nizza, S.T. and J.J. Campbell, *CD11b+ migratory dendritic cells mediate CD8 T cell cross-priming and cutaneous imprinting after topical immunization.* PLoS One, 2014. **9**(3): p. e91054.
172. Fosso, B., et al., *BioMaS: a modular pipeline for Bioinformatic analysis of Metagenomic AmpliconS.* BMC Bioinformatics, 2015. **16**: p. 203.
173. Gargari, G., et al., *Consumption of a Bifidobacterium bifidum Strain for 4 Weeks Modulates Dominant Intestinal Bacterial Taxa and Fecal Butyrate in Healthy Adults.* Appl Environ Microbiol, 2016. **82**(19): p. 5850-9.
174. Annunziato, F., et al., *Phenotypic and functional features of human Th17 cells.* J Exp Med, 2007. **204**(8): p. 1849-61.
175. Mora, J.R. and U.H. Von Andrian, *Specificity and plasticity of memory lymphocyte migration.* Curr Top Microbiol Immunol, 2006. **308**: p. 83-116.
176. Nishio, J., et al., *Requirement of full TCR repertoire for regulatory T cells to maintain intestinal homeostasis.* Proc Natl Acad Sci U S A, 2015. **112**(41): p. 12770-5.
177. Kamada, N. and G. Nunez, *Role of the gut microbiota in the development and function of lymphoid cells.* J Immunol, 2013. **190**(4): p. 1389-95.

178. Shulzhenko, N., et al., *Crosstalk between B lymphocytes, microbiota and the intestinal epithelium governs immunity versus metabolism in the gut.* Nat Med, 2011. **17**(12): p. 1585-93.
179. Mukhopadhya, I., et al., *IBD-what role do Proteobacteria play?* Nat Rev Gastroenterol Hepatol, 2012. **9**(4): p. 219-30.
180. Svensson, M. and W.W. Agace, *Role of CCL25/CCR9 in immune homeostasis and disease.* Expert Rev Clin Immunol, 2006. **2**(5): p. 759-73.
181. Takeda, K. and S. Akira, *Microbial recognition by Toll-like receptors.* J Dermatol Sci, 2004. **34**(2): p. 73-82.
182. Campbell, J.J., et al., *The chemokine receptor CCR4 in vascular recognition by cutaneous but not intestinal memory T cells.* Nature, 1999. **400**(6746): p. 776-80.
183. Santamaria Babi, L.F., et al., *Migration of skin-homing T cells across cytokine-activated human endothelial cell layers involves interaction of the cutaneous lymphocyte-associated antigen (CLA), the very late antigen-4 (VLA-4), and the lymphocyte function-associated antigen-1 (LFA-1).* J Immunol, 1995. **154**(4): p. 1543-50.
184. Sheridan, B.S. and L. Lefrancois, *Regional and mucosal memory T cells.* Nat Immunol, 2011. **12**(6): p. 485-91.
185. Lim, D.J. and B. Hussl, *Macromolecular transport by the middle ear and its lymphatic system.* Acta Otolaryngol, 1975. **80**(1-2): p. 19-31.
186. Oyoshi, M.K., et al., *Epicutaneous challenge of orally immunized mice redirects antigen-specific gut-homing T cells to the skin.* J Clin Invest, 2011. **121**(6): p. 2210-20.
187. Cueni, L.N. and M. Detmar, *New insights into the molecular control of the lymphatic vascular system and its role in disease.* J Invest Dermatol, 2006. **126**(10): p. 2167-77.
188. Liao, S. and N.H. Ruddle, *Synchrony of high endothelial venules and lymphatic vessels revealed by immunization.* J Immunol, 2006. **177**(5): p. 3369-79.
189. Bognar, P., et al., *Reduced inflammatory threshold indicates skin barrier defect in transglutaminase 3 knockout mice.* J Invest Dermatol, 2014. **134**(1): p. 105-11.

190. De Benedetto, A., et al., *Tight junction defects in patients with atopic dermatitis.* J Allergy Clin Immunol, 2011. **127**(3): p. 773-86 e1-7.
191. Ahrens, K., et al., *Mechanical and metabolic injury to the skin barrier leads to increased expression of murine beta-defensin-1, -3, and -14.* J Invest Dermatol, 2011. **131**(2): p. 443-52.
192. Miller, L.S., *Toll-like receptors in skin.* Adv Dermatol, 2008. **24**: p. 71-87.
193. Cogen, A.L., et al., *Selective antimicrobial action is provided by phenol-soluble modulins derived from Staphylococcus epidermidis, a normal resident of the skin.* J Invest Dermatol, 2010. **130**(1): p. 192-200.
194. Ushijima, T., M. Takahashi, and Y. Ozaki, *Acetic, propionic, and oleic acid as the possible factors influencing the predominant residence of some species of Propionibacterium and coagulase-negative Staphylococcus on normal human skin.* Can J Microbiol, 1984. **30**(5): p. 647-52.
195. Fan, L., et al., *Antigen presentation by keratinocytes directs autoimmune skin disease.* Proc Natl Acad Sci U S A, 2003. **100**(6): p. 3386-91.
196. Olaru, F. and L.E. Jensen, *Chemokine expression by human keratinocyte cell lines after activation of Toll-like receptors.* Exp Dermatol, 2010. **19**(8): p. e314-6.
197. Rigoni, R., et al., *Intestinal microbiota sustains inflammation and autoimmunity induced by hypomorphic RAG defects.* J Exp Med, 2016. **213**(3): p. 355-75.
198. Huggenberger, R. and M. Detmar, *The cutaneous vascular system in chronic skin inflammation.* J Investig Dermatol Symp Proc, 2011. **15**(1): p. 24-32.
199. Fuss, I.J., et al., *Disparate CD4+ lamina propria (LP) lymphokine secretion profiles in inflammatory bowel disease. Crohn's disease LP cells manifest increased secretion of IFN-gamma, whereas ulcerative colitis LP cells manifest increased secretion of IL-5.* J Immunol, 1996. **157**(3): p. 1261-70.
200. Ahern, P.P., et al., *Interleukin-23 drives intestinal inflammation through direct activity on T cells.* Immunity, 2010. **33**(2): p. 279-88.
201. Funderburg, N.T., et al., *Circulating CD4(+) and CD8(+) T cells are activated in inflammatory bowel disease and are associated with plasma markers of inflammation.* Immunology, 2013. **140**(1): p. 87-97.

202. Barnes, M.J. and F. Powrie, *Regulatory T cells reinforce intestinal homeostasis.* Immunity, 2009. **31**(3): p. 401-11.

203. Kawamoto, S., et al., *The inhibitory receptor PD-1 regulates IgA selection and bacterial composition in the gut.* Science, 2012. **336**(6080): p. 485-9.

204. Manichanh, C., et al., *The gut microbiota in IBD.* Nat Rev Gastroenterol Hepatol, 2012. **9**(10): p. 599-608.

205. Mora, J.R., *Homing imprinting and immunomodulation in the gut: role of dendritic cells and retinoids.* Inflamm Bowel Dis, 2008. **14**(2): p. 275-89.

206. Rakoff-Nahoum, S., L. Hao, and R. Medzhitov, *Role of toll-like receptors in spontaneous commensal-dependent colitis.* Immunity, 2006. **25**(2): p. 319-29.

207. Rivas, M.N., et al., *MyD88 is critically involved in immune tolerance breakdown at environmental interfaces of Foxp3-deficient mice.* J Clin Invest, 2012. **122**(5): p. 1933-47.

208. Fukata, M., et al., *The myeloid differentiation factor 88 (MyD88) is required for CD4+ T cell effector function in a murine model of inflammatory bowel disease.* J Immunol, 2008. **180**(3): p. 1886-94.

209. Schenten, D., et al., *Signaling through the adaptor molecule MyD88 in CD4+ T cells is required to overcome suppression by regulatory T cells.* Immunity, 2014. **40**(1): p. 78-90.

210. Cahenzli, J., et al., *Intestinal microbial diversity during early-life colonization shapes long-term IgE levels.* Cell Host Microbe, 2013. **14**(5): p. 559-70.

211. Carding, S.R., et al., *Developmentally regulated fetal thymic and extrathymic T-cell receptor gamma delta gene expression.* Genes Dev, 1990. **4**(8): p. 1304-15.

212. Kanamori, Y., et al., *Identification of novel lymphoid tissues in murine intestinal mucosa where clusters of c-kit+ IL-7R+ Thy1+ lympho-hemopoietic progenitors develop.* J Exp Med, 1996. **184**(4): p. 1449-59.

213. Vossen, J.M., et al., *Complete suppression of the gut microbiome prevents acute graft-versus-host disease following allogeneic bone marrow transplantation.* PLoS One, 2014. **9**(9): p. e105706.

214. Nielsen, M.M., D.A. Witherden, and W.L. Havran, *gammadelta T cells in homeostasis and host defence of epithelial barrier tissues.* Nat Rev Immunol, 2017. **17**(12): p. 733-745.

215. Mueller, S.N., A. Zaid, and F.R. Carbone, *Tissue-resident T cells: dynamic players in skin immunity.* Front Immunol, 2014. **5**: p. 332.
216. Albanesi, C., et al., *A cytokine-to-chemokine axis between T lymphocytes and keratinocytes can favor Th1 cell accumulation in chronic inflammatory skin diseases.* J Leukoc Biol, 2001. **70**(4): p. 617-23.
217. Dalessandri, T., et al., *IL-13 from intraepithelial lymphocytes regulates tissue homeostasis and protects against carcinogenesis in the skin.* Nat Commun, 2016. **7**: p. 12080.
218. Kong, H.H., et al., *Temporal shifts in the skin microbiome associated with disease flares and treatment in children with atopic dermatitis.* Genome Res, 2012. **22**(5): p. 850-9.
219. Song, P.I., et al., *Human keratinocytes express functional CD14 and toll-like receptor 4.* J Invest Dermatol, 2002. **119**(2): p. 424-32.
220. Bowe, W.P. and A.C. Logan, *Acne vulgaris, probiotics and the gut-brain-skin axis - back to the future?* Gut Pathog, 2011. **3**(1): p. 1.
221. Majamaa, H. and E. Isolauri, *Evaluation of the gut mucosal barrier: evidence for increased antigen transfer in children with atopic eczema.* J Allergy Clin Immunol, 1996. **97**(4): p. 985-90.
222. Parodi, A., et al., *Small intestinal bacterial overgrowth in rosacea: clinical effectiveness of its eradication.* Clin Gastroenterol Hepatol, 2008. **6**(7): p. 759-64.
223. Scher, J.U., et al., *Reply: To PMID 25319745.* Arthritis Rheumatol, 2015. **67**(8): p. 2280-2.
224. Zanvit, P., et al., *Antibiotics in neonatal life increase murine susceptibility to experimental psoriasis.* Nat Commun, 2015. **6**: p. 8424.
225. Jaskowski, T.D., et al., *IgA anti-epidermal transglutaminase antibodies in dermatitis herpetiformis and pediatric celiac disease.* J Invest Dermatol, 2009. **129**(11): p. 2728-30.
226. Mu, Q., et al., *Leaky Gut As a Danger Signal for Autoimmune Diseases.* Front Immunol, 2017. **8**: p. 598.
227. Xu, X.R., et al., *Dysregulation of mucosal immune response in pathogenesis of inflammatory bowel disease.* World J Gastroenterol, 2014. **20**(12): p. 3255-64.

228. Marzano, A.V., et al., *Cutaneous manifestations in patients with inflammatory bowel diseases: pathophysiology, clinical features, and therapy.* Inflamm Bowel Dis, 2014. **20**(1): p. 213-27.

229. Rothfuss, K.S., E.F. Stange, and K.R. Herrlinger, *Extraintestinal manifestations and complications in inflammatory bowel diseases.* World J Gastroenterol, 2006. **12**(30): p. 4819-31.

230. Timani, S. and D.F. Mutasim, *Skin manifestations of inflammatory bowel disease.* Clin Dermatol, 2008. **26**(3): p. 265-73.

231. van Wijk, F. and H. Cheroutre, *Mucosal T cells in gut homeostasis and inflammation.* Expert Rev Clin Immunol, 2010. **6**(4): p. 559-66.

232. Monteleone, G., F. Pallone, and T.T. MacDonald, *Emerging immunological targets in inflammatory bowel disease.* Curr Opin Pharmacol, 2011. **11**(6): p. 640-5.

233. Adams, D.H. and B. Eksteen, *Aberrant homing of mucosal T cells and extra-intestinal manifestations of inflammatory bowel disease.* Nat Rev Immunol, 2006. **6**(3): p. 244-51.